Toute commande sera adressée à:
EDITURA ACADEMIEI ROMÂNE, Calea 13 Septembrie nr. 13, Sector 5, P.O. Box 5–42, Bucureşti, România, Tel. 40-21-411 9008, Tel./Fax. 40-21-410 3983, 40-21-410 3448; e-mail: edacad@ear.ro
RODIPET S.A., Piaţa Presei Libere nr. 1, Sector 1, P.O. Box 35-37, Bucureşti, România, Tel. 40-21-222 4126, Fax 40-21-224 0558.
ORION PRESS IMPEX 2000 S.R.L., P.O. Box 77-19, Bucureşti, sector 5, România, Tel. 40-21-301 87 86, Fax 40-21-335 02 96.

Les manuscrits ainsi que toute correspondance seront envoyés à la rédaction; les livres et les publications proposés en échange seront adressés à: INSTITUTUL DE BIOLOGIE, Splaiul Independenţei 296, P.O. Box 56-53, 79651, Bucureşti.

EDITAT CU SPRIJINUL MINISTERULUI EDUCAŢIEI ŞI CERCETĂRII

REVUE ROUMAINE DE BIOLOGIE
SÉRIE DE BIOLOGIE ANIMALE
Calea Victoriei 125
R-79 717, Bucureşti, România
Tél. 650 76 80

Calea 13 Septembrie, nr. 13, sector 5
R-76 117, Bucureşti, România
Tél. 410 32 00; 40-21-411 90 08
Tél./Fax. 40-21-410 39 83

REVUE ROUMAINE DE BIOLOGIE

SÉRIE DE BIOLOGIE ANIMALE

TOME 45, N° 2 — Juillet-Décembre, 2000

SOMMAIRE

CONTRIBUTIONS TO THE STUDY OF MOLLUSCA FROM THE ROMANIAN STRETCH OF THE DANUBE

VIRGINIA POPESCU-MARINESCU, ELENA NEAGU

The investigations carried out during 1995–1996 throughout the length of the Romanian stretch of the Danube revealed at Mollusca level, lamellibranchiata' dominance. Excepting the values recorded at rkm 167 and 171, usually the highest values of mollusca numerical densities and their biomass were found in the Iron Gates I lake. This is the consequence of the newly created conditions following the damlake construction in 1970. As concerns the most important species, we mention: among lamellibranchiata, *Dreissena polymorpha, Sphaerium riviculum, S. corneum,* followed by *Unio tumidus*; and among gasteropods, *Viviparus acerosus, Lithoglyphus naticoides* followed at a certain distance, by *Bithynia tentaculata* and *Theodoxus danubialis.* But it is noteworthy the presence in the Romanian stretch of the Danube, of the three species of genus *Theodoxus (danubialis, transversalis and fluviatilis).* These latter forms, very demanding as concerns the environmental conditions, are in danger of disappearance due to the river pollution.

1. INTRODUCTION

In the last decades of the past century, the environmental conditions in certain sections of the Romanian stretch of the Danube underwent major changes from morpho-hydrological point of view. In this respect we mention the construction of the Iron Gates I damlake in 1970, a hydrotechnical work shortly followed by the second construction, Iron Gates II. The changes occurred in the upper section of the river concerned mainly the water flow velocity, the river depth and the substratum nature. They did not influence only the fauna from that section, but also that from downstream.

The environmental factors' changes influenced the mollusca fauna from the Danube both lamellibranchiata and gasteropods. A number of changes at the level of the aquatic assemblages' components from the lakes of the Iron Gates and from the river, including mollusca were evidenced by 1986 in a number of publications [1,3,4,6–13]. We especially mention the works by Grossu [2], Negrea and Popescu-Marinescu [5] which represent syntheses concerning the situation of gasteropods from the river throughout the length of the Romanian stretch of the river.

In this work we present the changes which occurred in the Danube among mollusca, after a 10 years period of time (1995–1996) since the last data were published by Negrea and Popescu-Marinescu.

REV. ROUM. BIOL. – BIOL. ANIM., TOME 45, N° 2, P. 113–123, BUCAREST, 2000

In this respect, throughout the length of the Romanian stretch of the Danube, in 1995–1996, quantitative samples of zoobenthos were collected* from the Danube, between rkm 1072,4 and the confluence with the sea through the Arms Sulina and Chilia. A major part of these samples included in their specific composition lamellibranchiata and gasteropods. The results of this material processing represent the present work object.

2. RESULTS AND DISCUSSION

From the data presented in the Tables 1 and 2 it results that from a quantitative point of view, the two mollusca groups, during 1995–1996 were well represented in the Romanian stretch of the Danube both as numerical density and as biomass, especially lamellibranchiata.

Regarding lamellibranchiata, the regions the most populated by these hidrobionts were the present damlakes, Iron Gates I and Iron Gates II in both studied years (Tables 1–4). The strong development of lamellibranchiata in the two lakes benefited by the new conditions created after 1970. Besides the depth and the substratum nature, another facilitating factor was the water flow velocity, diminished under the lake conditions compared to the situation existing in the river before the damlake construction. Maximal numerical densities of 131700 ind./m^2 (18759 g/m) were in 1996 at rkm 1072.4 at a water depth of 15.5 m and 120000 ind./m^2 (4687.39 g/m^2) at 10.2 m depth (Table 2). It is noteworthy that whereas at 15.5 m water depth, *Dreissena polymorpha* dominated with 122900 ind./m^2 (18480 g/m^2), at 10.2 m water depth, *Sphaerium* was dominant (by the two species, *riviculum* and *corneum*), with 18800 ind./m^2 (4490.05 g/m^2) (Table 4). The explanation of the dominance of one or another taxonomic species, on the same profile, at different water depths, consists mainly in the substratum nature.

If the maximal density is found at the tail of the Iron Gates I, we found the biomass maximum of 21740 g/m^2 in the lower part of the Romanian stretch of the Danube and namely at rkm 167. There, the water depth was of 19.2 m and the substratum was sandy. The respective weight in 1996 was due mostly (21730 g/m^2) to those 900 ind./m^2 of *Unio tumidus* (Table 4).

We outline the fact that, excepting the maxima recorded by lamellibranchiata at rkm 1072.4 and rkm 167, the other values found by us in 1995–1996 are similar

* We wish to thank Dr. Oaie G. from the Institute of Geology and Geoecology – Bucharest, as well as the team led by him, for their kindness in collecting the macrozoobenthic samples from the Danube.

to those mentioned by Russev et al. [13] for this group of organisms from the Danube between rkm 845 and 494 in 1971 and 1973.

A comparison concerning the spreading of the main lamellibranchiata taxa in the Romanian stretch of the Danube, in 1995–1996 (Tables 3 and 4) points out the fact that *Dreissena polymorpha* is present almost throughout the stretch length, whereas *Sphaerium*, represented by the species *riviculum* and *corneum*, is concentrated more in Iron Gates I and Iron Gates II lakes, particularly in 1995.

Table 1

Numerical density and biomass of mollusca in the Danube in 1995

THE D A N U B E			LAMELLIBRANCHIATA		GASTEROPODS	
Place of collecting	**Water depth (m)**	**Substratum nature**	**D ind./m^2**	**B g/m^2**	**D ind./m^2**	**B g/m^2**
rkm 1072.4	10.0	mud	12050	566.30	150	2.85
rkm 1072.4	11.0	sand, gravel	2750	335.00	3050	210.40
rkm 1048.7	18.3	stone, mud, sand	45800	8472.23	5300	896.33
rkm 1044.5	0.9	mud	-	-	50	0.40
rkm 1040.0	6.0	mud	50	16.62	-	-
rkm 999.0	16.7	mud	2700	1845.00	-	-
rkm 969.5	12.5	mud	50	1919.85	-	-
rkm 959.5	9.8	mud	400	523.25	-	-
rkm 952.0	25.0	mud	1950	84.83	-	-
rkm 911.0	14.8	sand	19100	3165.90	350	175.65
rkm 879.0	11.8	stone	32400	2135.35	150	123.79
rkm 866.0	20.0	stone, mud	1850	44.40	100	4.25
rkm 481.0	11.3	coarse sand	250	960.00	-	-
rkm 247.0	12.1	sand	-	-	50	0.25
rkm 171.0	6.0	mud, sand	15100	5359.91	8400	8888.27
rkm 167.0	4.0	mud	-	-	500	75.54
rkm 167.0	5.3	sand,tana-thocenosis	2200	465.00	1650	2209.00
rkm 167.0	18.0	sand	-	-	100	2.00
mile 78.0	7.5	mud	150	41.71	500	69.50
mile 34.0	4.8	mud, sand	150	1091.00	100	1.50
rkm 115.2	5.0	mud, sand	-	-	100	5.10
rkm 39.7	23.3	mud, sand	150	49.96	-	-
rkm 20.0	7.8	mud, sand	2750	3307.65	1650	3901.40

Table legend: rkm 1072.4–167.0 on the unique Danube; mile 78.0 and mile 34.0 on Tulcea Arm; rkm 115.2–20.0 on Chilia Arm. D = numerical density; B = biomass. Mollusca biomass includes the shell too.

Table 2

Numerical density and biomass of mollusca in the Danube in 1996

THE DANUBE			LAMELLIBRANCHIATA		GASTEROPODS	
Place of collecting	Water depth (m)	Substratum nature	D ind./m²	B g/m²	D ind./m²	B g/m²
rkm 1072.4	10.2	mud	120000	4687.39	1400	724.24
rkm 1072.4	15.5	mud, sand, stone	131700	18750.00	500	10.70
rkm 1048.7	18.3	sand, mud	1200	145.60	-	-
rkm 1044.5	10.0	sand	-	-	100	2.10
rkm 1040.0	10.5	sand	500	51.90	200	25.00
rkm 999,0	18.5	mud	-	-	100	364.53
rkm 999.0	31.0	mud	3800	20.30	2800	15.00
rkm 879.0	10.9	stone	2808	378.87	52	1.82
rkm 866.0	14.1	sand, stone	1300	145.14	-	-
rkm 481.0	5.3	sand	100	1669.84	-	-
rkm 481.0	8.9	sand	100	2.00	-	-
rkm 481.0	11.2	sand, gravel	100	3.00	-	-
rkm 375.0	9.2	mud, sand	300	1.50	1400	51.50
rkm 301.0	6.0	sand	700	67.54	100	22.20
rkm 301.0	13.5	sand	900	18561.42	2300	3363.00
rkm 167.0	19.2	sand	1300	21742.10	300	53.10
mile 78.0	18.0	sand	200	4.00	-	-
mile 34.0	3.0	mud	2400	2184.62	1200	338.33
mile 34.0	14.5	sand, gravel	7700	2104.13	900	1041.73
mile 33.1	12.3	sand	1100	147.32	-	-

Table legend: rkm 1072.4–167.0 on the unique Danube; mile 78.0 and mile 34.0 on Tulcea Arm; rkm 115.2–20.0 on Chilia Arm. D = numerical density; B = biomass. Mollusca biomass includes the shell too.

Table 3

Numerical density and biomass of the main lamellibranchiata species in the Danube in 1995

THE DANUBE			*Dreissena polymorpha*		*Sphaerium rivicu-lum + S. corneum*		*Unio tumidus*	
Place of collecting	Water depth (m)	Substratum nature	D ind./m²	B ex/m²	D ind./m²	B ex/m²	D ind./m²	B ex/m²
rkm 1072.4	10.0	mud	100	30.00	11900	436.30	50	100.00
rkm 1072.4	11.0	sand, gravel	2050	300.00	700	35.00	-	-
rkm 1048.7	18.3	stone, mud, sand	24600	4662.65	21150	622.20	50	3187.38
rkm 1040.0	6.0	mud	-	-	50	16.62	-	-
rkm 999.0	16.7	mud	-	-	2700	1845.00	-	-

Table 3 (continued)

THE DANUBE			*Dreissena polymorpha*		*Sphaerium rivicu-lum + S. corneum*		*Unio tumidus*	
Place of collecting	Water depth (m)	Substratum nature	D ind./m²	B ex/m²	D ind./m²	B ex/m²	D ind./m²	B ex/m²
rkm 969.5	12.5	mud	-	-	-	-	50	1919.85
rkm 959.5	9.8	mud	350	33.25	-	-	50	490.00
rkm 952.0	25.0	mud	-	-	1950	84.83	-	-
rkm 911.0	14.8	sand	16750	961.30	700	102.50	250	1480.00
rkm 879.0	11.8	stone	32350	1085.35	-	-	50	1050.00
rkm 866.0	20.0	stone, sand	1850	44.40	-	-	-	-
rkm 481.0	11.3	coarse sand	250	960.00	-	-	-	-
rkm 171.0	6.0	mud, sand	14300	4599.16	700	34.99	100	725.76
rkm 167.0	5.3	sand	-	-	2200	465.00	-	-
mile 78.0	7.5	mud	100	9.75	-	-	50	31.96
mile 34.0	4.8	mud, sand	100	21.00	-	-	50	1070.00
rkm 39.7	23.3	mud, sand	150	49.96	-	-	-	-
rkm 20.0	7.8	mud	2450	1207.78	150	38.76	100	950.05

Table legend: rkm 1072.4–167.0 on the unique Danube; mile 78.0 and mile 34.0 on Tulcea Arm; rkm 115.2–20.0 on Chilia Arm. D = numerical density; B = biomass. Mollusca biomass includes the shell too.

Table 4

Numerical density and biomass of the main lamellibranchiata species in the Danube in 1996

THE DANUBE			*Dreissena polymorpha*		*Sphaerium rivicu-lum + S. corneum*		*Unio tumidus*	
Place of collecting	Water depth (m)	Substratum nature	D ind./m²	B g/m²	D ind./m²	B g/m²	D ind./m²	B g/m²
rkm 1072.4	10.2	mud	1200	196.44	18800	4490.95	-	-
rkm 1072.4	15.5	mud, sand, stone	122900	18480.0	8800	270.00	-	-
rkm 1048.7	18.3	sand, mud	-	-	1200	145.60	-	-
rkm 1040.0	10.5	sand	200	15.45	300	36.45	-	-
rkm 999.0	31.0	mud	-	-	3800	20.30	-	-
rkm 879.0	10.9	stone	2808	378.87	-	-	-	-
rkm 866.0	14.1	stone	1200	123.91	100	21.23	-	-
rkm 481.0	5.3	sand	-	-	-	-	100	1669.84
rkm 481.0	8.9	sand	100	2.00	-	-	-	-
rkm 481.0	11.2	sand, gravel	100	3.00	-	-	-	-
rkm 375.0	9.2	mud, sand	300	1.50	-	-	-	-
rkm 301.0	6.0	sand	700	67.54	-	-	-	-
rkm 301.0	13.5	sand	-	-	400	41.42	500	18520.00

Table 4 (continued)

THE DANUBE			*Dreissena polymorpha*		*Sphaerium rivicu-lum + S. corneum*		*Unio tumidus*	
Place of collecting	Water depth (m)	Substratum nature	D ind./m²	B g/m²	D ind./m²	B g/m²	D ind./m²	B g/m²
rkm 167.0	19.2	sand	100	3.10	300	9.00	900	21730.00
mile 78.0	18.0	sand	200	4.00	-	-	-	-
mile 34.0	3.0	mud	2200	314.57	-	-	100	1865.34
mile 34.0	14.5	sand, gravel	7700	2104.13	-	-	-	-
mile 33.10	12.3	sand	1100	147.32	-	-	-	-

Table legend: rkm 1072.4–167.0 on the unique Danube; mile 78.0 and mile 34.0 on Tulcea Arm; rkm 115.2–20.0 on Chilia Arm. D = numerical density; B = biomass. Mollusca biomass includes the shell too.

As concerns *Unio tumidus*, in 1995, its area covered the entire Romanian stretch of the Danube, whereas in 1996 it was only in the lower part, where the sandy substratum was dominant (Table 4).

We have to mention that sporadically, *i.e.* in 1995, at rkm 911 and in 1996 at rkm 20, on The Chilia Arm, among our specimens, *Pseudanodonta complanata* appeared too, but in a small number.

A retrospective view concerning *Dreissena* and *Sphaerium* spreading and the quantities found in the periods of time preceding our investigations during 1995–1996, shows that *Dreissena polymorpha* was present in great number in some places at Iron Gates since 1942 [1], hence long before the damlake construction. After the Iron Gates I was created [12] this species proliferated particularly in the improperly so-called gulps Mraconia, Cerna, Bahna. The spreading of genus *Sphaerium* with its species *riviculum* and *corneum* is somewhat controversial. Thus, in 1962 Grossu [2] said that *Sphaerium riviculum* occurred "in the lower and middle regions of the Danube, beginning from Vienna up to the river mouth". According to Virginia Popescu-Marinescu [7], before the damlake construction, *Sphaerium sp.*, a specific composition of psamopelorheophilic assemblage, was present at Iron Gates, but scarcely. The same author [11] shows that after the damlake construction, in 1986, *Sphaerium riviculum* recorded a real explosive development. Russev et al. [13] show the *S. riviculum* spreading throughout the entire Romanian stretch of the Danube even prior to the construction of the Iron Gates I, and *S. corneum* was present from rkm 851 downstream to Tulcea, whereas Frank et al. in "Mollusca from the Danube from Schwartzland up to the Black Sea" synthesis published in 1990 [4] mentioned the *S. riviculum* spreading only from Giurgiu downstream and that of *S. corneum* only at Sulina. Regarding *Unio tumidus*, Frank et al. [4] mentioned it as being present in the Danube from Baziaş to Sulina. It is one of the lamellibranchiata species characteristic to the upstream section of the Romanian stretch of the Danube, prior to the damlake creation [7].

As concerns the gasteropods, this group is on the second place among the mollusca from the Romanian stretch of the Danube. They were present throughout the entire length of the analysed sector and underwent changes in the course of time, but as Negrea and Popescu-Marinescu [5] outlined, their changes were less profound than those of lamellibranchiata.

A biomass maximum of 8888.27 g/m² was found also in the lower part of the river, but at rkm 171 in 1995. Here the maximal numerical density of 8400 ind./m² (Table 1) was recorded as well. Among the conditions under which these values were obtained, we mention: a shallow water, a muddy substratum with sand and a water flow velocity of about 1 m/s. It is noteworthy mentioning that 98.45 % of the maximal biomass was given by *Viviparus acerosus*. This second dominant species among gasteropods had a density of 41.1% only. *Lithoglyphus naticoides*, the first dominant species as concerns the numerical density, held 55.36% and regarding the biomass, 1.46% only. Gasteropods also recorded at the Iron Gates I damlake, in 1995–1996, generally higher values, particularly as concerns the biomass, compared to the previous periods of time [12].

For the section between rkms 845–494, excepting the maximum at rkm 171, all the other biomass values are comparable to those mentioned by Russev et al. [13] for 1971 and 1973.

As concerns the gasteropods taxa from Romanian stretch of the Danube in 1995–1996,** *Viviparus acerosus* and *Lithoglyphus naticoides* were the most important. Regarding the spreading, both of them occupied the entire space of the Romanian Danube stretch, *L. naticoides* having a higher frequency (Tables 5–6). As a matter of fact, Grossu [2] noticed the fact that in the Romanian Danube stretch some prosobranchiata among which *L. naticoides* **are** in a large number and widespread. The above-mentioned author outlines also the fact that "almost in all the samples from Orşova-Coronini and Sulina, only *L. naticoides* individuals were found". Also, Frank et al. show that this species is spread throughout the entire Romanian stretch of the Danube [4].

Regarding the spreading, in the Romanian river stretch, *L. naticoides* are followed by *Viviparus acerosus* (Table 5–6), but more frequent at Iron Gates and between rkms. 301 and 171. Grossu [3] mentioned this species as a common one in the Danube basin, especially in its inferior part.

A more restrained spreading in the analysed sector, in the 1995–1996 was recorded by *Bithynia tentaculata* (Tables 5–6). This species was found in our samples in both of the investigated years only in the two lakes at the Iron Gates. But, Frank et al. [4] mentioned it just for the inferior section of the Romanian stretch of the Danube, beginning from rkm. 355 to the river mouth through the Sulina Arm. But Grossu considers it as being "a common one everywhere" in Romania [3].

** We express our thanks to Dr. Alexandrina Negrea from the Institute of Speleology-Bucharest, for the determinations she carried out.

Table 5
Numerical density and biomass of the main gasteropods species in the Danube in 1995

THE DANUBE			*Viviparus acerosus*		*Lithoglyphus naticoides*		*Bithynia tentaculata*		*Theodoxus transversalis*		*Theodoxus danubialis*	
Place of collecting	**Water depth (m)**	**Substratum nature**	**D ind./m²**	**B g/m²**	**D ind./m²**	**B g/m²**	**D ind./m²**	**B g/m²**	**D ind./m²**	**B g/m²**	**D ind./m²**	**B g/m²**
rkm 1072.4	10.0	mud	-	-	-	-	150	2.85	-	-	-	-
rkm 1072.4	11.0	sand, stone	-	-	-	-	3050	210.00	-	-	-	-
rkm 1048.7	18.3	stone, mud, sand	100	467.77	110	27.005	4900	390.56	50	5.5	50	5.5
rkm 1044.5	0.9	mud	-	-	50	4.00	-	-	-	-	-	-
rkm 911.0	14.8	sand	50	137.50	-	-	300	13.50	-	-	-	-
rkm 879.0	11.8	stone	150	123.79	-	-	-	-	-	-	-	-
rkm 866.0	20.0	stone, sand	-	-	50	3.50	50	0.75	-	-	-	-
rkm 247.0	12.1	sand	-	-	50	0.25	-	-	-	-	-	-
rkm 171.0	6.0	mud, sand	3450	8750.39	4650	129.49	-	-	250	7.0	50	1.4
rkm 167.0	4.0	mud	-	-	500	75.54	-	-	-	-	-	-
rkm 167.0	5.3	sand, tanathocenosis	1050	2200.00	600	9.00	-	-	-	-	-	-
rkm 167.0	18.0	sand	-	-	100	2.00	-	-	-	-	-	-
mile 78.0	7.5	mud	-	-	500	69.50	-	-	-	-	50	2.0
mile 34.0	4.8	mud, sand	-	-	100	1.50	100	1.50	-	-	-	-
rkm 115.2	16.8	sand	-	-	100	5.10	-	-	-	-	-	-
rkm 72.3	4.5	mud	-	-	350	1.25	-	-	-	-	-	-
rkm 20.0	7.8	sand	1400	3878.38	100	19.30	-	-	150	3.9	-	-

Table legend: rkm 1072.4–167.0 on the unique Danube; mile 78.0 and 34.0 on the Tulcea Arm; rkm 115.2–20.0 on the Chilia Arm; D = numerical density; B = biomass. Mollusca biomass includes the shell too.

Table 6
Numerical density and biomass of the main gasteropods species in the Danube, in 1996

THE DANUBE			*Viviparus acerosus*		*Lithoglyphus naticoides*		*Bithynia tentaculata*		*Theodoxus danubialis*	
Place of collecting	**Water depth (m)**	**Substratum nature**	**D ind./m²**	**B g/m²**	**D ind./m²**	**B g/m²**	**D ind./m²**	**B g/m²**	**D ind./m²**	**B g/m²**
rkm 1072.4	10.2	mud	1000	703.24	-	-	400	21.00	-	-
rkm 1072.4	15.5	mud, sand, stone	-	-	-	-	400	1.00	100	7.00
rkm 999.0	18.5	mud	100	364.53	-	-	-	-	-	-
rkm 999.0	31.0	mud	-	-	2800	15.00	-	-	-	-
rkm 879.0	10.9	stone	-	-	-	-	26	0.52	26	1.30
rkm 375.0	7.0	mud, sand	-	-	1400	51.50	-	-	-	-
rkm 301.0	6.0	sand	-	-	-	-	-	-	100	22.20
rkm 301.0	13.5	sand	1500	3323.00	800	40.00	-	-	-	-
rkm 167.0	19.2	sand	300	53.10	-	-	-	-	-	-
mile 34.0	3.0	mud	800	258.00	300	50.00	-	-	100	30.33
mile 34.0	14.5	sand, gravel	500	1036.10	300	11.73	-	-	-	-

Table legend: rkm 1072.4–167.0 on the unique Danube; mile 34.0 on Tulcea Arm; D = numerical density; B = biomass. Molusca biomass includes the shell too.

Genus *Theodoxus* species deserves a particular attention. They are organisms more sensitive to oxygen deficiency and pollution. Popescu-Marinescu states [12] that *Theodoxus* species, in the course of time, restrained both the spreading area and the number of individuals. Nevertheless, in 1995–1996, *Th. danubialis* species was present in some sections, especially in the lake Iron Gates as well as between rkms 301–167 (Tables 5–6). Grossu [2] as well as Negrea and Popescu-Marinescu [5] mention it as being the most widespread species of this genus in the Danube. More seldom in a living state in our samples, *Th. transversalis* individuals appeared. Only once living individuals of *Th. fluviatilis* were found (at the mile 34 on the Sulina Arm) and once in tanathocenosis (at rkm 20 on the Chilia Arm). Frank *et al.* [4] present *Th. danubialis* and *Th. transversalis* as being spread throughout the Romanian stretch of the Danube. As concerns *Th. fluviatilis*, they mentioned it only from Jirlău-Borcea downstream to Sulina. Since 1942 these species have been found by Băcescu [1] at Iron Gates (it is that in a smaller number of individuals compared to the other two species).

Besides all these mentioned species, in our samples, in 1995–1996, *Esperiana esperi, E. acicularis* and *Succinea putris* were found in a living state, but much more seldom.

In many Danube sections (rkms. 959.5, 596, 481, 426, 171, 68.1, mile 34), a tanathocenosis existed, rich in species, where *Lithoglyphus naticoides, Viviparus acerosus, Bithynia tentaculata* were dominant and *Theodoxus transversalis, Th. danubialis, Planorbis corneus, Esperiana esperi, E. acicularis, Valvata piscinalis, Lymnaea stagnalis* were found more rarely and *Theodoxus fluviatilis* very rarely.

3. CONCLUSIONS

1. In 1995–1996, generally, in the Romanian stretch of the Danube, the quantity of mollusca, both as numerical density and as biomass, was higher as compared to previous years, as a consequence of the river water eutrophication.

2. The superior section of the Romanian stretch of the Danube, the Iron Gates lake proved to be the most rich in mollusca, during the two investigated years.

3. At the level of mollusca from the river, the lamellibranchiata dominance is to be noticed, and in a direct relation with the environmental factors.

4. The main species found during our researches period in the investigated section are: among lamellibranchiata *Dreissena polymorpha, Sphaerium riviculum, S. corneum,* followed by *Unio tumidus;* among gasteropods *Viviparus acerosus, Lythoglyphus naticoides,* followed by *Bithynia tentaculata* and *Th. danubialis.*

5. But it is noteworthy the presence of the species *Theodoxus danubialis, Th. transversalis* and *Th. fluviatilis* in some sections of the Romanian stretch of the Danube.

REFERENCES

1. BĂCESCU M., Quelques observations sur la faune benthonique du défilé roumain du Danube: son importance zoogeographique et pratique; la description d'une espece nouvelle de Mermithide, *Pseudomermis cazanica* n. sp., Ann. Sci. Univ. Jassy, **31** (1948).
2. GROSSU AL., Noi contribuţii la cunoaşterea moluştelor din cursul inferior al Dunării, Hidrobiologia, **4**, 337–359, Bucureşti (1963).
3. GROSSU AL., Gasteropoda romaniae **1**, 117–311, Bucureşti (1986).
4. C. FRANK, J. JUNGBLUTH, A. RICHNOVSZKY, *Die Mollusken der Donau vom Schwarzwald bis zum Schwarzen Meer*, 21–128, Budapest (1990).
5. NEGREA ALEXANDRINA, POPESCU-MARINESCU VIRGINIA, Gasteropode din sectorul românesc al Dunării găsite pâna în prezent, Hidrobiologia, **20**, 75–110, Bucureşti (1992).
6. POPESCU ECATERINA, PRUNESCU-ARION ELENA, Contribuţii la studiul faunei bentonice din Dunăre, în regiunea cataractelor (km 1042–955), St. cerc. biol., Seria biol. anim., **13**, 2 (1961).
7. VIRGINIA POPESCU-MARINESCU, Componenţa şi structura biocenozelor din Dunăre,C. Biocenozele bentonice din zona litorală şi de adâncime in: "Monografia zonei Porţilor de Fier", 85–110, Edit. Acad. R.S.R., Bucureşti, 1970.
8. VIRGINIA POPESCU-MARINESCU, Etappen der Zoobenthos-Entwicklung in der Donau, im Gebiet des "Eisernen Tors", Abschnitt Mraconia, Rev. roum. biol., Biol. anim., **31**, *1*, 73–80, Bucarest (1986).
9. V. MARINESCU (POPESCU-MARINESCU), Die Entwicklung der Benthos-Zoozönose in der Donau in Bereich des Stausees Eisernes Tor II, 26. Arbeitstagung der IAD, Passau/Deutschland, 1987, Wissenschaftliche Kurzreferate,152–155 (1987).
10. VIRGINIA POPESCU-MARINESCU, Die Struktur der Benthos-Zoozönosen aus der Donau bei Ceatal Izmail (km 80), in der Zeitspanne 1981–1985, Rev. roum. biol., Biol. anim., **34**, *1*, 43–48, Bucarest (1989).
11. VIRGINIA POPESCU-MARINESCU si ION DIACONU, Structura zoocenozelor bentonice din lacul de baraj Porţile de Fier I (profilele Mraconia, Cerna, Brahna) in anul 1986, St. cerc. biol., Seria biol. anim., **41**, *1*, 71–76, Bucureşti (1989).
12. POPESCU-MARINESCU VIRGINIA. Structura zoocenozelor din Dunare, în sectorul românesc, in perioada 1971–1986, Hidrobiologia 20, 111–134, Bucureşti (1992).
13. B. RUSSEV, VICTORIA CURE, VIRGINIA POPESCU-MARINESCU, Die Veränderungen der Strömungsgeschwindigkeit und ihre Auswirkungen auf die Plankton und Benthosbiozönosen der Donau, Hidrobiologia, **17**, 93–148, Bucureşti (1983).

Received July 26, 2000.

National Institute for Biological Sciences,
296, Splaiul Independenţei, Bucharest

NEW THRIPS SPECIES (CL. INSECTA: ORD. THYSANOPTERA) FOR THE FAUNA OF SWEDEN

LILIANA VASILIU-OROMULU[1], RICHARD ZUR STRASSEN[2], HANS LARSSON[3]

The work presents 12 new thrips species for the fauna of Sweden: *Aeolothrips astutus* Priesner, 1926, *Aeolothrips propinquus* Bagnall, 1924, *Aptinothrips elegans* Priesner, 1924, *Iridothrips iridis* (Wat., 1924), *Rhaphidothrips longistylosus* Uzel, 1895, *Sericothrips bicornis* Karny, 1910, *Scolothrips uzeli* (Schille, 1910), *Haplothrips angusticornis* Priesner, 1921, *Haplothrips alpester* Priesner, 1914, *Haplothrips setiger* Priesner, 1921, *Haplothrips statices* (Haliday, 1836) and *Phlaeothrips bispinosus* Priesner, 1919.

Key words: Thysanoptera, new species, Sweden.

1. INTRODUCTION

Thysanoptera are pterigote insects with reduced dimensions, from 0.5 to 1–2 mm in the temperate zones, to 15 mm in the tropical ones. They are distributed on all continents, from the sea level to the highest altitudes; the majority is phytophagous, some zoophagous representing, in their turn, the food for some invertebrates and vertebrates, too.

There are more than 5100 species in the world, in Sweden are published 109 species.

2. MATERIALS AND METHODS

The insects were collected in different places of Sweden: in Löddösness (Sk), a natural reservation, on *Iris pseudacorus*'s leaves, on *Juniperus* sp. in Miles Garden in Stockholm.

The thrips were sampled by the shaking method, some from different plants, some from the branches of *Juniperus*, or directly between the *Iris*'s leaves, and all preserved in AGA solution. The slides can be found in Sweden, in Stockholm, Lund Museum's collections and Alnarp, in Romania, Institute of Biology's collections, in Bucharest and in Germany, in Senckenberg Museum's collection, Frankfurt am Main.

REV. ROUM. BIOL. – BIOL. ANIM., TOME 45, N° 2, P. 125–135, BUCAREST, 2000

3. RESULTS AND DISCUSSIONS

New records are represented by:

Aeolothrips astutus Priesner, 1926

Thysanop. Europas (1926/28): 109; Titschack: Verh. Ver. naturw. Heimatf. Hamburg **34** (1960): 62–74; Titschack: ebenda **36** (1964): 61–65; Jacot-Guillarmod (1970): 105–106.

The species belongs to the: S/Order Terebrantia, Haliday, 1836, Family Aeolothripidae, Uzel, 1895, S/Family Aeolothripinae, Bagnall, 1913.

The genus Aeolothrips comprises about 85 species, most of which are found in the holarctic region. The species have black and white banded forewings. The larvae are creamy yellow to white and they are at least partially predaceous in some species. When mature, the larvae spin a silken cocoon in the soil or leaf litter. *A. fasciatus* L. is regarded, after Mound, 1976, as a nomen dubium and regarded as *A. intermedius* but there have been good criteria to differentiate these two species lately.

Location of type: Simontornya
Find: Hungary
Habitat: *Anchusa officinalis, Echium vulgare*
Distribution: European
Key to species: Body dark brown, forewings with 2 dark transversal bands (Fig.1), antennal segments, exception the apex of II and ¾ of yellow III, brown, *Aeolothrips astutus* is a polyphagous, floricolous, and xerophilous species.

In Sweden: leg Qvick, from *Anchusa officinalis*, 3.07.1977, 1 female, Eskilstuna /Söndermanland/ det. R. zur Strassen (SMF T 14754).

Aeolothrips propinquus Bagnall, 1924

Entomologist's mon. Mag. **60** (1924): 269; Titschack: Verh. Ver. naturw. Heimatf. Hamburg **34** (1960): 62–74; Titschack: ebenda **36** (1964): 61–65; Jacot-Guillarmod (1970): 149–150.

The species belongs to the: S/Order Terebrantia, Haliday, 1836, Family Aeolothripidae, Uzel, 1895, S/Family Aeolothripinae, Bagnall, 1913.

Location of type: Woldingham

New thrips species for the fauna of Sweden

Find: England
Habitat: Verbascum, Onobrychis, Echium
Distribution: European
Key to species: Head and thorax uniformly dark brown, ring vein around apex of forewing darker than the membrane it surrounds; sensorium on each of antennal segments III and IV more than 0.5 times as long as the corresponding

segment; accessory setae on sternite VII of female closer to the posterior margin of the sternite than their length (after Mound) (Fig. 2).

Aeolothrips propinquus is a polyphagous, floricolous, mesophilous species.

In Sweden: leg Qvick, from *Anchusa officinalis*, 3.07.1977, 1 female, Eskilstuna /Söndermanland/ det. R. zur Strassen (SMF T 14754).

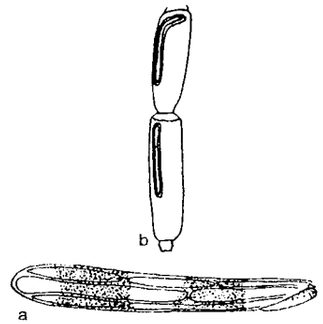

Fig. 1 – *Aeolothrips astutus* a – forewing b – antennal segments (after Titschack in Schliephake).

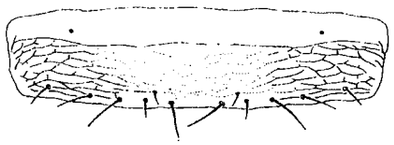

Fig. 2 – *Aeolothrips propinquus* female sterniteVII (after Mound).

Aptinothrips elegans Priesner, 1924[Fig. 28 after Mound, pg. 21; fig. 53, pg. 136 Schliephacke]

Sitz.-Ber. Akad. Wien **133** (1924):528; Priesner (1926/28): 161; Jacot-Guillarmond (1974): 593–596.

The species belongs to the: S/Order Terebrantia, Haliday, 1836, Family Thripidae, Haliday, 1836, S/Family Thripinae, (Stephens) Karny, 1921, Tribus Thripini, Priesner, 1949, S/Tribus Aptinohripina, Karny, 1921.

Location of type: Simontornya
Find: Hungary
Habitat: *Lathyrus tuberosus*
Distribution: Ponto-mediterranean

All three species of the genus Aptinothrips are apterous, feed and breed within the leaf sheaths of grasses.

Key to species: Lateral pair of posteromarginal setae on sternites III – VI of both sexes arising in font of margin; posteromedian setae and pores of tergite IX of female nearer posterior margin than lateral setae; tergites II – VIII with 0 – 4 discal setae; base of antennal segment II usually broad and flat (Fig. 3) (after Mound).

Aptinothrips elegans is a polyphagous, thermophilous, xerophilous, graminicolous species.

In Sweden: leg. Qvick, from *Alopecurus pratensis*, 27.05.1979, 3 female Husby-Rekarne/ Södermanland/, det. R. zur Strassen (SMF T 14797).

Fig. 3 – *Aptinothrips elegans* antennal segments I – II (after Mound).

Iridothrips iridis (Watson, 1924)

Entomologist's mon. Mag (1924): 253 (*Bregmatothrips iridis*) Priesner (1926/28): 267–269; Stannard (1968): 320–321; Prisner (1964): 65; Jacot-Guillarmod (1974): 838–839.

The species belongs to the: S/Order Terebrantia, Haliday, 1836, Family Thripidae, Haliday, 1836, S/Family Thripinae, (Stephens) Karny, 1921, Tribus Thripini, Priesner, 1949, S/Tribus Thripina, Priesner, 1957.

Location of type: unknown
Find: the Netherlands, Bassenheim
Habitat: *Iris pseudacorus*
Distribution: European

Key to species (Mound, 1976): female usually micropterous; males always micropterous; metanotum with equangular reticulations, median setae less than half as long as metanotum (Fig. 4): unusually large; brown species with antennal segments III and IV as well as fore tibiae, yellow.

We have found only micropterous females and males, in a great number, on *Iris pseudacorus*.

Iridothrips iridis is an oligophagous, folicolous, hygrophilous species, in leaf funnels of different *Iris* sp.

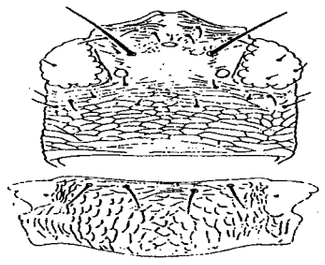

Fig. 4 – *Iridothrips iridis* head and metanotum (after Mound).

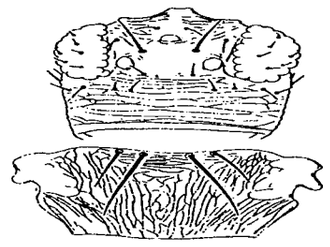

Fig. 5 – *Frankliniella tenuicornis* head and metanotum (after Mound).

In Löddösness reservation, in the poximity of *Iris pseudacorus* it was a population of *Acorus calamus*, a hygrophilous plant, which was inhabited by the species *Frankliniella tenuicornis* (Fig. 5), a graminicolous thrips, anemochorous distributed from the crops area, so not at all by *Iridothrips iridis* which is specific only for Leg. L. Vasiliu-Oromulu and H. Larsson, det. L. Vasiliu-Oromulu, 1998.

Rhaphidothrips longistylosus Uzel, 1895

Monog. Ord. Thysanoptera (1895): 131 (Typusart); Priesner (1926/28): 264–266; Jacot-Guillarmod (1974): 953–955.

The species belongs to the: S/Order Terebrantia, Haliday, 1836, Family Thripidae, Haliday, 1836, S/Family Thripinae, (Stephens) Karny, 1921, Tribus Thripini, Priesner, 1949, S/Tribus Thripina, Priesner, 1957.

Location of type: unknown
Find: Czechoslovakia
Habitat: Poaceae
Distribution: Holarctic

Key to species: Colour dark brown, tarsi and antennal segments III and IV yellow, antennal segments VII and VIII very long, (Fig. 6) head with 1 pair of long ocellar setae and postocular setae (Fig. 7); tergites without ctenidia laterally, but VIII with posteromarginal comb of microtrichia; wings variable in length.

Rhaphidothrips longistylosus is a polyphagous, hygrophilous, graminicolous species.

Leg. L. Cederholm on *Orchis maculata*, Kullaberg (Sk) in 10. 06. 1954, det. L. Cederholm, slide in Stockholm Museum's collection, verified by L. Vasiliu-Oromulu.

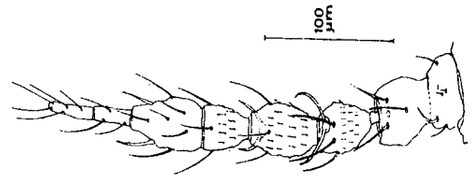

Fig. 6 – *Rhaphidothrips longistylosus* antenna (after Schliephake).

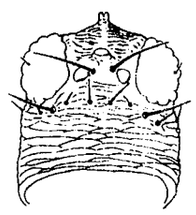

Fig. 7 – *Rhaphidothrips longistylosus* head (after Mound).

Sericothrips bicornis Karny, 1910

Mitt. Nat. Ver. Univ. Wien **7** (1909): 270 (*Euthrips abnormis*); Priesner (1926/28): 166 (*Sericothrips staphylinus* var. *bicornis*); Jacot-Guilarmod (1971): 363–367.

The species belongs to the: S/Order Terebrantia, Haliday, 1836, Family Thripidae, Haliday, 1836, S/Family Thripinae, (Stephens) Karny, 1921, Tribus Thripini, Priesner, 1949, S/Tribus Thripina, Priesner, 1957.

Location of type: Hainburg, 13.06.1909
Find: Austria
Habitat: Fabaceae
Distribution: European

Sericothrips is a large genus with species in most parts of the world. Many species have the median part of the posterior two-thirds of the pronotum defined by prominent dark apodeme (after Mound).

Key to species: Antennal segments I, II yellow, IV – VIII brown (Fig. 8), body dark brown, femora brown at apex yellow, tibia brownish yellow, tarsus yellow.

Sericothrips bicornis is a polyphagous, floricolous, mesophilous species.

In Sweden: from *Lotus corniculatus,* 6.06.1979, 2 females, Ärea/ Söndermanland/ det. R. zur Strassen (SMF T 14818).

Scolothrips uzeli (Schille, 1910)

Akad. Wiss. Krakau 14 Sep. (1910): 5; (*Chaetothrips uzeli*); Priesner 1926 (28): 241–242; Jacot-Guillarmond (1974): 966.

The species belongs to the: S/Order Terebrantia, Haliday, 1836, Family Thripidae, Haliday, 1836, S/Family Thripinae, (Stephens) Karny, 1921, Tribus Thripini, Priesner, 1949, S/Tribus Thripina, Priesner, 1957.

Location of type: unknown.
Find: the Netherlands
Habitat: *Juniperus communis*
Distribution: European.

There are more than 12 species in sub-tropical regions, and probably predators on red spider mites (Eotetranychus sp.) (Mound, 1976).

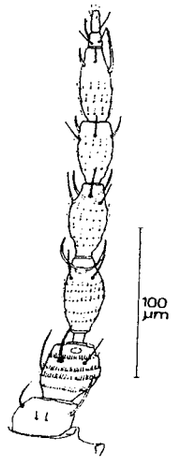

Fig. 8 – *Sericothrips bicornis* antenna (after Schliephake).

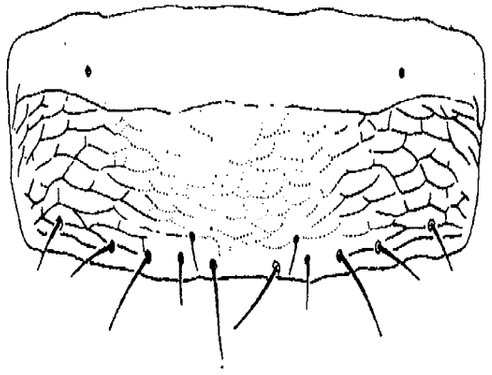

Fig. 9 – *Scolothrips uzeli* pronotum (after Schliephake).

Key to species: pronotum with 12 long setae, each at least half as long as median length of the pronotum (Fig. 9); forewing pale with 2 narrow dark cross bands, setae on veins about twice as long as median width of wing.

8 antennal segments, 3 articles maxillary palps, meso- and metasternum with spinula, the VIII abdominal tergite without microtrichia.

It is a small species, body color yellow, antennal segments I – VIII from hyaline to grey, ocelli pigment red till brown grey. The setae very light; the III and IV antennal articles forked, female macroapterous, male apterous (Schliephake, 1979) porose glandular area on sternite III – VIII.

Scolothrips uzeli is a monophagous, folicolous, floricolous, mesophilous and predaceous species.

In Sweden: leg. L.Vasiliu-Oromulu on *Juniperus communis* in Miles Garden, in Stockholm; det. L.Vasiliu-Oromulu.

Haplothrips alpester Priesner, 1914

Ent. Z. Frankfurt, **27**, 45 (1914) (*Haplothrips distinguendus* var. *alpestris*); Priesner (1926/28):580

The species belong to: S/Ord. Tubulifera, Haliday, 1836, Fam. Phlaeothripidae, Uzel, 1895, S/Fam. Phlaeothripinae, Priesner, 1928, Tribus Haplothripini, Priesner, 1928, S/Tribus Haplothripina, Priesner, 1928.

Location of type: Bruch, 1.06.1913
Find: Austria
Habitat: Asteraceae
Distribution: European

The 12 species of Haplothrips found in Sweden are usually easily recognized by the presence of a well-developed maxillary bridge and constricted forewings.

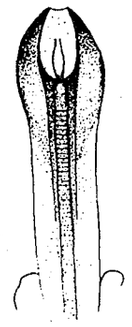

Fig. 10 – *Haplothrips alpester* aedeagus.

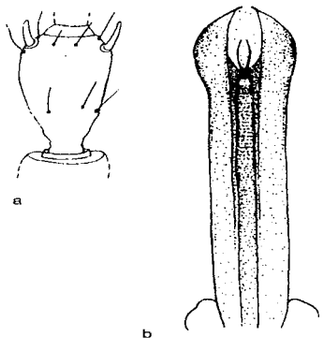

Fig. 11 – *Haplothrips angusticornis* a-antennal segment III, b-aedeagus (after Schliephake).

Key to species: Antennal segment III symmetrical dark yellow at base, light brown at apex; forewings with 7–13 (11) duplicated cilia, male genitalia with a lanceolate aedeagus (Fig. 10) (after Schliephake).

Haplothrips alpester is a polyphagous, floricolous, mesophilous specis.

In Sweden: leg. L. Cederholm on *Matricaria inodora*, Kullaberg (Sk) 13.07.1957, det. L. Cederholm, the slides are in Lund Museum's collection, verified by L. Vasiliu-Oromulu.

Haplothrips angusticornis Priesner, 1921

Treubia **2**, 1 (1921): 12 (*Haplothrips trifolii* var. *angusticornis*); Priesner (1926/28): 617.

The species belongs to the: S/Ord. Tubulifera, Haliday, 1836, Fam. Phlaeothripidae, Uzel, 1895, S/Fam. Phlaeothripinae, Priesner, 1928, Tribus Haplothripini, Priesner, 1928, S/Tribus Haplothripina, Priesner, 1928.

Location of type: Linz, 8.07.1920
Find: Austria
Habitat: Asteraceae (Achillea , Anthemis, Matricaria).
Distribution: West Palearctic

Key to species: Antennal segments I and II brown, III brownish yellow, with 2 sens cones (Fig. 11 a) forewings, with 4–10 (7) duplicated cilia; male genitalia with aedeagus with lanceolate apex (Fig. 11 b) (after Schliephake).

Haplothrips angusticornis is a polyphagous, floricolous, mesophilous species.

In Sweden: leg. L. Cederholm on *Matricaria inodora*, Kullaberg (Sk) 13.07.1957, det. L. Cederholm, the slides are in Lund Museum's collection, verified by L. Vasiliu-Oromulu.

Haplothrips setiger Priesner, 1921

Treubia **2**, 1 (1921): 11; Priesner (1926/28): 588; Priesner: Stett. Ent. Ztg. **94**, 2 (1933): 210; Mound (1968): 117.

The species belongs to: S/Ord. Tubulifera, Haliday, 1836, Fam. Phlaeothripidae, Uzel, 1895, S/Fam. Phlaeothripinae, Priesner, 1928, Tribus Haplothripini, Priesner, 1928, S/Tribus Haplothripina, Priesner, 1928.

Location of type: Wegscheid, 8.07.1920
Find: Austria
Habitat: Flowers
Distribution: West Palearctic

Key to species: Distal cilia of forewing distinctly barbed (Fig. 12); male genitalia with aedeagus slightly constricted medially (Fig. 13); all pronotal setae minute except epimerals (after Mound).

It is a polyphagous, floricolous, mesophilous species.

In Sweden: in Sk, 2 female, det. Liliana Vasiliu-Oromulu.

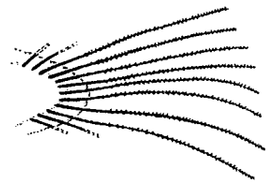

Fig. 12 – *Haplothrips setiger* forewing apex (after Mound).

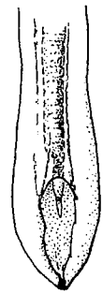

Fig. 13 – *Haplothrips setiger* aedeagus (after Mound).

Haplothrips statices (Haliday, 1836)

Ent. Mag. **3** (1836): 442 (*Phloeothrips statices*); Priesner (1926/28): 579; Karny: Trud. Poltava 6 (1913): 8.

The species belongs to the: S/Ord. Tubulifera, Haliday, 1836, Fam. Phlaeothripidae, Uzel, 1895, S/Fam. Phlaeothripinae, Priesner, 1928, Tribus Haplothripini, Priesner, 1928, S/Tribus Haplothripina, Priesner, 1928.

Location of type: unknown
Find: unknown
Habitat: Armeria species
Distribution: European

Key to species: postocular setae (Fig. 14) usually little more than 0.5 times as long as antennal segments III; forewing usually pale brown; male genitalia with aedeagus lanceolate (Fig. 15) (after Mound).

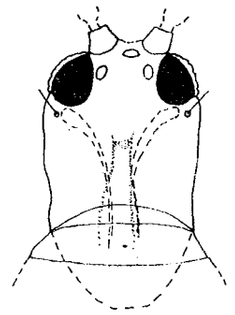

Fig. 14 – *Haplothrips statices* head (after Schliephake).

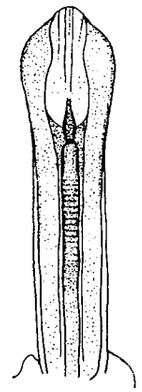

Fig. 15 – *Haplothrips statices* aedeagus (after Schliephake).

It is a polyphagous, floricolous species.

In Sweden: in Sk, Up, 2 female, det. Liliana Vasiliu-Oromulu

Phlaeothrips bispinosus Priesner, 1919

Sitz.-Ber. Akad. Wien **128** (1919): 136; Priesner (1926/28): 656 .

The species belongs to: S/Ord. Tubulifera, Haliday, 1836, Fam. Phlaeothripidae, S/Fam. Phlaeothripinae, Priesner, 1928, Tribus Phlaeothripini, Priesner, 1928, S/Tribus Phlaeothripina, Priesner, 1960.

Location of type: Ruskuli, 1918
Find: Albanien
Habitat: on dead branches, airplankton
Distribution: West Palearctic + Mongolia

Genus Phlaeothrips are more than 20 nominal species in the world; they can be distinguished from Hoplandrothrips species by the parallel-sided wings, the broad pelta, the median dorsal setae on tergite IX of the female scarcely one-third as long as the tube and the absence of the male a tubercle on the fore femur and a glandular area on sternite VIII (after Mound).

Key to species: Lateral margins of head with few tubercles, antennal segment III less than 2.0 times as long as wide, brownish-yellow, weakly yellow near apex, pelta triangular, male genitalia with aedeagus in V-form, enlarged by spatula (Fig.16).

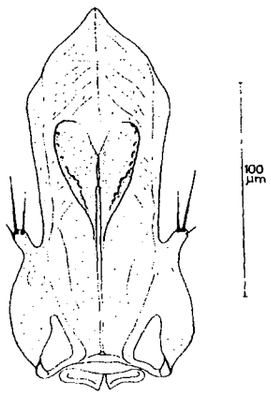

Fig. 16 – *Phlaeothrips annulipes* male genitalia (after Schliephake).

Phlaeothrips bispinosus is a polyphagous, arboricolous, corticolous, mycophagous species.

In Sweden: in Vr.

4. CONCLUSIONS

There are 12 thrips species new for the fauna of Sweden: *Aeolothrips astutus* Priesner, 1926, *A. propinquus* Bagnall, 1924, *Aptinothrips elegans* Priesner, 1924, *Iridothrips iridis* (Wat., 1924), *Rhaphidothrips longistylosus* Uzel, 1895, *Sericothrips bicornis* Karny, 1910, *Scolothrips uzeli* (Schille, 1910), *Haplothrips angusticornis* Priesner, 1921, *Haplothrips alpester* Priesner, 1914, ***Haplothrips setiger*** Priesner, 1921, ***Haplothrips statices*** (Haliday, 1836) and *Phlaeothrips bispinosus* Priesner, 1919.

REFERENCES

JACOT-GUILLARMOD C.F., 1970–1979–1986, *Catalogue of the Thysanoptera of the World Ann., Cape Prov.Mus.(Nat.Hist.),* Albany Museum, **7** p. 1, 1–216; p. 2/1971, 217–515; p. 3/1974, 516–976; p. 4/1975, 977–1255; p. 5/1978, 1257–1556; p. 6/1979, 1557–1724; 17 p. 1/1986 1–93.

MALTBAEK J., FRYNSEVINGER (Thysanoptera). *Et Bidrag til Kundskaben om Haderslev Katedralskoles Aarsskrift* (1927), 2 (1928).

MORISON G.D., Thysanoptera of the London area, Lond. Nat. Suppl., **26,** 1–36; **27,** 37–75; **28,** 76–131, (1947–49).

MOULTON D., *Thysanoptera – new species and notes.* Bull. Brooklyn Entom. Soc., **22**(4), 181–201 (1927).

MOUND L.A., MORISON D.G., PITKIN R.B., PALMER J.M., *Thysanoptera*, Royal Ent.Soc.London, **I** (II): 1–79 (1976).

PRIESNER H., *Die Thysanopteren Europas*, Wagner-Verlag, Wien, 1–755, 1926.

PRIESNER H., *Ordnung Thysanoptera.* Bestimmungsbücher zur Bodenfauna Europas, **2,** 1–242 (1964).

QVICK U., New records and notes on the Swedish Thrips Fauna (Thysanoptera). Ent. Tidskr., **98**, 127–131 (1977).

SCHLIEPHAKE G., KLIMT, K., , *Thysanoptera*, Fransenflügler VEB Gustav Fisch. Ver., Jena, 1–477 (1979).

STANNARD L.J., The Thrips, or Thysanoptera of Illinois, Bull. Ill.. St. Nat. Hist. Surv., **29**, 215–552 (1968).

STRASSEN R. ZUR, On some rare fungivorous phlaeothripid Thysanoptera (Insecta) from Germany and Sweden. Proceed. Work Thys. Beijing, China, and Sym. Thys. Halle, Germany, 1992, CFS **178,** 115–119 (1994).

WATSON J.R., A new Bregmatothrips (Thysanoptera) from England and Holland. Entom. Monthly Magaz., **40**, 253–254, (1924).

Received September 1, 2000.

[1] *Institute of Biology, Spl. Independenţei 296, PoBox 56–53, Bucharest – 79651, Romania*

[2] *Forschungsinstitut Senckenberg, Senckenberganlage 25, D- 60325 Frankfurt am Main, Germany*

[3] *Dept. Pl. Forest Prot. Alnarp, Po Box 44, 23053 – Sweden*

ZOOPLANKTON OF THE DANUBE DELTA LACUSTRIAN ECOSYSTEMS 2. DYNAMICS OF STRUCTURE, PRODUCTIVITY AND BIOMASS RECYCLATION

VICTOR ZINEVICI, LAURA PARPALĂ

The interannual and intraannual spatial dynamics of taxonomic structure, numerical abundance, biomass, productivity and turnover of zooplankton from the Danube Delta ecosystems are analysed. The study was done in 12 ecosystems representative for the mentioned area, on 20 years period. The Danube Delta ecosystems are situated in different stages of ecological succession. This fact and the hydrological regimes of various kind, due to the localization in the net of shallows, channels and river branches, determined significant spatial changes of taxonomic structure, numerical abundance, biomass, productivity and turnover of the zooplankton. The natural variations of hydrological and thermal regimes, as well as those of ecosystem trophic stage, caused by the anthropic factor, significantly influenced the interannual and intraannual evolution of the mentioned ecological parameters of zooplankton communities which characterise the Danube Delta lacustrian ecosystems.

1. INTRODUCTION

The analysis of structure, productivity and turnover of zooplankton from the Danube Delta lacustrian ecosystems evidenced large spatial or temporal variations. These are the result of the cumulative effect of natural and anthropic factors. Among the causes of the mentioned variations are the following:

– the ecosystems are in different stages of ecological succession;

– hydrological regime differences (for example intensity and duration of water masses flow) owing to the lake location in the net of shallows, channels and river branches;

– the interannual and intraannual changes of river flow, thermal regime, pollutant and nutrient concentrations, that directly affected the structure and productivity of the primary producer types.

2. MATERIAL AND METHODS

The zooplankton studies were carried out in 12 lacustrian ecosystems being in the first stage of ecological succession: Roşu, Roşuleţ, Porcu, Puiu, Uzlina, Isac, Iacub, Merhei, Matiţa, Babina, Bogdaproste and Băclăneşti, during 1975–1995 period. Among these, the lakes Roşu and Puiu are the youngest ones, characterised

REV. ROUM. BIOL. – BIOL. ANIM., TOME 45, N° 2, P. 137–149, BUCAREST, 2000

by large surfaces, most favourable hydrological conditions, the biggest depths and the lowest values of the shoreline development. The Porcu, Băclăneşti, Merhei and Uzlina lakes are situated to another extreme, characterised by small surfaces (excluding Merhei lake), reduced depths, high values of the shoreline development and a slow flow of water masses. Some of these (for example Porcu Lake) could belong to the second stage of succession after other criteria.

The sampling was performed monthly (from March to November) with Patalas-Schindler sampler. 50 liters of water were filtered for each sample, through a 60 μm mesh net. The samples were collected in 3–5 stations of each ecosystem, from the entire water column, in each station.

The parameter calculations were referred to each species, taxonomic group, trophic level and also to total zooplankton. The literature gravimetric data with regard to species, sexes and sizes were used for the biomass calculation (expressed as μg wet weight/l). The productivity (μg wet weight/l/24 h) was assessed by the methods: Ilkowska-Stankzykowska (in the case of Lamellibranchia planktonic larvae), Galkowskaya (for Rotatoria), Winberg, Pechen and Sushkina (for Copepoda and Cladocera) (1). The biomass recyclation was determined using two coefficients: P_{24h}/B (daily turnover rate) and B/P_{24h} (daily recyclation time or biomass recyclation time).

3. RESULTS AND DISCUSSIONS

Spatial dynamics. The taxonomic diversity reflects to a great extent the variations of environmental heterogeneity, which, in turn, express the changes of submerged macrophytes/phytoplankton ratio. The absolute maximum value noted in an ecosystem within a vegetation period (189 taxons) (Iacub lake, in 1975) (Fig. 1), represented the effect of particularly high values of the two environmental parameters. The high taxonomic diversity of Roşu and Puiu lakes (164 taxons in 1975, respectively 142 in 1977) represented a convenient conjunction of a large lacustrian surface, abundant development of submerged macrophytes and optimum water circulation. A high value of taxonomic diversity presented Porcu lake (157 taxons in 1976), the smallest lake among the studied ones. The factors, which influenced the taxonomic diversity, were represented, in this case, by the abundance of submerged macrophytes and a good ratio between shoreline length and the lacustrian surface. Also a relative high value of the mentioned parameter was noted in the case of Merhei lake (145 taxons in 1980). Certainly, this value would be higher if favourising factors (large surface, optimum of the shoreline, high abundance of submerged macrophytes) were not counteracted by the

unfavourable water circulation. Generally, in the case of young ecosystems the eutrophication impact upon the taxonomic structure was stronger, more rapid and the recovery was late. In concordance with this dynamics, a pronounced taxonomic diminution was registered in Roşu lake, in 1983 year (69.51% related to the reference value, which is considered that of 1975 year). As for ecosystems being in advanced stages of ecological succession, the impact often had lesser intensity, appeared later and the recovery occurred more quickly. To this category belong Bogdaproste and Băclăneşti lakes.

Conversely, in Merhei lake, in wrong ecological conditions owing to the unfavourable water circulation, the reduction of the taxonomic spectrum was almost the same as that in Roşu lake (respectively 68.28% of initial value, of 1981 year). However, in Merhei lake, the maximum effect of the impact is evidenced not later than 1987–1989 period. In the conditions of this dynamics, the annual minimum values of the taxonomic spectrum belong to Merhei and Roşu lakes (46 and respectively 50 taxons) (1975–1989 period, respectively 1983) (2).

In the case of numerical (3) and gravimetrical (5) abundance or productivity (4) entirely different characteristics of the dynamics were noted. This is the consequence of the dependence of these ecological parameters on different factors. Thus, if in the case of taxonomic diversity was noticed an important role of environment heterogeneity, whose ascendant dynamics depends on the submerged macrophyte abundance increase, as for other parameters the phytoplankton abundance was the determinant factor.

The spatial dynamics of numerical abundance showed the absolute maximum value in Matiţa lake (2470 ind/l) (in 1981 year) (Fig. 2). In the case of biomass and productivity the absolute maximum value occurred in Isac lake (313888 μg/l, respectively 4451 μg wet weight/l/24h) (in 1983 year) (Figs. 3,4). High values of numerical abundance were registered also in Babina lake (2193 ind/l) (in 1986 year), Merhei lake (2181 ind/l) (in 1992 year) and Isac lake (1991 ind/l) (in 1983 year). In the case of biomass and productivity high values were noticed in Babina lake too (19568 μg wet weight/l, respectively 1905 μg wet weight/l/24h) (in 1986 year) and in Roşu lake (16481 μg/l, respectively 1727 μg/l&24h) (in 1989 year). The minimum values of the numerical abundance were evidenced in Porcu and Băclăneşti lakes (60 ind./l) (in 1978, respectively 1986 year), as well as in Roşu lake (61 ind./l) (in 1975 year). As regards biomass and productivity the lowest values occurred in Băclăneşti lake (194 μg/l, respectively 15 μg wet weight/l/24h) (in 1984 year), in Roşu lake (201 μg/l, respectively 18 μg wet weight/l/24h) (in 1975 year) and in Puiu lake (272 μg/l, respectively 24 μg wet weight/l/24h) (in 1978 year).

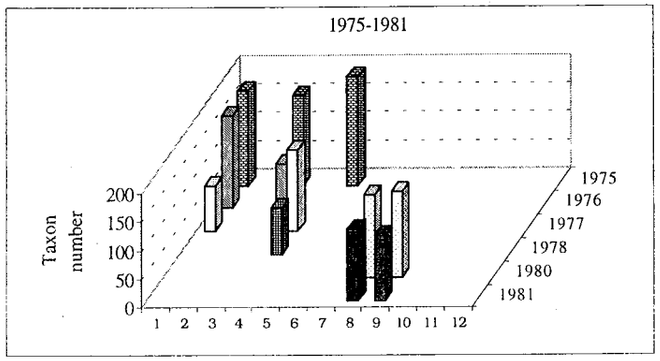

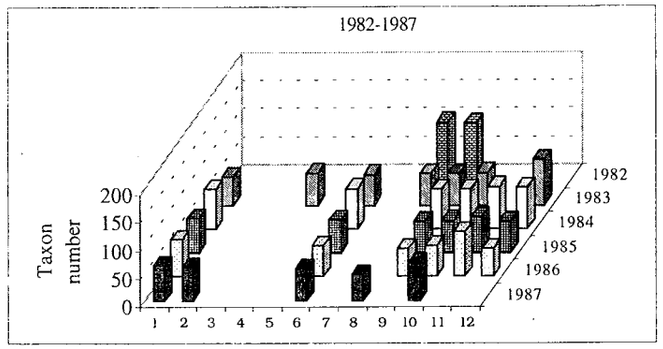

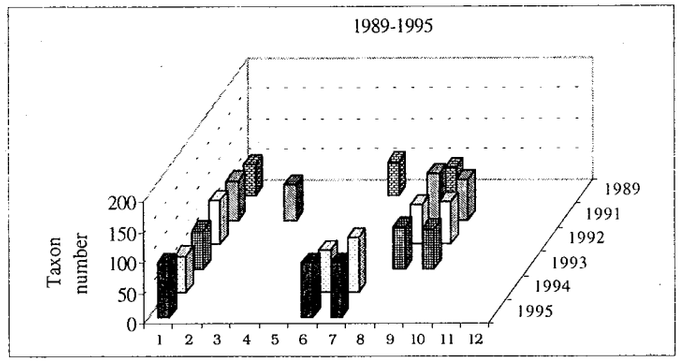

1 = L. Roşu; 2 = L. Roşuleţ; 3 = L. Porcu; 4 = L. Puiu; 5 = L. Iacub; 6 = L. Isac; 7 = L. Uzlina; 8 = L. Merhei; 9 = L. Matiţa; 10 = L. Babina; 11 = L. Bogdaproste; 12 = L. Băclăneşti

Fig. 1 – The spatial and temporal dynamics of the annual averages of lacustrian zooplankton taxonomic diversity (1975–1995 period).

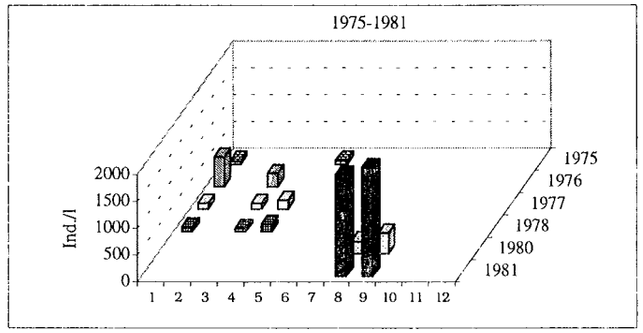

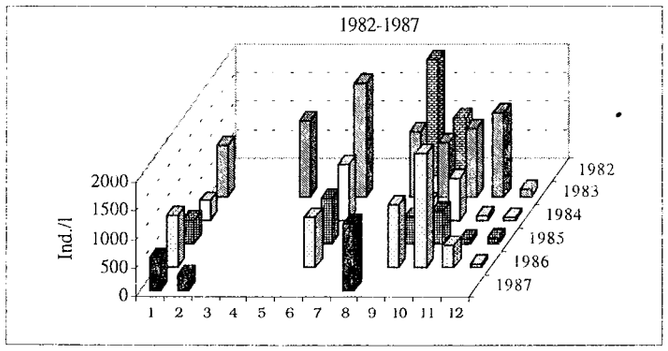

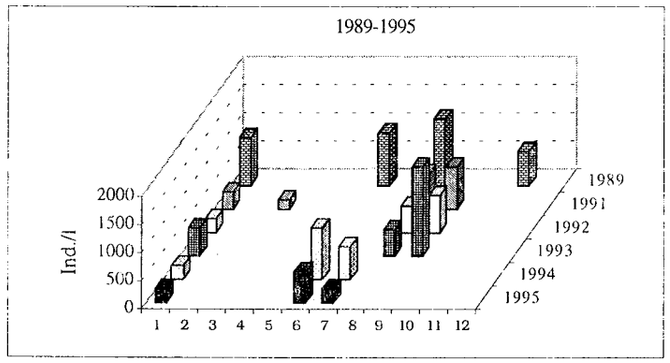

1 = L. Roşu; 2 = L. Roşuleţ; 3 = L. Porcu; 4 = L. Puiu; 5 = L. Iacub; 6 = L. Isac; 7 = L. Uzlina; 8 = L. Merhei; 9 = L. Matiţa; 10 = L. Babina; 11 = L. Bogdaproste; 12 = L. Băclăneşti

Fig. 2 – The spatial and temporal dynamics of the annual averages of lacustrian zooplankton numerical density (1975–1995 period).

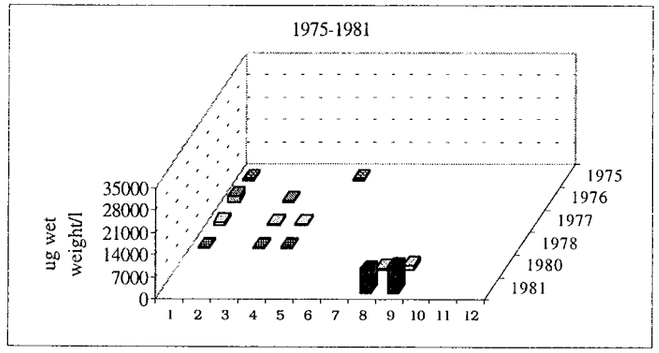

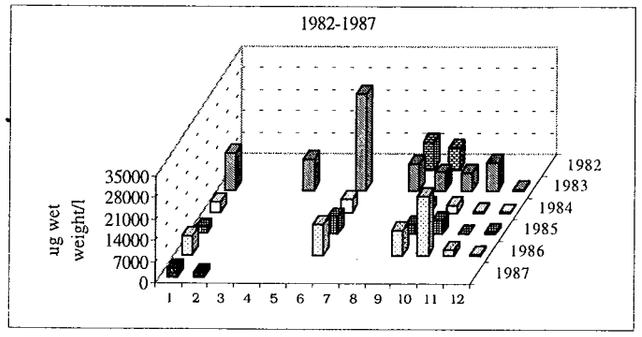

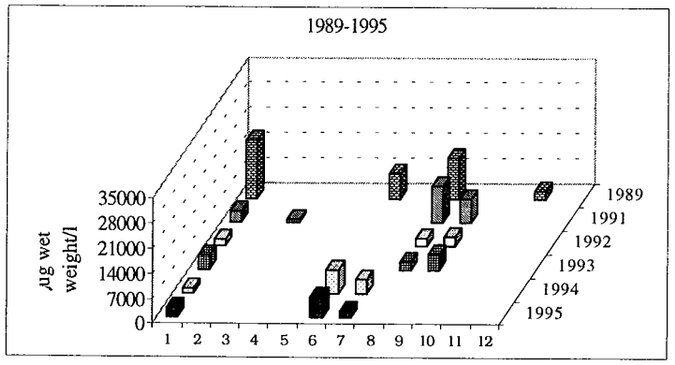

1 = Roşu; 2 = Roşuleţ; 3 = Porcu; 4 = Puiu; 5 = Iacub; 6 = Isac; 7 = Uzlina; 8 = Merhei; 9 = Matiţa; 10 = Babina; 11 = Bogdaproste; 12 = Băclăneşti

Fig. 3 – The spatial and temporal dynamics of the annual averages of lacustrian zooplankton biomass (µg wet weight/l) (1975–1995 period).

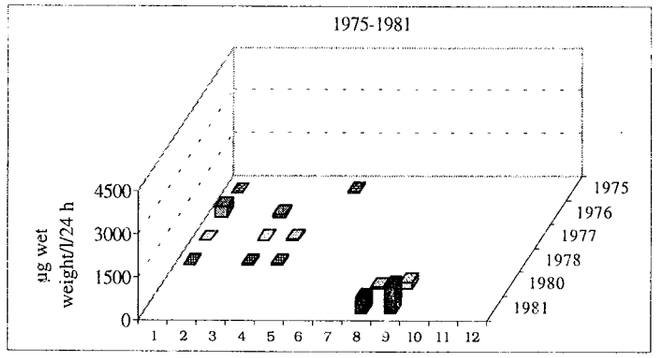

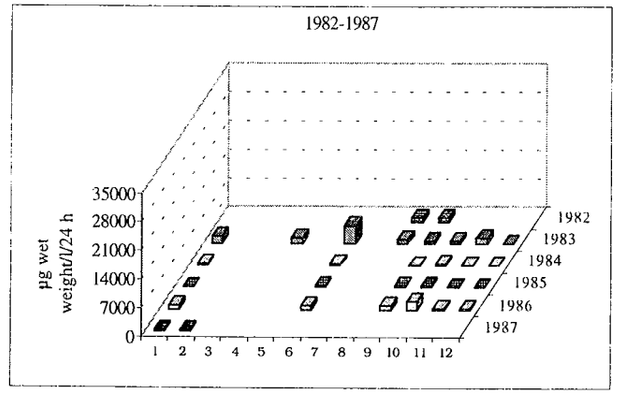

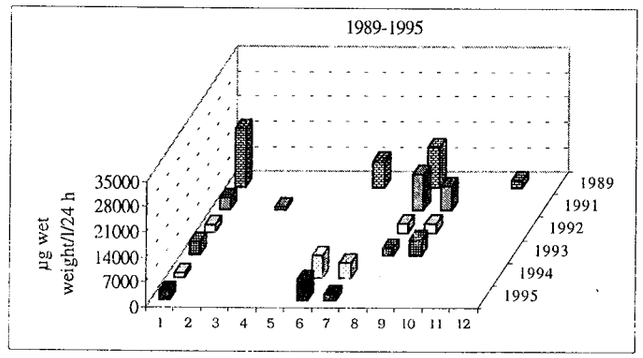

1 = L. Roşu; 2 = L. Roşuleţ; 3 = L. Porcu; 4 = L. Puiu; 5 = L. Iacub; 6 = L. Isac; 7 = L. Uzlina; 8 = L. Merhei; 9 = L. Matiţa; 10 = L. Babina; 11 = L. Bogdaproste; 12 = L. Băclăneşti

Fig. 4 – The spatial and temporal dynamics of the annual averages of lacustrian zooplankton productivity (µg wet weight/l/24h) (1975–1995 period).

Interannual dynamics. The interannual dynamics reflects especially three factors among those which determine structural and functional variations of the zooplankton communities of lacustrian ecosystems: Danube hydrological regime variations; thermal regime changes; eutrophication process ones.

The dynamics of the annual taxonomic diversity averages/ecosystem showed very high values in ecosystems when ecological equilibrium was uninfluenced intensely by anthropic factors (1975–1980), the absolute maximum value being in 1975 (176 taxons/ecosystem) (Fig. 5).

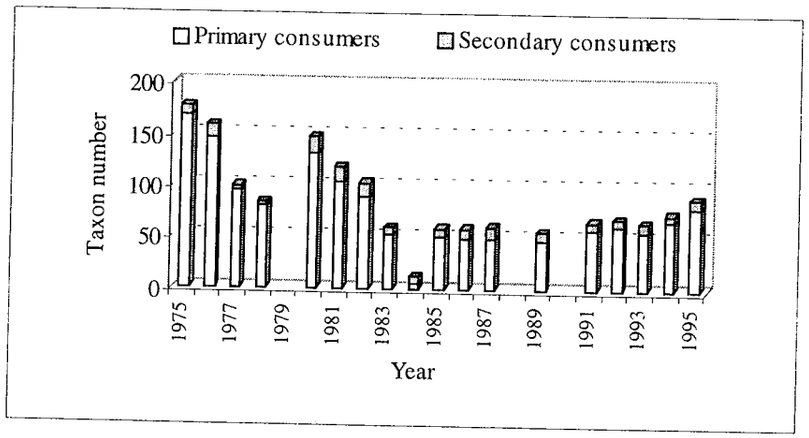

Fig. 5 – The annual average dynamics (1975–1995 period) of lacustrian zooplankton taxonomic diversity related to ecosystem (taxon number/ecosystem).

A marked reduction of annual averages was noted in the period of maximum eutrophication (1981–1990), with an absolute minimum value in 1989 year (55 taxons/ ecosystem). This dropped to 31.44% from 1975 value. A slight recovery tendency of taxonomic diversity was observed in 1991–1995 period. The value registered in 1995 (89 taxons/ecosystem) represents only 50.59% of the mentioned reference value (2). The calculation of 5 years period averages excluded the unsignificant variations, resulting a clearer image of temporal dynamics. These data regarding the taxonomic diversity in 1975-1995 period are the followings: 133 → 82 → 58 → 73 taxons/ecosystem.

The interannual dynamics of the numerical abundance showed other characteristics comparatively to taxonomic diversity since, usually, an inverse correlation exists between the two parameters. Thus, the dynamics of the annual averages of the numerical abundance evidenced reduced values in the period before eutrophication (1975–1980) with an absolute minimum value in 1975 year (66 ind/l) (Fig. 6). A gradual increase of them was observed in 1981–1985 period, an absolute maximum value, respectively a 32.8 times increase, being in 1981

(2164 ind/l). A slight decrease tendency was evidenced in 1986–1990 period, which was enhanced in 1991–1995. However, the minimum value of descendant period, corresponding to 1995 year, was 5.8 times greater than that of the reference year (1975). In spite of more dispersed annual averages as compared to taxonomic diversity, the temporal evolution of numerical abundance is clearly seen in the succession of the averages calculated on 5 years periods: 225 → 1145 → 740 → 534 ind/l.

The interannual dynamics of the biomass and productivity (5), (4) was directly correlated to the numerical abundance temporal evolution, all of them being caused by similar factors. Though, some distinctions can be evidenced, due to the later reaction of the biomass and productivity to the changes produced by the ascendant dynamics of the trophic level. In these cases too, the averages calculated in the period before eutrophication were low and the absolute minimum values of the two parameters (257 µg/l, respectively 27.5 µg/l/24 h) occurred in 1975 (Figs. 7, 8). Ten years later, very high averages alternate to low ones. The absolute maximum values of this period (10 622 µg/l, respectively 52.2 µg/l/24 h) surpassed 41.3 and respectively 52.2 times the values of 1975 year. They appeared in 1983, the third year of impact, while the numerical abundance in the first one (1981). The 1991–1995 period is characterized by a decreasing tendency of the two parameter values, but not as low as those registered in 1975-1980 period. The minimum values of the last period (2262 µg/l, respectively 266.3 µg/l/24 h) surpass 8.8 times and respectively 9.7 times the reference ones of 1975 year. Similarly to the case of absolute maximum values, the numerical abundance minimum value (recorded in 1995), of 1991–1995 period, does not correspond in time to biomass (1992) or productivity (1994) minimum values.

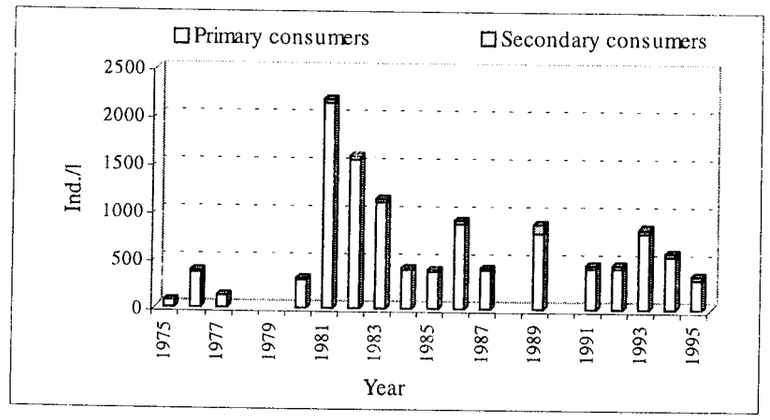

Fig. 6 – The annual average dynamics (1975–1995 period) of lacustrian zooplankton numerical density (exemplar number/l).

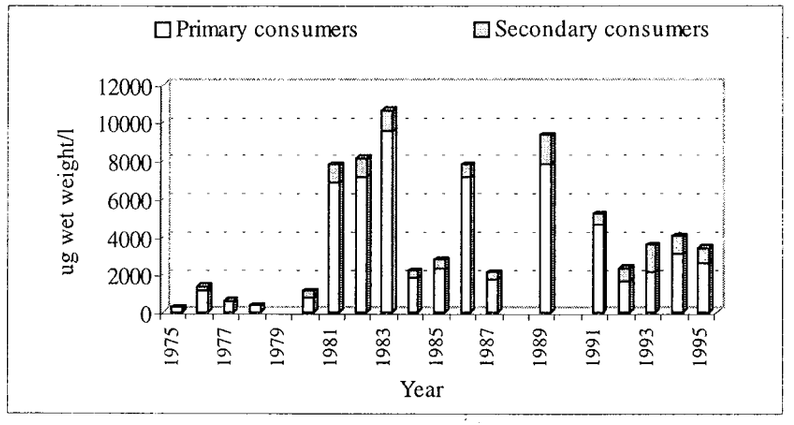

Fig. 7 – The annual average dynamics (1975–1995 period) of lacustrian zooplankton biomass (μg wet weight/l).

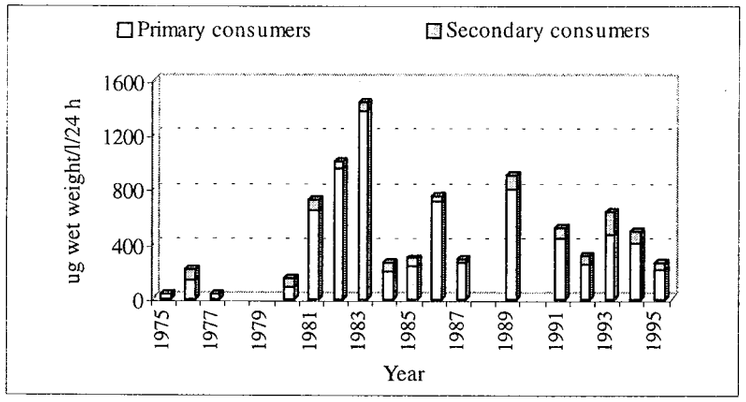

Fig. 8 – The annual average dynamics (1975–1995 period) of lacustrian zooplankton productivity (μg wet weight/l/24h).

The biomass and productivity annual averages are characterized by a quite great dispersion, as the numerical abundance, which is avoided by average calculation on 5 years periods. Thus, we obtain the following: 736 → 6299 → 6389 → 3678 μg/l, respectively 107.1 → 744.3 → 644.1 → 444.8 μg/l/24 h. In the case of the

biomass, the maximum value appeared in 1986–1990 period, as to the numerical abundance and productivity, was recorded in 1981–1985 period.

Seasonal dynamics shows month to month variations of biological parameter values, during a year or a vegetation cycle (April to October). Of course, the temperature is the determinant factor of this dynamics.

Both in the case of numerical abundance, and biomass or productivity, the minimum values within 10 months of study were evidenced in the coldest periods, situated at extremities of the cycle (March and December). But the examination of the most significant points of the dynamics during the vegetation cycle (April to October) evidences clear differences between the considered parameters. Thus, the numerical abundance dynamics showed a gradual increase from April to August, when the maximum value (1352 ind/l) was reached, and a decrease in September-October period (Fig. 9).

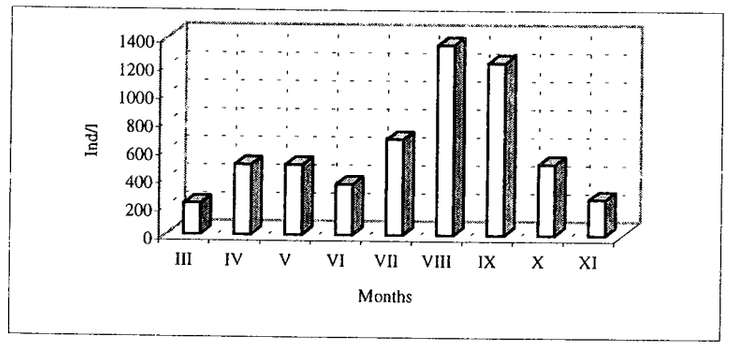

Fig. 9 – The monthly average dynamics of lacustrian zooplankton numerical density (exemplar number/l) in 1975–1995 period.

It should be noted in this case the discrepancy between the high values of August and September, against any other month of the vegetation cycle. Also, it is remarkable the decrease registered in June, in an ascendant tendency period.

The biomass and productivity seasonal dynamics showed more dispersed monthly data than those of the numerical density dynamics.

In the case of the biomass there were three maximum values in May, July and September (5225–5860–9286 μg/l) (Fig. 10), in concordance with the succession of populations important by the gravimetric point of view. As is seen, the September value represents the maximum value of the vegetation cycle, whereas the minimum one was registered in March (474 μg/l) (4).

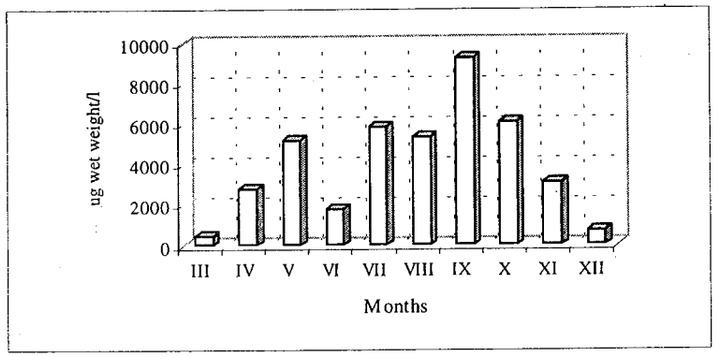

Fig. 10 – The monthly average dynamics of lacustrian zooplankton biomass (µg wet weight/l) in 1975–1995 period.

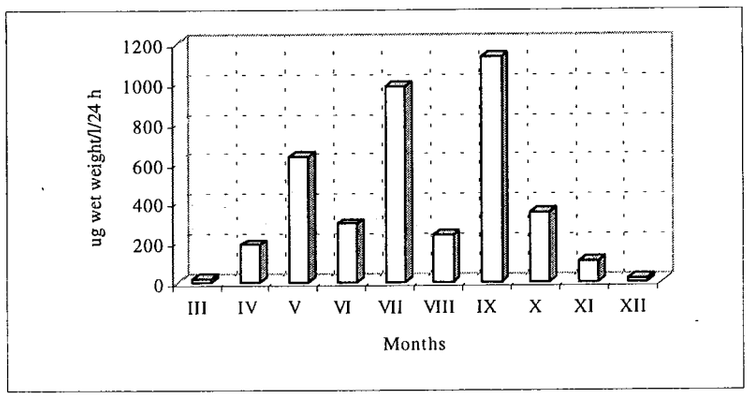

Fig. 11 – The monthly average dynamics of lacustrian zooplankton productivity (µg wet weight/l/24h) in 1975–1995 period.

The seasonal dynamics of productivity (5) presented three maximum values too, which were registered in May, July and September (627–983–1129 µg/l/24 h), the last one being the absolute maximum value of the whole seasonal cycle (Fig. 11). The minimum values (188–293–232 µg/l/24 h) were between the maximum ones, in April, June, and August respectively, the most pronounced being the first one.

4. CONCLUSIONS

– The Danube Delta lacustrian ecosystem state, in different stages of ecological succession and the existence of hydrological regimes of various kind,

due to the lake localization in the net of shallows, channels and river branches, determined significant spatial changes of taxonomic structure, numerical abundance, biomass, productivity and turnover of the zooplankton in the mentioned ecosystem type;

– The natural temporal variations of hydrological and thermal regimes, as well as those of ecosystem trophic stage, caused by the anthropic factor, significantly influenced the interannual and intraannual evolution of the mentioned ecological parameters of the zooplankton communities which characterize the Danube Delta lacustrian ecosystems.

REFERENCES

1. EDMONSON W.T., *A manual on methods for the assessment of secondary productivity in fresh waters*. I. B. P. Handbook 17, Oxford, 1971.
2. ZINEVICI V., TEODORESCU LAURA, *Dinamica structurii taxonomice a zooplanctonului lacurilor mari din Delta Dunării în perioada 1975–1995*. An. Şt. ale Inst. Delta Dunării, **5** (1), 63–75, Tulcea, 1996.
3. ZINEVICI V., PARPALĂ LAURA, *The dynamics of zooplankton numerical density in the great lakes Danube Delta (1975–1995 period)*. Proceedings of the Institute of Biology, 1, 53–66, Bucharest, 1997.
4. ZINEVICI V., TEODORESCU LAURA, *Dinamica productivităţii zooplanctonice în lacurile mari din Delta Dunării (perioada 1975–1995)*. An. Şt. ale Inst. Delta Dunării, 7, 439–451, Tulcea, 1999.
5. ZINEVICI V., PARPALĂ LAURA, *The zooplankton biomass dynamics in Danube Delta big lakes, 1975–1995 period*. Proceedings of the Institute of Biology, 2, 55–64, Bucharest, 1999.

Received July 24, 2000.

Institute of Biology
Spl. Independenţei nr. 296, P.O. Box 56–53,
Bucharest 79651, Romania

BIOMASS RECYCLATION TIME OF PLANKTONIC COPEPODS FROM LAKE ROŞU (THE DANUBE DELTA)

LAURA PARPALĂ, VICTOR ZINEVICI

The paper analyses the "turnover time" (B/P_{24h}) in some planktonic copepod dominant species from lake Roşu (the Danube Delta), in 1994–1996 period. It was concluded that "turnover time" increases from juvenile stages towards adult ones. The value of this coefficient is about 23 days in calanoids and 24 days in cyclopids. At last, 9 copepod generations succeed in Lake Roşu during a vegetation period.

1. INTRODUCTION

The biomass recyclation time ("turnover time") represents the average lifespan of a species, in determined conditions.

"Turnover time" (expressed in days) is evidenced by the B/P_{24h} coefficient (Winberg, 1971).

Numerous scientists, especially in the USA, determine this coefficient, which in fact, is the inverse of "turnover rate" (P_{24h}/B) coefficient, utilized in the determination of the biomass recyclation rate.

It is well known that a greater productivity depends on the biomass renewal rate (Botnariuc and Vădineanu, 1982). Thus, "turnover time", similarly to "turnover rate" of planktonic copepod, is an expression of their ecological role. The copepods support a specified number of consumers, thus providing for continuous renewal of the trophic base for those consumers. In another words, copepods contribute to trophic base renewal necessary to whole ecosystem function. Obviously, copepod gravimetric changes of structural or functional nature are reflected specifically in the dynamics of biomass recyclation process.

The authors concluded that the accelerated evolution of the Danube Delta lacustrian ecosystems was caused by the increase of the water nutrient quantities. It was materialized at the primary producer level through the replacing of submerged macrophytes by phytoplankton, and determined a tendency of increase of biomass recyclation rate at functional level (Zinevici and Teodorescu, 1991).

2. MATERIAL AND METHODS

Studies were carried out on several planktonic copepod species from Lake Roşu, in 1994–1996 period. It is not a random selection of these species. On the one side, their ecological importance (constance, numerical dominance, gravimetrical dominance, productivity dominance) was taken into account. On the

REV. ROUM. BIOL. – BIOL. ANIM., TOME 45, N° 2, P. 151–154, BUCAREST, 2000

other side, it was chosen a species in which all developmental stages, from embryo to adult, were observed. Further, it was intended that selected species belong to both trophic levels of planktonic consumers: filtrators (*Diaptomida*) and predators (*Cyclopida*). Thus, the selected species are the following: *Calanipeda aquae-dulcis*, *Eudiaptomus gracilis*, *Eurytemora velox*, *Heterocope caspia* among filtrators and *Acanthocyclops vernalis*, *Cyclops vicinus vicinus*, *Mesocyclops csrassus*, *M.leuckarti*, *M.oithonoides* among predators.

The B/P_{24h} coefficient (Winberg, 1971) was used to determine the biomass recyclation time.

3. RESULTS AND DISCUSSIONS

An increase of development stage duration was observed in planktonic copepods, as they develop from embryo to adult. Thus, the development period of 4, respectively 7.16 days (calanoids) in the case of embryos and nauplial forms, or 5.44 respectively 5.98 days (cyclopids), doubles in the copepodide stage (11.98 days for calanoids and 12.89 days for cyclopids) (Figs. 1,2).

The cumulation of days required by each copepod metamorphosis stage results in an average of 23.14 days of biomass recyclation period in calanoids, and 24.31 days in cyclopids.

Our data are close to literature ones (generally obtained at 18 °C, or in a vegetation period of 180 days). For example, Winberg (1971) reported for Cyclops genus 21.8 days. Andronikova *et al.* (1970) noted 29.5 days in a 180 days vegetation period, comparatively to our value of 24.33 days. Andronikova found for *Mesocyclops leuckarti* 35.8 days for a generation, for *M. oithonoides* 24.90 days and for *Eudiaptomus gracilis* 19.22 days. Gras (1983) determined a 33 days development period for *Mesocyclops leuckarti* from Tchad lake, supplied from the Chari river, at 30 °C temperature.

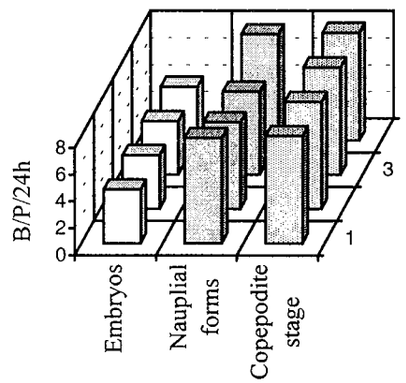

1 = *Calanipeda aquae-dulcis*;
2 = *Eudiaptomus gracilis*;
3 = *Eurytemora velox*;
4 = *Heterocope caspia*

Fig. 1 – Development period of juvenile stages of some species of *Diaptomida* from Lake Roşu, in 1994–1996 period.

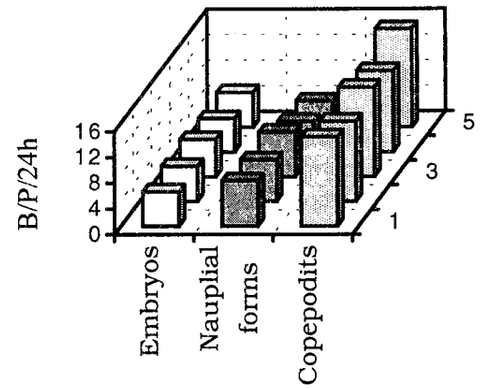

1 = *Acanthocyclops vernalis*; 2 = *Cyclops vicinus vicinus*;
3 = *Mesocyclops crassus*; 4 = *M.leuckarti*; 5 = *M.oithonoides*

Fig. 2 – Development period of juvenile stages of some *Cyclopida* species from Lake Roşu, in 1994–1996 period.

It is important to note that our values (Fig. 3) were obtained at an average temperature of 19.5 °C and a vegetation period of 244 days/year.

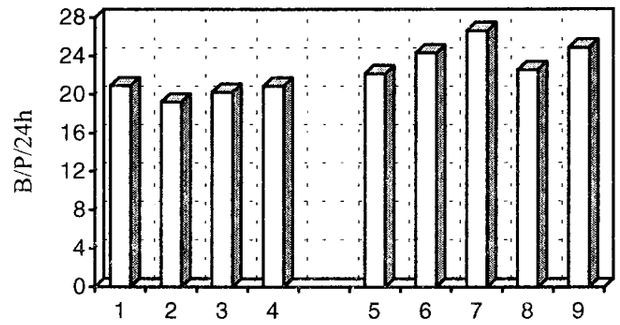

1 = *Canalipeda aquae-dulcis*; 2 = *Eudiaptomus gracilis*; 3 = *Eurytemora velox;*
4 = *Heterocope caspia*; 5 = *Acanthocyclops vernalis*; 6 = *Cyclops vicinus vicinus;*
7 = *Mesocyclops crassus*; 8 = *M. leuckarti*; 9 = *M. oithonoides*

Fig. 3 – Biomass recyclation time of planktonic copepod from Lake Roşu, in 1994–1996 period.

Generally, calanoid "turnover time" was more rapid than cyclopid one.

The "turnover time" in calanoids ranged between 19.22 days (*Eudiaptomus gracilis*) and 20.92 days (*Calanipeda aquae-dulcis*), while in cyclopids between 26.62 days (*Mesocyclops crassus*) and 22.56 days (*Mesocyclops leuckarti*).

According to our opinion the variations of the biomass recyclation period from a year to another, from one species to another, represents the way the planktonic consumers accomplish the increase of efficiency of the nutritive resource valorification (Zinevici and Teodorescu, 1991).

Lake Roşu, considered representative for delta biome (its surface, ecological characteristics, as well as for a long period of study), allows to develop annually 9 generations of planktonic copepods (along a vegetation period which lasts from April till November).

4. CONCLUSIONS

- Development period of juvenile stages of planktonic copepods increases as they develop from embryo towards adult;
- Average duration of biomass recyclation of calanoids from Lake Roşu is about 23 days, while that of cyclopids 24 days;
- 9 generations of copepods succeed in Lake Roşu during a vegetation period (from April till November);
- We may generalize the copepod regeneration period (certainly, known as polycyclic species) from Lake Roşu to delta biome level, with respective variations, caused by a specific structure, or by the ecological factor dynamics, as well as by the evolution stage of each ecosystem.

REFERENCES

1. ANDRONIKOVA I.N., DRABKOVA W.G., KUZMENKO K.N., MICHAYLOVA N.F. STRAVINSKAJA E.A., *Biological productivity of the main communities of the Red lake. Productivity problems of freshwaters*, UNESCO – IBP Symposium: 1–12, Warszawa, 1970.
2. BOTNARIUC N., VĂDINEANU A., *Ecologie*. Ed.Did. şi Pedag., Bucureşti, 1982.
3. GRAS R., SAINT-JEAN L., *Production du zooplankton du lac Tchad*. Rev. Hydrobiol. trop., **16**, *1*, 57–77 (1983).
4. WINBERG G.C., *Methods for the Estimation of Production of Aquatic Animals*. Academic Press, London and New York, 1971.
5. ZINEVICI V., TEODORESCU L., *Dinamica reciclării biomasei zooplanctonice în ecosisteme de tip lacustru din Delta Dunării (perioada 1975–1987) sub impactul procesului de eutrofizare*. St.Cerc.Biol., S.Bol.Anim., **43**, *1–2*, 109–113, Bucureşti, 1991.

Received July 24, 2000.

Institute of Biology
Spl. Independenţei nr. 126, P.O.Box 56–53,
Bucharest 79651, Romania

INVESTIGATIONS OF BOAR SEMEN PRESERVATION BY FREEZING*

AL. G. MARINESCU[1,2], I. ARIŞANU[2], T.FEREDEAN[2], A.G. MARINESCU[3]

Using the Hulsenberg procedure described by Westendorf et al. (1975), after thawing (freezing in liquid nitrogen), we obtained samples with live spermatozoa with 0–30% motility. These results were obtained in the absence of a cryoprotector substance for semen, such as Orvus-ES paste (or its analogues), as currently in use worldwide.

1. INTRODUCTION

Several attempts have been made lately to find an adequate way of preserving the boar semen by freezing, procedure that may maintain for a longer period the fertilization properties of the spermatozoon, very sensitive in this species.

The first such attempts (Polge 1956) used different preservation media, an important role in protecting the spermatozoon membrane during freezing and thawing being attributed to glycerin. Positive results were recorded concerning mobility and less the fertilizing capacity. Subsequently, the attention focused on spermatozoon reactivity in relation to the intensity and duration of the different hypothermic regimens, under the conditions of reducing the proportion of glycerin below 5% (Grove et al., 1968, Polge *et al.*, 1970).

Pursel and Johnson (1971), using Beltsville – F_3 preservative, proposed an original method of changing the stages of pre-freezing cooling, obtaining 74% rate of fertility, comparable to the insemination with fresh semen. Graham *et al.* (1971) used another cryoprotector, Orvus-ES paste, instead of glycerin and obtained after freezing 5 piglets from one of the eight sows.

Subsequently, Crabo and Einarsson (1971), Hillmann (1972), Paquignon (1973), Westendorf *et al.* (1975) brought several improvements to the methodology and technical procedure of freezing.

The investigators from Hulsenberg (Germany), using an original procedure of sperm freezing as straws (changed preservative and thermal treatment) obtained 70% fertility and an average litter of 9.9 piglets (Westendorf *et al.*, 1975). The same procedure experimented in two breeding complexes from Jugoslavia obtained 60% fertility and litters of 9.0 piglets (Schrader, 1976).

*With the support of Al. von Humboldt Foundation (Germany).

Under the conditions of the industrial exploitation of this particularly valuable species for any country, especially under the present conditions, the issue of sperm freezing is very important both for a quick and efficient improvement in the large complexes and for obtaining (possible) imports, much cheaper, of improved semen.

2. MATERIAL AND METHOD

2.1. EXPERIMENTAL ANIMALS

The boar semen was taken from 5 Landrace and Large White boars grown in ICCCP – Periş complex. All boars were currently used for reproduction and were kept in normal conditions of housing and utilization.

Sixteen ejaculates were used for the purpose of the experiment.

2.2. SEMEN COLLECTION AND ANALYSIS

The semen was collected in Periş complex, in the morning in the dummy pen using the manual method. Immediately after collection, the sperm was transferred into a bowl at approximately 37°C.

Semen quality was assessed by determining its volume, aspect, motility, viability and degree of agglutination, as well as the spermatozoa count, in million/cm^3.

Spermatozoa motility was determined with an optical microscope, the blades being warmed up before examination.

2.3. SPERM PREPARATION FOR FREEZING

Immediately after collection and examination, the semen was prepared according to the procedure of Hulsenberg, described by Westendorf et al. (1975):

– The ejaculate was diluted 1:2 with the so-called "diluter 8", brought to the same temperature (about 32–37°C). ("Diluter 8": 57.5 g glucose, 2.5 g lactose, 4.5 g Na-citrate-2-H_2O, 3.5 g EDTA, 1.2g $NaHCO_3$, 0.4 g KCl, 1.0 g sulfanilamide, 990000 IU penicillin, 1.0 g streptomycin, ad 1000 ml aq. bidist.).

– The mixture was cooled to 15°C for 2–6 hours (original method: 6 hours) in Janetzki-type cooling centrifuges.

– After the diluted semen was cooled to 15°C,it was centrifuged for about 8 minutes at 800 × g (according to the amount of liquid and container size, about 2–300 U/min).

– The obtained supernatant was centrifuged 30' at 2200 × g and kept in the freezer. The sediment was re-suspended 1:2 in a solution of freezer pre-diluter (marked by us TG-1) and cooled for 2 hours to 5°C (in Janetzki centrifuges). (Pre-diluter TG-1: lactose solution 11% (100 ml); egg yolk (25 ml) – kept in the refrigerator, cooled to 15°C immediately before re-suspension).

– The sediment was diluted again with part of the inner mixture, with a freezing post-diluter (denoted by us TG-2), obtaining in the end a ratio of 1:3 between the sediment with spermatozoa and the two freezing diluters. (Post-diluter TG-2: lactose solution 11%, egg yolk (25 ml), glycerin (9 ml)). (It is noteworthy the absence of Orvus-ES paste, produced by Procter and Gamble (USA), for its cryoprotective properties, according to the original Hulsenberg protocol).

2.4. SEMEN FREEZING

After the above-mentioned stages were completed, the temperature for each stage being strictly monitored, the prepared semen was introduced in small sealable plastic vials (Eppendorf, Germany), in batches of about 1 ml, quickly passed into a plastic container (100 ml), submerged previously in the freezing liquid (nitrogen).

The entire operation took a few seconds, thereafter the container with the vials was stored into a container with liquid nitrogen (Union Carbide-type).

2.5. THAWING AND SEMEN EXAMINATION

After 1–5 days, the samples of frozen semen were thawed, being transferred rapidly into a bath with warm water (50–60°C) (according to Hulsenberg procedure) for about 30".

The content of the vial with thawed semen was agitated and examined with an optical microscope. The main analysis was the determination of viability motility percentage. In both samples we also determined the morphological changes and GOT activity (transaminase), as damage indicator for cell membrane.

According to the research phase for 1997, we did not use the frozen semen for insemination; this was to be done the next year.

3. RESULTS

The results on spermatozoa viability and motility after freezing in liquid nitrogen and thawing in water bath at 50–60°C, according to Hulsenberg procedure (including the changes of duration and thermal treatment), are presented in Table 1.

It may be observed that the proportion of live spermatozoa and particularly the proportion of highly motile spermatozoa ranged between 0–30% and 0–20%, respectively.

The analysis of semen motility (viability) index at different stages of the preparation process for freezing (Table 1) shows quite small differences between most analyzed ejaculates. Lower motility was observed, however, after the 5°C step and after dilution with TG-1 and TG-2, in the samples with the lowest viability after thawing.

There was no obvious difference between the ejaculates from the two boar breeds, Landrace and Large White.

Table 1

Spermatozoa viability and motility after thawing

Ejaculate number	Breed	Ejaculate quality		Semen quality before freezing				Semen quality after freezing	
		Motility	Agglutination	$S+D_8$ immediately	$S+D_8$, 15°C	$S+D_8$ TG_1, 5°C	$S+D_8$ TG_1, + TG_2	Viability, %	Motility, %
1	Landrace	70-80	-	++	++	+	+	-	-
2	Large White	80	5	++	++	++	++	10	5
3	Large White	80	-	++	++	++	++	10	5
4	Landrace	80	-	++	++	++	-+	5	2
5	Large White	80	5	++	++	+	+	-	-
6	Large White	75-80	-	+++	++	++	++	10	5
7	Landrace	80	-	++	++	++	++	15	10
8	Landrace	80	-	++	++	++	++	20	10
9	Large White	80	-	++	+	+	+	5	2
10	Large White	80	-	+++	++	++	++	30	20
11	Large White	80	5	++	++	++	++	25	15
12	Large White	80	-	+++	++	+	+	10	5

Caption: S = semen; D_8 = Hulsenberg diluter; G_1 = h diluter; TG_2 = freezing; +++ = very good semen (70–80%); ++ = good semen (40–60%); + = poor semen (10–30%); - no motility (below 1).

4. DISCUSSION

Our results are generally consistent with most experiments of this type mentioned in the literature (between 10–30% motility, more exactly viability) (Pursel and Johnson, 1971, 1975; Hillmann and Treu, 1973; Westendorf *et al.*, 1975).

It is interesting to note that the positive results that have been obtained (Pursel and Johnson, 1975; Westendorf *et al.*, 1975) materialized into a high index of fertility (around 70%) after insemination with frozen semen, used compulsorily a substance with cryoprotective action (next to glycerin) such as Orvus-ES paste. Westendorf *et al.* (1975) communicated very poor results (below 5%) in the absence of this cryoprotector, while the use of such products, Orvus E-S paste or its analogues OEP-4343 A or Texapon TH, resulted in good and very good rates (30–50%).

Our results are better in this respect (up to 20–30% motility). Considering the recommendation to use in practice (according to Thorpe Willoughby Pig Breeding Center – England 1976) frozen semen samples with at least 20% motility, we consider that the large industrial complexes may already inseminate the sows with the semen samples having this minimum threshold of viability (motility).

Because the method recommended by Visser and Salamon (1974) (quoted by [8]) did not result in the high rates obtained subsequently particularly by Westendorf et al. (1975), with a procedure that we have also used for this experiment, even if the first authors used only glycerin as cryoprotective substance and obtained higher post-thawing rates (30–35%), we consider that the more recent method should be used in the future. We still have to assess, however, the effect of not using Orvus-ES paste on the fertility and litter size and we still have to improve this procedure and possibly develop a Romanian cryoprotector.

5. CONCLUSIONS

1. Using the Hulsenberg procedure described by Westendorf *et al.* (1975), after thawing (freezing in liquid nitrogen), we obtained samples with live spermatozoa with 0–30% motility.

2. These results were obtained in the absence of a cryoprotector substance for semen, such as Orvus-ES paste (or its analogues), as currently in use worldwide.

REFERENCES

1. CRABO B.G. and EINARSSON S., Acta Vet. Scand., **12**, 125–127 (1971).
2. GRAHAM E.F., RAYAMANNAN A.H.J., SCHMEHL M.K.L., MAKILAURILA M., BOWER R.E., A.I. DIGEST, **19**, *1*, 12–14 (1971).
3. HILLMANN K.H., *Untersuchungen zur Tiefgefrierkonservierung von Ebersamen mit Beltsville-F3-Verdunner,* Dissertation, Tierarztl. Hochschule Hannover (1972).
4. HILLMANN K.H. und TREU H., Zuchthyg., **8**, 105–112 (1973).
5. MARINESCU Al.G., RICHTER DANA, DINU DIANA, ANDREUȚĂ S., MARINESCU A., Rev.Roum.Biol., Biol.Anim., **44**, 104–108 (1978).
6. PAQUIGNON M.J., Rech.Porc.France, 49–57 (1973).
7. POLGE C.und SALAMON S., Vet.Rec., **87**, 424–428 (1956).
8. PURSEL V.G.and Johnson L.A., J.Anim.Sci., **40**, 99–102 (1975).
9. SCHRADER H., Dtsch.Tier.Wschr., **84**, 1, 9–11 (1977).
10. WESTENDORF P., RICHTER L. und TREU H., Dtsch. Tier.Wschr., **82**, 261–267 (1975).

Received September 30, 2000.

[1]*Institute of Biology, Bucharest, Spl. Independenței 296*
[2]*ICCP Periș, Academy of Agriculture and Forestry Sciences*
[3]*"C. Davila" University of Medicine and Pharmacy, Bucharest*

HISTOCHEMICAL LOCALIZATION OF MERCURY IN THE KIDNEY OF *Carassius auratus gibelio*

OTILIA ZĂRNESCU, VIORICA MANOLACHE, LOTUS MEȘTER

The deposition of mercury in the kidney was studied in the crucian carp, *Carassius auratus gibelio*. The fish were exposed to 1µg/l $HgCl_2$ in the water, for 24 hours, eight days and one month.
Tissues from trunk kidney were fixed and sections were developed by autometallography.
Silver amplification revealed accumulation of mercury in the epithelium of certain proximal tubules where they formed a dark layer in the supranuclear region and at the level of brush border. In addition, silver enhanced mercury was found in glomeruli of renal corpuscles and Bowman's capsule. In the intertubular space, the mercury could be visualized in the melanomacrophage centers and in the interstitial tissues.

1. INTRODUCTION

Mercury can exist in three oxidation states in natural waters: Hg^0, Hg^{1+}, and H^{2+}. The distribution of these forms depends upon the pH, redox potential and availability of anions that form stable complexes with mercury. Inorganic mercury occurs, in addition to metallic mercury, in compounds such as mercurous mercury (Hg_2Cl_2) or mercuric mercury ($HgCl_2$).

Fish accumulate mercury as a result of an efficient uptake and a slow rate of elimination (22). Mercury is highly toxic in fish, inducing morphological lesions (18), physiological defects (20) and behavioral abnormalities (24).

The vertebrate kidney is composed of many different types of cells with varying sensitivities to toxic trace metals: proximal, intermediate and distal tubule cells. The most sensitive are, owing to their reabsorptive functions, the proximal tubule cells. Mercury from plasma is filtered by renal glomerulus and subsequent uptake by means of endocytosis by proximal tubule cells of the renal cortex and sequestered in lysosomes until the cells are damaged and lost in the urine (14).

Autometallography (AMG) is one of the most sensitive methods for detecting mercury and it was used in fish for localization of this heavy metal in the kidney and the liver of *Oncorhynchus mykiss* (3) and in the ovary of *Carassius auratus gibelio* (19, 27).

In the present study, we used the autometallographic technique to detect mercury deposits in the trunk kidney of *Carassius auratus gibelio*, exposed to sublethal concentrations of mercuric chloride ($HgCl_2$).

REV. ROUM. BIOL.–BIOL. ANIM., TOME 45, N° 2, P. 161–165, BUCAREST, 2000

2. MATERIALS AND METHODS

Animals: Female crucian carps, weighing between 30–40 g, were purchased from the Nucet Station. The specimens were acclimatized to laboratory conditions for two weeks, at room temperature in glass aquarium, containing tap water (500 l).

Mercury exposure: $HgCl_2$ was added to aquarium water (30 l) as a mercuric chloride solution at the beginning of the experiments, one hour before addition of fish. The concentration of mercury used in this study was 1 μg/l. The animals were sacrificed after 24 hours, 8 days and one month. There was no mortality as a result of the exposure to mercuric chloride. Five fish were kept in clean freshwater, serving as controls.

Histological procedures: After mercury treatment, the fish were sacrificed by medullary transection. Small pieces of trunk kidney were dissected, immersed in Bouin's solution (overnight), dehydrated in ethanol, cleared in xylene and embedded in paraffin. Sections (5μ) were silver-enhanced for microscopic analysis following the autometallographic method of Danscher (8) and Danscher and Moller-Madsen (9). Following physical development, the sections were stained with hematoxylin-eosin or hematoxylin only.

3. RESULTS AND DISCUSSION

Twenty-four hours after metal exposure the connective interstitial tissue was disorganized and contained many macrophages. The cells of proximal nephron were vacuolated with pycnotic nuclei. Moreover, the architecture of the renal corpuscles was altered (Fig. 1A). Silver amplification revealed the presence of the mercury deposits in the cytoplasm of macrophages from the intertubular tissue (Fig. 1B). In the nephron the mercury precipitates were observed in the parietal layer of Bowman's capsule, in the glomerular cells and in the apical surface of certain proximal tubules cells (Fig. 1C).

At the eight days after mercury exposure in the blood vessels, there are many cytolyzed cells and the interstitial tissue contained more macrophages, comparatively with the previous type of experiment. Moreover, in some renal corpuscles the Bowman's capsule was dilated (Fig. 2A). The density of mercury deposits in the cytoplasm of macrophages (Fig. 2B), interstitial tissue (Fig. 2C) and in the cells of proximal tubules (Fig. 2D) was higher than after 24 hour of mercury exposure.

After one month of mercury exposure, the kidney is characterized by the presence of a significant number of pycnotic nuclei and by the massive accumulation of melanomacrophages. Autometallographic development of the mercury indicated numerous mercury deposits in the intertubular tissue. The melanomacrophage centers contained cellular debris and macrophages loaded with

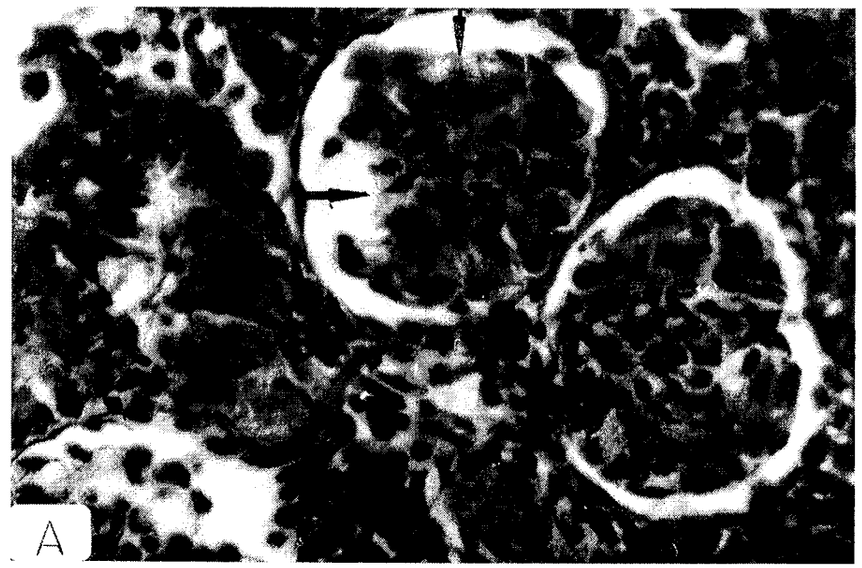

Fig. 1A–C – 24 h after $HgCl_2$ exposure.
A – Renal corpuscles have an altered morphology (arrows);
G – glomerulus; H&E ×400. B – Deposits of silver-enhanced mercury in the cytoplasm of macrophages (arrows). × 400. C – Localisation of mercury deposits in apical surface of proximal tubule cells (arrows). × 400.
B–C – autometallography.

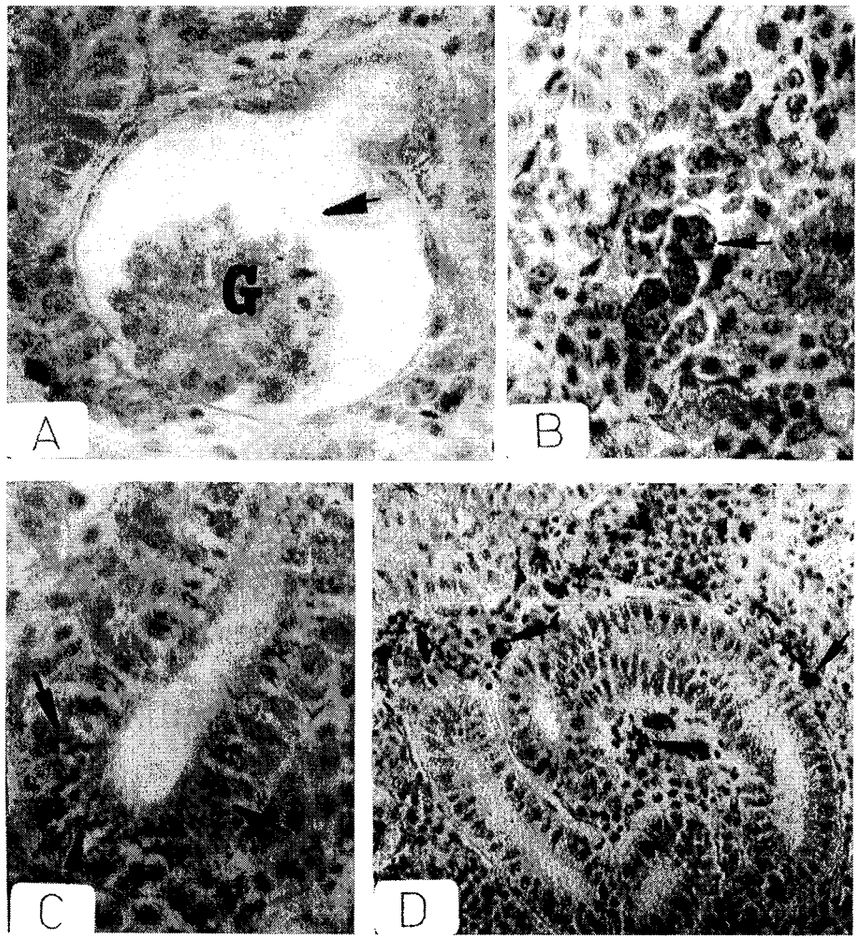

Fig. 2A–D – 8 days after $HgCl_2$ exposure.
A – Hypertrophy of Bowman's capsule (arrow).
G – glomerulus. The density of mercury deposits in the macrophages (B, arrow), proximal tubule cells (C, arrows) and interstitial tissue (D, arrows) was higher than after 24 hours of mercury exposure.
Autometallography. A, B, C × 400; D × 200.

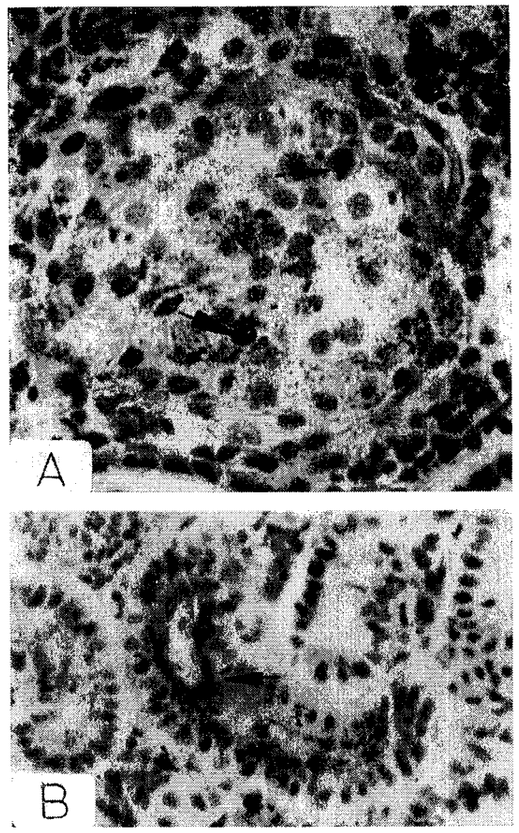

Fig. 3A–B – One month after $HgCl_2$ exposure.
A – Melanomacrophage center with cellular debris and macrophages loaded with mercury grains (arrows). × 400.
B – Mercury deposits at the level of the brush border of proximal nephron (arrow).
Autometallography. × 200.

mercury grains (Fig. 3A). The mercury deposits were found within lysosomes and at the level of the brush border of a proximal nephron (Fig. 3B).

Exposure to metals from the environment caused histopathological damages in the renal parts of the kidney in the fish.

Quantitative studies have shown that inorganic mercury is concentrated in the kidney of fish as *Carassius auratus* (26), *Onchorynchus mykiss* (22), *Salvelinus fontinalis* (18) and this organ contained the highest accumulation of mercury. Mercury is present in the kidney as a complex with metallothionein (MT) that is responsible for the long-term stability of mercury. Mercury has an especially strong affinity for MT, as much as that it displaces copper and zinc from the molecule (11).

The abnormalities in the renal corpuscles of *Carassius auratus gibelio* are similar to those noted in *Channa punctatus* (4) and dilation of the renal corpuscles that suggests an increase of the filtration rate was reported at *Clarias batrachus* exposed to organic pollutants (17).

Our autometallographic findings demonstrated that mercury was accumulated in the parietal layer of Bowman's capsule, in the glomerulus of renal corpuscle, in the cytoplasm and brush border of proximal tubule cells. There is one report on autometallography of fish kidney of rainbow trout exposed 14 days to $HgCl_2$ (3). In this study, the mercury deposits were detected at the ultrastructural level in basal lamina of proximal tubules and in lysosomes of tubule cells. Moreover, in rats, mercury was detected in glomerular and tubular basement membrane (10) and brush border. Few mercury grains were seen in the mesangial matrix and lysosomes of the mesangial cells (21).

Necrosis of epithelial cell from the trunk kidney of crucian carp may be correlated with uptake and rapid elimination of mercury. This aspect observed also by Banerjee and Bhattacharya (4) suggests that the protein-bound mercury was conveyed to the nephron, which was toxic to the tubular epithelium causing necrosis.

In mammals, inorganic mercury in the plasma is filtered at the glomerulus and is taken up by the epithelial cells of the proximal tubule by pinocytosis (14). Some of the mercuric ions (both inorganic and organic) taken up by the kidney are first delivered to the luminal and basolateral surfaces of epithelial cells lining the proximal tubule as a complex with glutathione (*e.g.*, GSH-Hg-GSH or GSH-Hg-cysteine). In addition, there is some support for the notion that once complexes of inorganic mercury and GSH reach the luminal membrane of the epithelial cells lining the proximal tubule, the mercuric ions may actually be cotransported into the proximal tubular epithelial cells with cysteine or cysteinylglycine by the sodium-dependent amino acid or dipeptide transport system after the actions of γ-glutamyl-transferase and cysteinylglycinase on the luminal membrane (5).

In our experiments, a great amount of mercury grains was accumulated in the interstitial tissue and in melanomacrophage centers. Teleost melanomacrophage centers have been proposed to be involved in defense mechanisms and different pathological conditions (12). Moreover, previous studies have demonstrated that $HgCl_2$ may activate fish immune response (16).

In conclusion, our study demonstrated that mercury was accumulated progressively in the trunk kidney, both in the tubular and interstitial compartment.

REFERENCES

1. ALDEN C.L., FRITH C.H., *Kidney*. In: Handbook of Toxicological Pathology, 320–372 (1991).
2. ALLEN P., *Distribution of mercury in the soft tissues of the blue tilapia Oreochromis aureus (Steindachner) after acute exposure to mercury (II) chloride*. Bull. Environ. Contam. Toxicol., **53** (1994).
3. BAATRUP E., NIELSEN M.G., DANSCHER G., *Histochemical demonstration of two mercury pools in trout tissues: Mercury in kidney and liver after mercuric chloride exposure*. Ecotoxicol. Environ. Saf., **12**, 267–282 (1986).
4. BANERJEE S., BHATTACHARYA S., *Histopathology of kidney of Channa punctatus exposed to chronic nonlethal level of elsan, mercury, and ammonia*. Ecotoxicol. Environ. Saf., **29**, 265–275 (1994).
5. BARFUSS D.W., GANAPATHY V., LEIBACH F.H., *Evidence for active dipeptide transport in isolated proximal straight tubules*. Am. J. Physiol., **255**, F177-F181 (1988).
6. CUVIN-ARALAR M.L.A., FURNESS R.W., *Tissue distribution of mercury and selenium in minnows Phoxinus phoxinus*. Bull. Environ. Contam. Toxicol., **45**, 775–782 (1990).
7. DALLINGER R., *Mechanisms of metal incorporation into cells*, In: Cell Biology in Environmental Toxicology. Cajaraville M.P., Ed., Serv. Ed. Univ. Del Pais Vasco, Bilbao, Spain, 135–154 (1995).
8. DANSCHER G., *Autometallography. A new technique for light and electron microscopic visualization of metals in biological tissues (gold, silver, metal sulphides and metal selenides)*. Histochemistry, **81**, 331–335 (1984).
9. DANSCHER G., MOLLER-MADSEN B., *Silver amplification of mercury sulfide and selenide. A histochemical method for light and electron microscopic localisation of mercury in tissue*. J. Histochem. Cytochem., **33**, 219–228 (1985).
10. DANSCHER G., RUNGHBY J., *Differentiation of histochemically visualized mercury and silver*. Histochem. J., **18**, 109–114 (1986).
11. HEATH A.G., *Uptake, accumulation, biotransformation, and excretion of xenobiotics*. In: Water pollution and fish physiology, Heath A. G., Ed., Boca Raton, CRC Press, 79–124 (1995).
12. HERRAEZ M.P., ZAPATA A.G., *Structural characterization of the melanomacrophage centres (MMC) of goldfish Carassius auratus*. Eur. J. Morphol., **29**, 89–102 (1991).
13. HILMY A.M., DOMIATY E., DAABEES A.Y., MOUSSA F.I., *Short-term effects of mercury on survival, behaviour, bioaccumulation and ionic pattern in the catfish Clarias lazera*. Comp. Biochem. Physiol., **87**, 303–308 (1987).
14. HULTMAN P., ENESTROM S., *Localisation of mercury in the kidney during experimental acute tubular necrosis studied by the cytochemical silver amplification method*. Br. J. Exp. Pathol., **67**, 493–503 (1986).
15. KENDALL M.W., *Acute effects of methyl mercury toxicity in channel catfish (Ictalurus punctatus)*. Bull. Environ. Contam. Toxicol., **13**, 570–576 (1975).

16. MACDOUGAL K.C., JOHNSON M.D., BURNETT K.G., *Exposure to mercury alters early activation events in fish leukocytes*. Environ. Health Perspect., **104**, 1102–1106 (1996).
17. MANDAL P.K., KULSHRESTHA A.K., *Hisopathological changes induced by the sub-lethal Sumithion in Clarias batrachus (Linn.)*. Indian J. Exp. Biol., **18**, 547–552 (1980).
18. McKIM J.M., OLSON G.F., HOLOCOMBE G.W., HUNT E.P., *Long-term effects of methylmercuric chloride on three generations of brook trout (Salvelinus fontinalis): Toxicity, accumulation, distribution, and elimination*. J. Fish. Res. Board Canada, **33**, 2726–2739.
19. MEŞTER R., ZĂRNESCU O., *Histochemical localization of mercury in the ovary of crucian carp, Carassius auratus gibelio, after exposure to mercuric chloride*. Rev. Roum. Biol. – Biol. Anim., **41**, 25–34 (1996).
20. MENEZES M.R., QASSIM S.Z., *Effects of mercury accumulation on the electrophoretic patterns of the serum haemoglobin and eye lens proteins of Tilapia mossambica (Peters)*. Water Res., **18**, 153–161 (1984).
21. NORGAARD J.O.R., MOLLER-MADESEN B., DANSCHER G., *Autometallographic localization of mercury in rat kidney-interaction between mercury and selenium*. In: Progress in Histo- and Cytochemistry, vol. 23: Histo- and Cytochemistry as a Tool in Environmental Toxicology, Graumann W., Drukker J., Eds, Fischer Verlag, 187–193 (1991).
22. OLSON K.R., BERGMAN H.L., FROMM P.O., *Uptake of methyl mercuric chloride by trout: A study of uptake pathways into the whole animal and uptake by erythrocytes in vitro*. J. Fish Res. Board. Canada, **30**, 1293–1299 (1973).
23. OLSON K.R., SQUIBB K.S., COUSINS R.J., *Tissue uptake, subcellular distribution, and metabolism of $^{14}CH_3HgCl$ and $CH_3{}^{203}HgCl$ by rainbow trout, Salmo gairdneri*. J. Fish. Res. Bd. Canada, **35**, 381–390 (1978).
24. RODGERS D.W., BEAMISH F.W.H., *Dynamics of dietary methylmercury in rainbow trout, Salmo gairdneri*. Aquat. Toxicol., **2**, 271–290 (1982).
25. TAYLOR M.G., *Mechanisms of metal immobilization and transport in cells*. In: Cell Biology in Environmental Toxicology, Cajaraville M.P., Ed., Serv. Ed. Univ. Del. Pais Vasco, Bilbao, Spain, 11–23 (1995).
26. WEISBART M., *The distribution and tissue retention of mercury-203 in the goldfish (Carassius auratus)*. Can. J. Zool., **51**, 143–150 (1973).
27. ZĂRNESCU O., LAZĂR S., MEŞTER R., *Ultrastructural localisation of mercury accumulations in the ovary of crucian carp, Carassius auratus gibelio, after exposure to mercuric chloride*. In: Proceedings of 13th National Electron Microscopy Congress, METU, Ankara (Turcia), Tekin E., Canberk Y., Eds, 450–456 (1997).

Received September 28, 2000.

Faculty of Biology
Spl. Independenţei 91–95, Bucharest
E-mail: otilia@ibd.dbio.ro

GIANT CELLS IN FAT NECROSIS

C-C. PRUNESCU, PAULA PRUNESCU

The morphology and ultrastructure of the fat necrosis granulomas from the dorso-lumbar region of the normal hamsters, were described. In the subcutaneous fatty tissue there were observed granulomas composed of neutrophil granulocytes, monocytes, macrophages, epithelioid cells and multinucleated giant cells. The macrophages and the epithelioid cells were loaded with electron-dense granules, lipid vacuoles and irregular, racemouse, secondary lysosomes. The multinucleated giant cells presented the nuclei arranged in the submarginal cytoplasm, a large lipid vacuole occupying the most of the cell volume and numerous Ziehl-Neelsen positive vacuoles. The continuous growing of the central lipid vacuole seemed to be the main cause of the destruction of the large-sized giant cells.

1. INTRODUCTION

The necroses of fatty tissue are phenomena known in human pathology as lesions of enzymatic and/or traumatic nature, as particular forms of foreign body reactions to endogenous and/or exogenous lipids (1, 4, and 15).

The progress of the fat necrosis described in this paper was observed in the normal hamsters and seemed to represent a spontaneous degradation way of the adipose cells from certain body areas.

2. MATERIAL AND METHODS

Golden yellow fat necrosis zones were detached from the adipose subcutaneous symmetrical masses situated in the dorso-lumbar region of normal adult hamsters of both sexes. Fragments of necrotic fatty tissue were fixed in Helly's solution or in 4 % saline formalin. In some cases the tissue fragments were postchromized. 5 μm thick paraffin sections were stained with Sudan black B and examined in aqueous medium, for detection of the neutral fats. Also the Ziehl – Neelsen staining was realised, to make evident the acid – fast lipofuscins (14). The control preparations were stained with Hemalum – Eosin.

Small fragments removed from fat necrosis areas were fixed in 3% glutaraldehyde in Milonig buffer, *p*H 7.2 the postfixation was made in 1.3% osmium tetroxide solution in the same buffer. Pieces were embedded in a resin of Vestopal type. The ultrathin sections obtained with a Tesla ultramicrotome were double contrasted with uranyl acetate and lead citrate. The examination and photography were realised with a JEM 7 electron microscope.

REV. ROUM. BIOL. – BIOL. ANIM., TOME 45, N° 2, P. 167–175, BUCAREST, 2000

3. RESULTS

The fat necrosis zones were adjacent to normal adipose tissue. The fat necrosis area presented the structure of a granuloma with neutrophil granulocytes, macrophages, epithelioid cells and multinucleated giant cells (Fig. 1). Capillaries, also venules and arterioles were observed in the fat necrosis area similarly to the adjacent unaffected fatty tissue.

Lipid vacuoles varying in size from 0.5–5 μm were present in the cytoplasm of the macrophages and epithelioid cells. Some lipid inclusions were fine and diffuse. This material was Ziehl-Neelsen positive. The fatty inclusions were arranged in several vacuoles but often there was a large vacuole with central localisation. These vacuoles were slight Ziehl-Neelsen positive, and stained strongly positive with Sudan black B.

The size of the giant cells ranged from 20–100 μm or more. The nuclei of the giant multinucleated cells with large lipid vacuoles were arranged in the marginal strip of the cytoplasm (Fig. 1). Some giant cells presented cytolysis, in the areas where the marginal nuclei were sparse or absent.

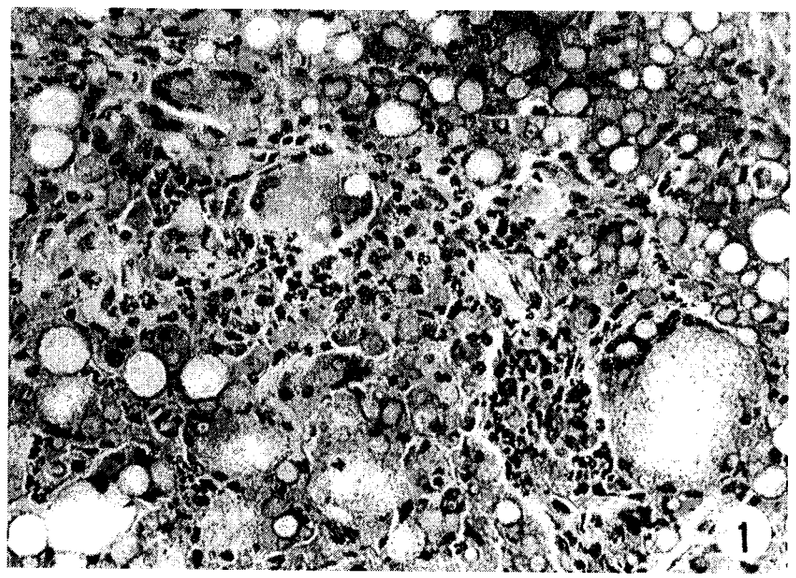

Fig. 1 – Fat necrosis granuloma: adipocytes, neutrophil granulocytes, monocytes, macrophages. multinucleated giant cells. Ziehl-Neelsen, 450 ×.

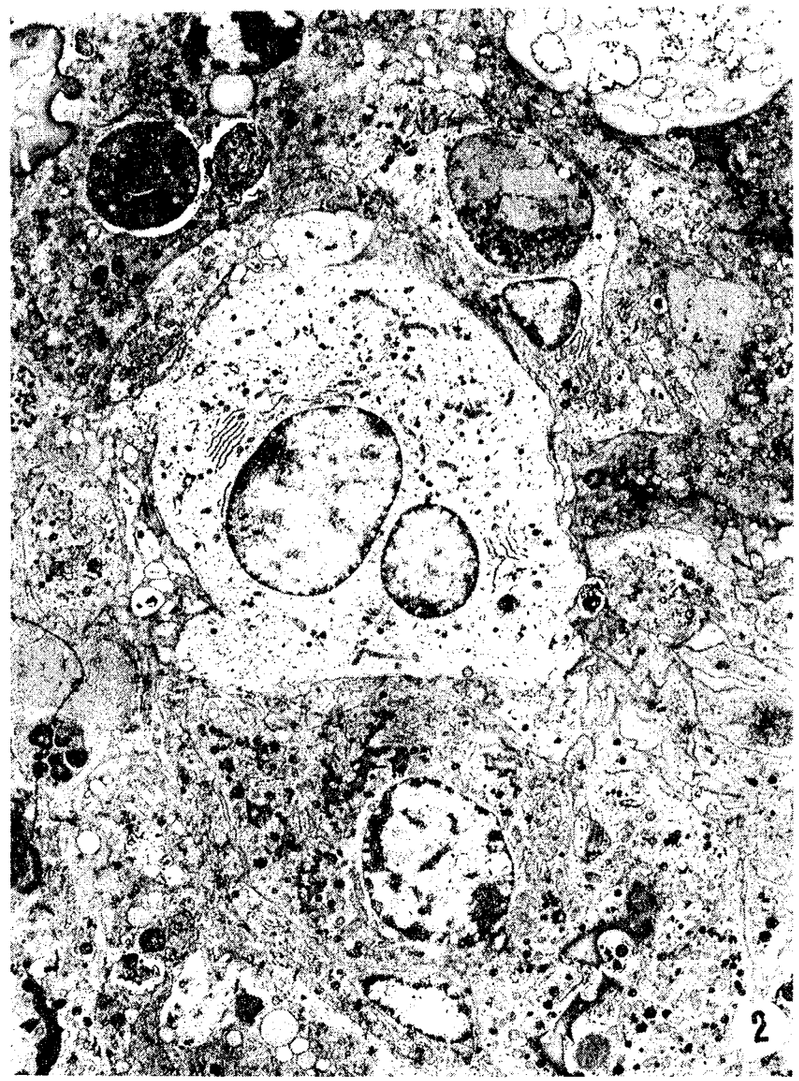

Fig. 2 – Fat necrosis granuloma. Macrophages loaded with apoptotic bodies and electrondense granules. An epithelioid cell with clear cytoplasm and two nuclear profiles. Note, abundant cytoplasmic processes of the cells in this area. 3,000 ×.

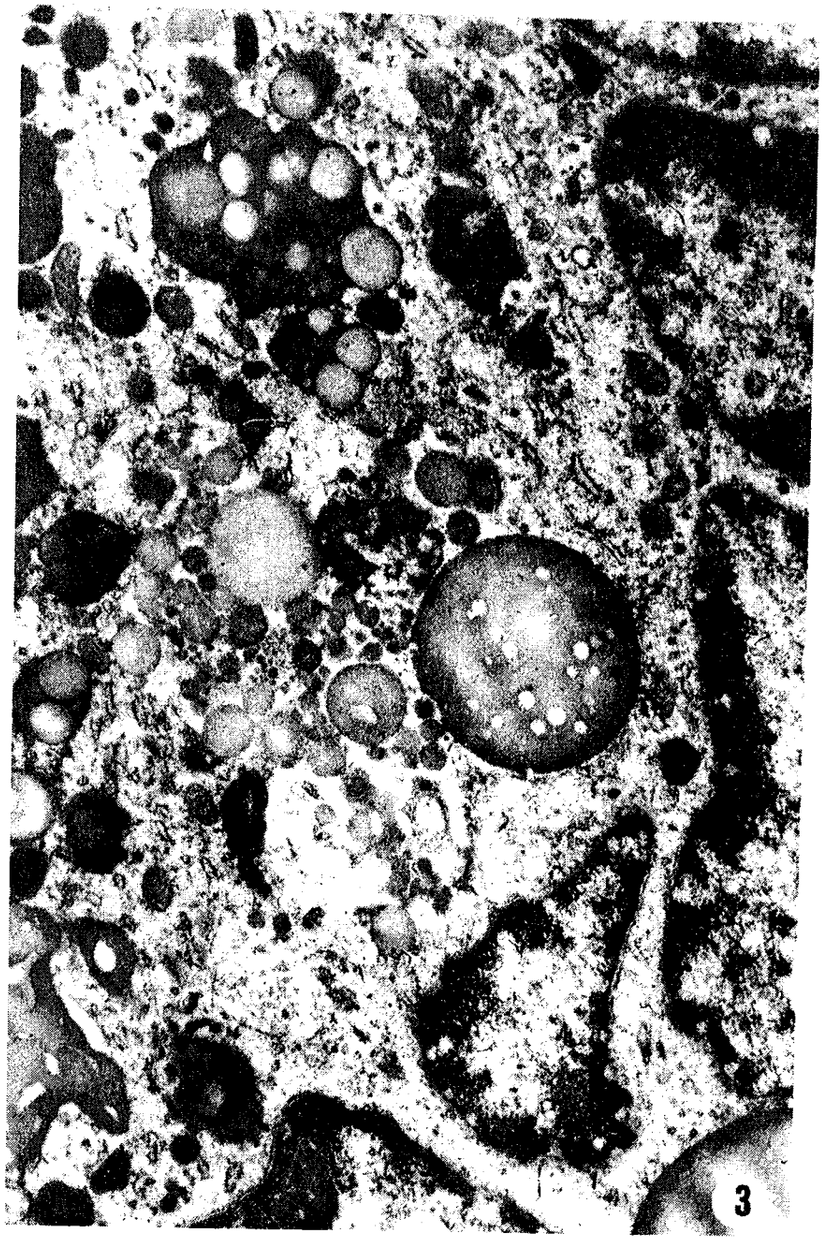

Fig. 3 – Fat necrosis giant cell (detail). Near the peripheral row of the nuclei there are fat droplets of various sizes and polyvesicular structures containing electrondense material and translucent vacuoles. 13,700 ×.

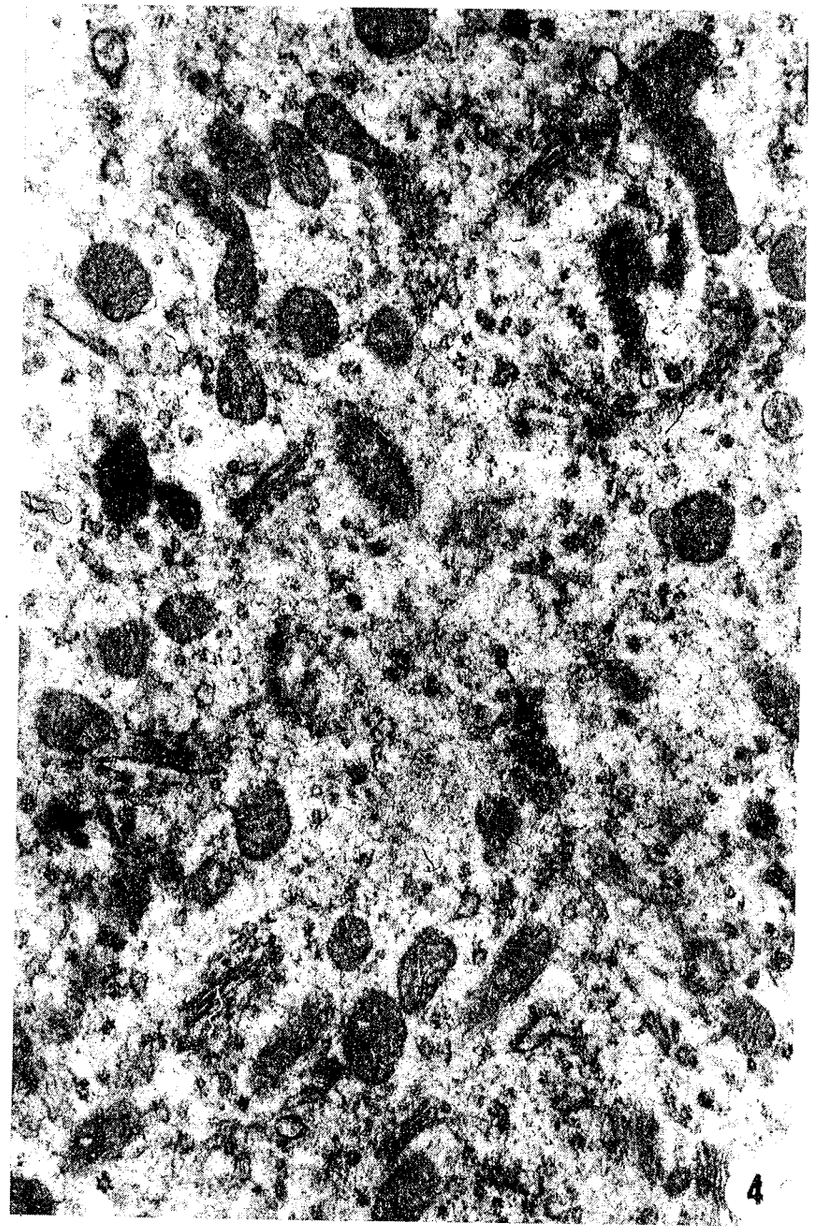

Fig. 4 – Cytocentrum of a giant multinucleated cell. Numerous active Golgi structures, two centriols and small mitochondria with dense matrix. 20,000 ×.

Fig. 5 – The narrow strip of cytoplasm separating the plasmalemma from the central lipid vacuole is devoid of cellular organelles.
In the lipid mass of the vacuole cytoplasmic processes are present. 22,000 ×.

The ultrastructure of different cell types in the fat necrosis territory (Fig. 2) was analysed. The neutrophil granulocytes presented frequently a normal appearance but often were in an apoptotic state (Fig. 2). The macrophages were numerous and presented in the cytoplasm lipid inclusions of varying dimensions. Some macrophages endocytosed apoptotic bodies. Others presented a multitude of fine electrondense granules and moderately electrondense ovoid or irregular secondary lysosomes. Macrophages presented small mitochondria with dense matrix, polyribosomes and few canals of rough endoplasmic reticulum. The marginal cytoplasm was extended by tortuous projections (Fig. 2). The epithelioid cells were characterised by a clearer appearance of the cytoplasm, the presence of parallel running canals of the rough endoplasmic reticulum and a profusion of electrondense fine granules (Fig. 2). Often, the macrophages and the epithelioid cells presented numerous interpenetrating projections of the cytoplasm. In the multinucleated giant cells were present some specific cellular zones:

– at the cellular periphery, a row of nuclei was arranged which presented the heterochromatin distributed along the nuclear membrane. Fat inclusions were never seen in the nuclei (Figs. 1, 3);

– in the deeper cytoplasm there were numerous small electrondense granules, small mitochondria with dense matrix and polyvesicular structures composed of translucent vacuoles and coarse bodies of variable electron opacity, representing lipofuscin-like pigments (Fig. 3);

– in the inner part of the nuclei row many cytocentra were present. A cytocentrum was organised by the association of numerous Golgi structures radially oriented and an area with centrioli (Fig. 4). From the extremities of the flattened saccules of the Golgi structures a multitude of coated vesicles detached;

– in the central area of the giant cell, a large lipid vacuole was obviously noted. Cytoplasmic processes from the surrounding cytoplasm penetrated into the lipid vacuole (Fig. 5). Near the lipid vacuole, the cytoplasm was devoid of cellular organelles.

4. DISCUSSION

The evolution of the granulomas involving the differentiation of the monocytes to macrophages, epithelioid cells and giant cells is a subject of interest. Fat necrosis granuloma seemed to have an evolution similar to various other experimental or pathologic granulomas (2, 8, 11, 12, 13, 16, 17, and 18). A sequential development of the experimental fat necrosis granuloma was presented in the rat with ligature of the epididymis peduncle (6).

To determine the fat necrosis granuloma appearance, certain cellular events succeeded: a minute lesion to induce the necrosis of some adipocytes and the

storage fats released in the intercellular space. Such lesions might be of different origins (trauma, age, vitamin E deficiency) (7, 9, and 19). The lesions of the adipose tissue elicited an inflammatory reaction: neutrophil granulocytes, monocytes and macrophages migrated in the inflammatory zone. The storage lipids in the extracellular localisation became the object of the oxidative reactions following the release of the superoxide and other reactive oxygen intermediates secreted by neutrophil granulocytes and macrophages (5, 7, and 10). Also, the granulocytes and macrophages phagocytosed the adipocytes, lipidic remnants and other cellular debris.

The phagocytic vacuoles with lipid content were made evident with Ziehl-Neelsen staining as red-violet acid-fast material in the macrophages cytoplasm. Also, an electrondense material was noted in the secondary lysosomes of the macrophages. A similar situation was described in rats, in experimental granuloma with cholesterol (3).

In the cytoplasm of the fat necrosis giant cells the electron-light lipid vesicles associated with coarse electrondense bodies and a great central lipid vacuole of different electron-translucence were observed. The large central vacuoles of the giant multinucleated cells were always positive for Sudan black B and slightly positive for Ziehl-Neelsen staining. In fact, the Ziehl-Neelsen positive containing of the macrophages vacuoles fainted as the syncyalization of the macrophages progressed, to the formation of the giant cell. The diminution to the loss of the Ziel-Neelsen positive reaction in the vacuoles of the giant cells suggested an intense process of lipoproteolysis.

The lipid overloaded giant cells presented the tendency to degrade, as the result of an autolytic process which advanced from the great central vacuole area towards the narrow cytoplasm strip devoid of the nuclei. In this way, the lipids were once more released and the cycle of the fat necroses was taken again. This might be the explanation for the self-regeneration process of the fat necrosis in the adipose dorso-lumbar tissue of the normal hamsters. The occurrence of the fat necrosis in normal hamsters could be due to the postural position at rest of this species, which may determine mechanical pressure and tissue damage.

REFERENCES

1. AHO H.J., STERNBY B., NEVALAINEN T.J., *Fat necrosis in human acute pancreatitis: An immunohistological study,* Acta Pathol. Microbiol. Immunol. Scand., Sect. A, Pathol. **94,** *2,* 102–106 (1986).
2. BAUM H-P., THOENES W., *Differentiation of granuloma cells (epithelioid cells and multinucleated giant cells): a morphometric analysis*, Virchows Arch. B (Cell Path.), **50**, 181–192 (1985).
3. BAYLISS O.B., *The giant cell in cholesterol resorption,* Br. J. Exp. Path., **57,** *5*, 610–618 (1976).

4. CHANDRASOMA P., TAYLOR C.R., *Concise Pathology*, Appleton and Lange, Stamford, Connecticut, 72–81 (1998).
5. CRICHTON R.R., *Inorganic Biochemistry of Iron Metabolism,* Ellis Horwood Series, J. Burgess Editor, 194–196 (1991).
6. GROSS V.M., HARNISH J.R., *Histomorphologie der experimentellen Fettgewebeneckrose*, Virchows Arch. Abt. B, Zell Pathol., **14**, 135–145 (1973).
7. HARMAN D., *Lipofuscin and Ceroid Pigments,* edited E.A. Porta. Plenum Press, 3–13 (1990).
8. HONMA T., HAMASAKI T., *Ultrastructure of multinucleated giant cell apoptosis in foreign-body granuloma*, Virchows Arch., **428,** *3*, 165–176, 1996.
9. JONES D., GRESHAM G.A., LLOYD N.G.. HOWARD A.N., *Yellow fat in the wild rabbit*, Nature (Lond), **207**, 205–206 (1965).
10. NATHAN C.F., *Secretory products of macrophages,* J. Clin. Invest. **79**, 319–326 (1987).
11. PAPADIMITRIOU J.M., ARCHER M., *The morphology of murine foreign body multinucleate giant cells*, J. Ultrastr. Res., **49**, 372–386, (1974).
12. PRUNESCU C-C., PRUNESCU P., *Giant multinucleated iron-containing cells in the liver of polymaltosated iron injected rats,* Rev. Roum.Biochim., **25**, *4*, 355–362 (1988).
13. PRUNESCU P., PRUNESCU C-C., *Pigment-bearing multinucleated cells in the liver of malarian rodents during recovery*, Rev. Roum. Biol. (Zool). **20,** *2*, 107–111 (1975).
14. PUTT F.A., *Manual of Histopathological Staining Methods,* John Wiley & Sons, p. 279 (1972).
15. ROSS J.S., PROUT G.R. jr., *Retroperitoneal fat necrosis producing ureteral obstruction,* J.Urol. **115,** 5, 524–529 (1976).
16. SEITZER U., SHEEL-TOELLNER D., TOELLNER K.M., REILING N., HAAS H., GALLE J., FLAD H. D., GERDES J., *Properties of multinucleated giant cells in a new "in vitro" model for human granuloma formation,* J. Pathol., **182**, *1*, 99–102 (1992).
17. SMETANA K. jr., *Multinucleated foreign-body giant cell formation*, Exp. Mol. Path., **46,** 258–265 (1987).
18. STOKEL D.D., GRANSTROM L., BACKMAN L., DAHLGREN S., *Inflammatory response to subcutaneously implanted MARLEX and GORE-TEX in massive obese patients,* Biomaterials, **13**, *4,* 261–263 (1992).
19. WOLMAN M., *Biological peroxidation of lipids and membranes*, Israel J. Med. Sci., **11,** suppl., 1–248 (1975).

Received August 3, 2000.

Institute of Biology of the Romanian Academy,
Spl. Independenţei 296, P.O.Box 56–53,
Bucharest, 79651, Romania

HISTOLOGICAL AND HISTOCHEMICAL STUDY OF THE SKIN IN PADDLEFISH, *Polyodon spathula*

LOTUS MEŞTER, OTILIA ZĂRNESCU

Polyodon spathula skin morphology, structure, distribution of acidic glycoconjugates, elastin and collagen fibres were investigated by different methods.
Being an endangered sturgeon species, of a great scientific interest, *Polyodon* presents some structural peculiarities of the skin. The epidermis of *Polyodon* is different from that of the other teleosts by the absence of fully differentiated mucous gland cells, large irregular spaces between epithelial cells in some regions of the body and by the presence of epithelial invaginations on the outer surface of the operculum. Dermis varies also on different parts of the body, separated in two strata: laxum and compactum. The elastic fibres (sparse in general in fish) were found in a great number on the sides and forming fibres, mainly horizontal, in the deep plexus of the stratum compactum from the belly and gill membrane.
The acidic glycoconjugates appear to be more concentrated in the dermis from the paddle and opercular inner zone. Chondroitin sulphate immunoreactivity was associated with collagen bundles of stratum compactum and denticles. In denticles this activity shows a similar pattern with those of mammalian bones.

1. INTRODUCTION

The North American paddlefish is one of the two living species of Polyodontidae, the other being the Chinese paddlefish, *Psephurus gladius* (2, 5).

Polyodon spathula is a fish of economic value, introduced from the USA in our country, at Nucet Station. Numerous studies have been published on fish integument, but only one of these has dealt with paddlefish, that has a unique skin (3, 7, 12, 14). Most of these studies focused on epidermis and scales.

The objective of this study was to investigate the general morphology of the skin from different body sites, distribution of acidic glycoconjugates, elastin and collagen fibres, and immunohistochemical detection of chondroitin sulphate.

2. MATERIALS AND METHODS

Three years old *Polyodon spathula* were purchased from the Nucet Station. Following capture, the fish were sacrificed by medullary transection and skin samples were taken from various sites of the body (sides, belly, operculum, rostrum and gill membrane) for fixation in Bouin-Hollande solution. After

REV. ROUM. BIOL. – BIOL. ANIM., TOME 45, N° 2, P. 177–181, BUCHAREST, 2000

fixation, the samples were dehydrated in ethanol, cleared in toluene, embedded in paraffin and sectioned. 7 µm-thick sections were stained with hematoxylin-eosin (H&E), Alcian Blue, *p*H-2.5 (for acidic glycoconjugates), Orcein (for elastic fibres) and Van Gieson (for collagen).

For immunohistochemistry the sections were rinsed in 0.1M PBS and sequentially incubated in methanol:H_2O_2 (9:1) to remove endogenous peroxidase (30 min), PBS plus 10% normal rabbit serum to remove non-specific background staining (1h), mouse monoclonal anti-chondroitin sulphate, primary antibody (Sigma), diluted 1:150 (overnight, at 4°C), rabbit anti-mouse IgG peroxidase conjugate (Sigma), diluted 1:150 (1h, at room temperature). Each incubation step was followed by four 5 min rinses in PBS. To visualize the primary antibody binding sites, the slides were incubated for 5-15 min in a solution of 3,3'-diaminobenzidine (0.05%) and 0.015% hydrogen peroxide, dissolved in 0.1M PBS.

3. RESULTS AND DISCUSSION

The skin of *Polyodon spathula* as in most teleosts is composed of two main layers: the epidermis, formed by several rows of strongly interconnected cells and the underlying dermis. Skin thickness differs over various body parts of the same fish (Table 1). Moreover, the skin of the outer surface of the gill membrane is folded (Fig. 1).

Polyodon spathula is covered by a stratified squamous epithelium and in contrast with other fish species has epithelial cells only. The number of layers varies from eight (rostrum) to 12 (gill membrane). The epidermis comprises an irregular row of cells, most of which are either rounded, oblong or irregular in form. The surface layer of the epidermis is composed of 2–3 irregular rows of squamous cells with pyknotic nuclei. Among squamous cells can be observed acidophilic cells (Fig. 2). These eosinophilic leukocytes are round with centrally located granules that displaced the nucleus to the cell periphery. The functions of acidophilic cells in the fish epidermis have not been satisfactorily elucidated. Large numbers of eosinophilic cells appeared to be associated at salmonid fish with ectoparasite species (1). In the middle layer of the epidermis there are polyhedral cells which can contain or not granules, that stained blue with Alcian Blue, pH-2.5, suggesting the presence of acidic glycoconjugates (Fig. 3). From this point of view the epidermis of the *Polyodon* is different from other teleosts and *Acipenser* in the absence of fully differentiated mucous gland cells (14). The basal layer of the epidermis is formed by cuboidal cells situated on the basal membrane that separates the epidermis from dermis.

Fig. 1 – Histology of the skin from the outer surface of the gill membrane. H&E, Alcian Blue, × 300.

Fig. 2 – Eosinophilic cells (arrows). H&E, × 600.

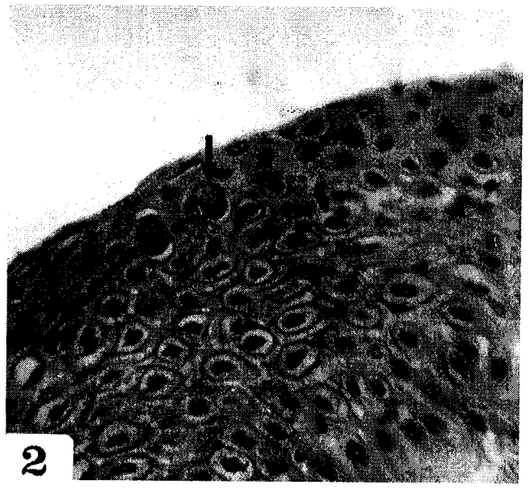

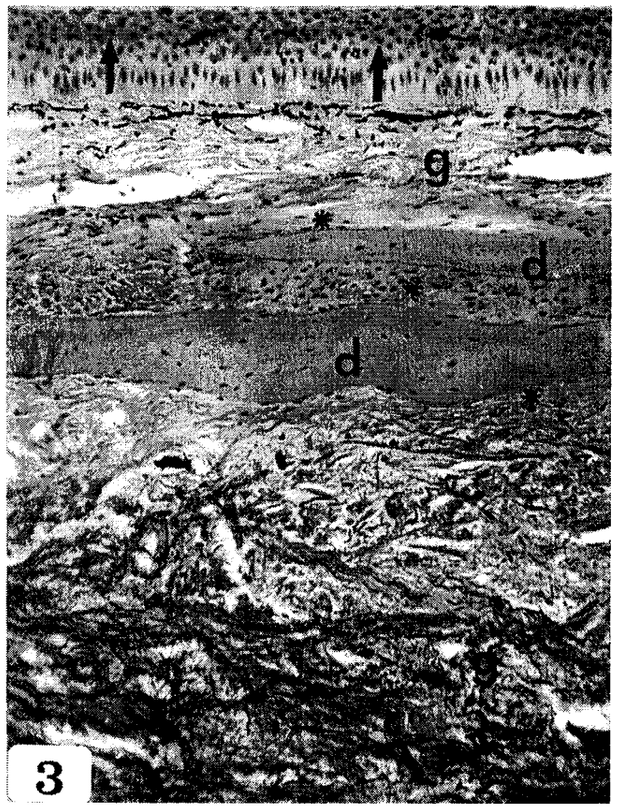

Fig. 3 – Histology of the skin from the rostrum. Note the presence of the mucus in the middle layer of the epidermis (arrows). c – collagen fibers; d – denticles; g-glycoconjugates; * – dense connective tissue. H&E, Alcian Blue. × 150.

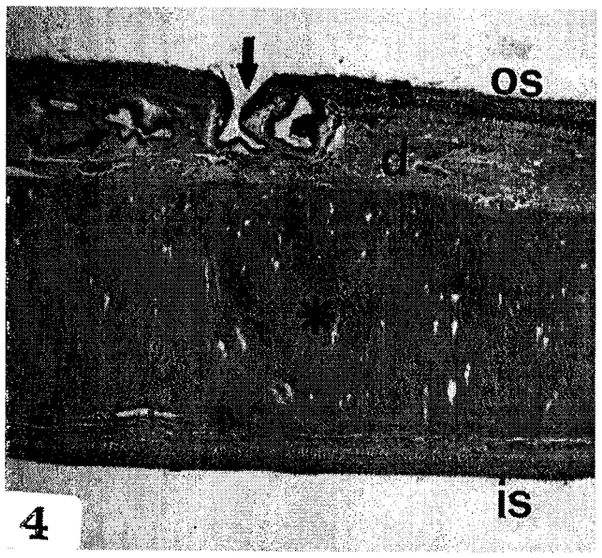

Fig. 4 – Histology of the operculum. Surface pits (arrows). d – dermis; e – epidermis; IS – inner surface; OS – outer surface; * – inner part. H&E, Alcian Blue, × 52.5.

Fig. 5 – Histology of the skin from the belly. SL – stratum laxum; SC – stratum compactum. H&E. Alcian Blue, × 150.

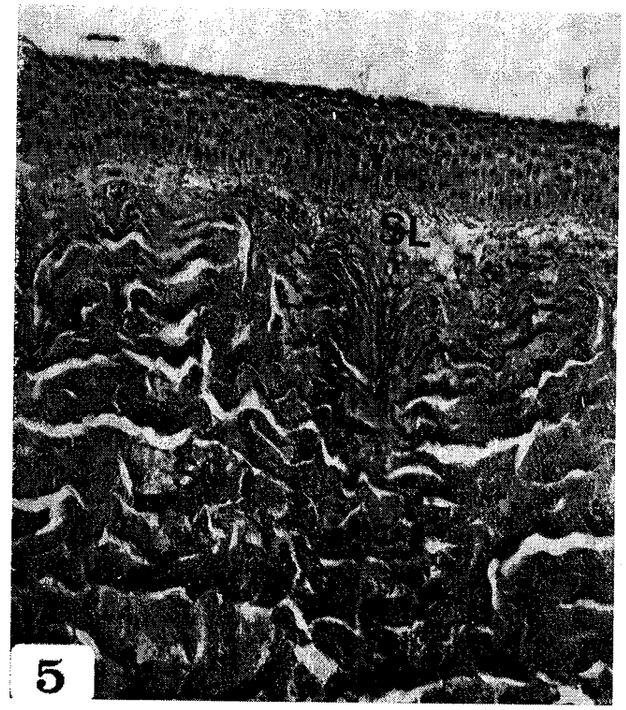

Fig. 6 – Orcein staining (arrows) of the skin from the sides. × 150.

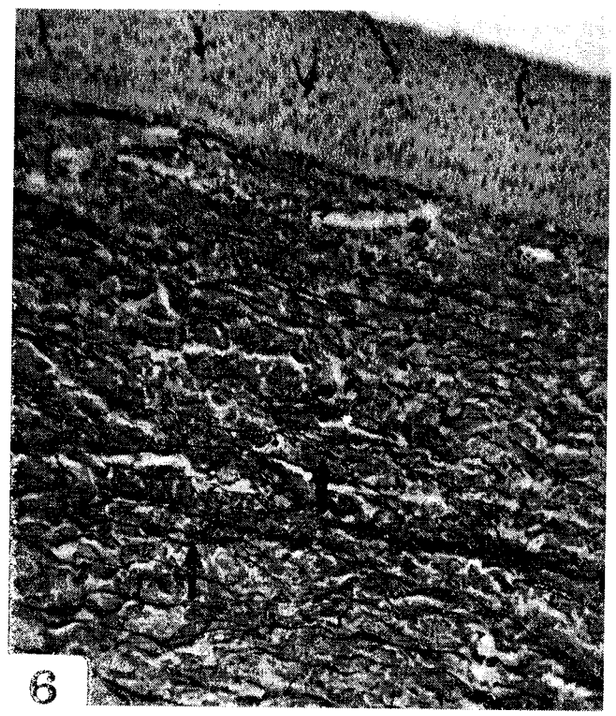

Fig. 7– In the belly, the elastic fibers were associated with the deep plexus of the stratum compactum (arrows). × 150.

Fig. 8 – Stratum compactum of the dermis shows chondroitin sulphate immunoreactivity between collagen bundles (arrows). SL – stratum laxum; SC – stratum compactum. × 320.

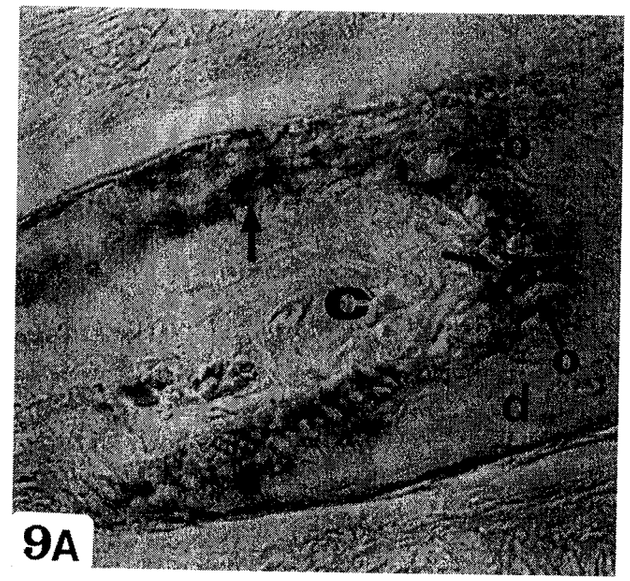

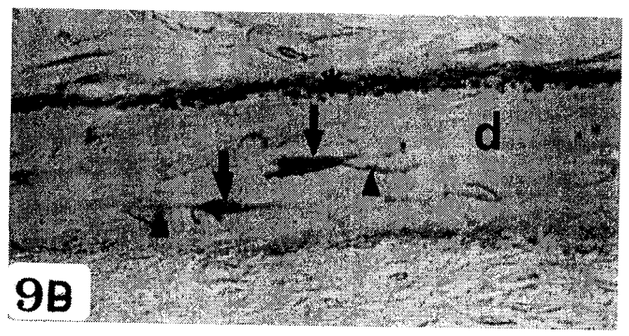

Fig. 9A–B – The chondroitin sulfate immunoreactivity was associated with pericellular areas of osteoblasts (A, arrows), with margins of the denticles (B, *) and with cytoplasm of osteocytes (B, arrows) and its canaliculi (B, arrow head). c-connective tissue; d-denticles. O – osteocytes. × 375.

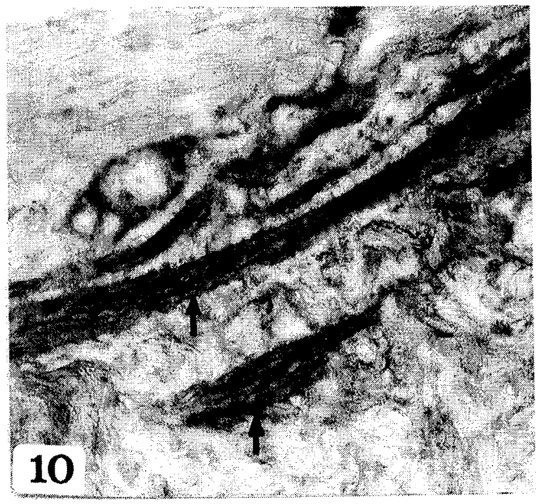

Fig. 10 – Distribution of chondroitin sulphate in the lower part of stratum compactum from the belly skin (arrows). × 375.

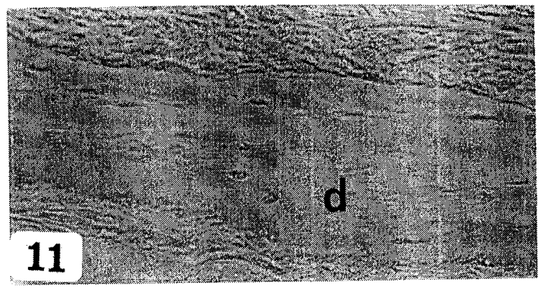

Fig. 11 – The specificity of the reaction was seen by the absence of immunolabelling in control sections reacted with nonimmune serum. d-denticles. × 375.

Table 1

Comparison of skin thickness in paddlefish

Skin region	Skin thickness (μm)	
	Epidermis	Dermis
Sides	178–267	1008–1500
Belly	890–116	1152–1440
Outer surface of tip operculum	133–223	223–356
Inner surface of tip operculum	89	90–133
Rostrum	133	1440–1560
Outer surface of gill membrane	133	223–625
Inner surface of gill membrane	71.36	133–223

In some regions of the body, there are large irregular spaces between epithelial cells. These channels were associated with stress, parasites or virus infections at other species (16).

Melanocytes are present in the epidermis from back, sides, outer surface of the operculum and rostrum. The morphology of these cells was irregular, with many cytoplasmic processes that are insinuated between epithelial cells.

On the outer surface of the operculum, there are present epithelial invaginations, surface pits (Fig. 4). At the lips of the pits epidermis is similar to regular skin but at the neck, surface cells shift from simple squamous to polyhedral cells. The floor of pits is composed of a single layer of cuboidal and columnar cells. Pits were identified previously at *Polyodon spathula*, on the head, operculum, rostrum (12) and throat (14). Surface pits are not a sensory organ (14) and from this point of view they are similar to nonsensory pits of Esocidae (9, 10).

Dermis, like the epidermis, varies on different parts of the body (Table 1). In paddlefish, the dermis contains two strata: laxum and compactum (Fig. 5). The thickness of stratum laxum situated at the base of epidermis is variable in different parts of the body and contains collagen fibers, nerves, capillaries, fibroblasts and pigment cells. Melanocytes are found beneath basement membrane, more abundant in the upper part of the stratum laxum from the rostrum, sides and outer surface of the operculum. On the outer face of the operculum the melanocytes are more frequent around the pits. While epidermal pigment cells may be of variable shape, dermal chromatophores, especially those actively engaged in physiological color change, are more or less flattened.

Stratum compactum of the dermis is formed by densely compressed bundles of collagen fibers that run mostly parallel to the skin surface. At regular intervals, there are observed perpendicular collagen fibers as well as blood capillaries and nerves that traverse the stratum compactum.

The sturgeons have reduced the dermal ossifications to bony scutes. The bony denticles lack from the skin of the throat and belly. The denticles or bony scutes are elongated or irregular and surrounded by a dense connective tissue

(Fig. 3). They are composed of bone with lacunae that contain osteocytes. There are few canaliculi that run from the lacunae. Previous studies described five types of scales in the skin of *Polyodon spathula*: the dorsal and ventral fulcra on the caudal fin, rhomboidal scales on the caudal lobe, horny denticles over the pectoral girdle, calcareous denticles over the trunk and the anchor-shaped plates on the rostrum (8, 14).

Using Orcein staining, the elastic fibers were seen associated with the entire stratum compactum on the sides (Fig. 6) and as long aggregates forming fibers, sometimes branched, arranged mainly horizontally in the deep plexus of the stratum compactum, from belly and gill membrane (Fig. 7). In fish, elastic fibers are sparse, except in special cases such as the puffer fish (11). Elastic tissue was found in lamprey dermis adjacent to the dermal endothelium and with vertical collagen bundles passing to the stratum compactum (16). In mammals, elastic fibers are characteristics of the intermediate dermis, while mature elastic fibers are found deeper in the tissue, because of its relationship to the subpapillary vascular plexus (6).

The alcianophilia of the dermis was variable in intensity in different sites. The strongest staining for Alcian Blue was associated with entire dermis from the rostrum (Fig. 3) and inner part of the operculum (Fig. 4). Dermis of gill membrane was weakly alcianophilic.

Chondroitin sulphate immunoreactivity was associated with collagen bundles of stratum compactum (Fig. 8) and denticles. In denticles immunolabelling was observed surrounding the osteoblasts (Fig. 9A), in the cytoplasm of osteocytes, in its canaliculi (Fig. 9B), and on the margins of bone. Moreover, the immunolabelling of chondroitin sulphate had the same distribution as elastin fibres detected with orcein in the lower part of stratum compactum from the skin of belly and gill membrane (Fig. 10). The control sections incubated with nonimmune serum were negative (Fig. 11). There is relatively little information on glycosaminoglycans of fish dermis. Rathemtulla *et al.* (13) found hyaluronic acid in the species investigated. Moreover, it was demonstrated that hagfish had in addition dermatan sulphate and polysulphate, lampreys dermatan sulphate or chondroitin sulphate depending on the species, and *Chimaera* chondroitin sulphate. In some teleosts, histochemical reactions suggest that a pad of glycoproteins is present in the scale pocket above the scale (15). The distribution of chondroitin sulphate in denticles of *Polyodon spathula* shows a similar pattern with those of mammalian bones. In mammals, chondroitin sulphate was located in pericellular areas and in osteocytic lacunae (4). The major glycosaminoglycans (GAG) in mammalian skin are hyaluronic acid (which exists free in the tissue as a GAG), and a chondroitin sulphate/dermatan sulphate, assembled into large and small proteoglycans in the dermal matrix (6).

REFERENCES

1. BLACKSTOCK N., PICKERING A.D., *Acidophilic granular cells in the epidermis of the brown trout, Salmo trutta* L. Cell Tissue Res., **210**, 359–369 (1980).
2. BREMIS W., FINDEIS E.K., GRANDE L., *An overview of Acipenseriformes.* Env. Biol. Fish., **48**, 28–71 (1997).
3. COLLINGE W.E., *The sensory canal system of fish I. Ganoidei.* Quart. J. Microsc. Sci. (N.S), **36**, 499–537 (1894).
4. GEHRON ROBEY P., BIANCO P., TERMINE J.D., *The cellular biology and molecular biochemistry of bone formation.* In: Disorders of Bone and Mineral Metabolism. F.L. Coe, M.J. Favus, eds, Raven Press Ltd., 241–263 (1992).
5. GRAHAM K., *Contemporany status of the North American paddlefish, Polyodon spathula.* Env. Biol. Fish., **48**, 279–289 (1997).
6. HOLBROOK K.A., SMITH L.T., *Morphology of connective tissue: Structure of the skin and tendon.* In: Connective Tissue and its Heritable Disorders. Wiley-Liss Inc., 51–71, 1993.
7. KISTLER H.D., *The primitive pores of Polyodon spathula.* J. Comp. Neur., **16**, 294–298 (1906).
8. MACALPIN A., *Paleopsephurus wilsoni, a new polyodontid fish from the upper Cretaceous of Montana, with a discussion of allied fish, living and fossil.* Contrib. Mus. Paleont. Univ. Mich., **6**, 167–234 (1947).
9. MERRILEES M.J., CROSSMAN E.J., *Surface pits in the family Esocidae. I. Structure and types.* J. Morphol., **141**, 307–320 (1973).
10. MERRILEES M.J., CROSSMAN E.J., *Surface pits in the family Esocidae. II. Epidermal-dermal interaction and evidence for aplasia of the lateral line sensory system.* J. Morphol., **141**, 321–344 (1973).
11. MITTAL A.K., BANERJEE T.K., *Functional organization of the skin of the "green-puffer fish", Tetraodon fluviatilis (Ham.-Buch).* Zoomorph., **84**, 195–209 (1976).
12. NACHTRIEB H.F., *The primitive pores of Polyodon spathula (Walbaum).* J. Exp. Zool., **9**, 455–468 (1910).
13. RATHEMTULLA F., HOGLUND N.G., LOVTRUP S., *Acid mucopolysaccharides in the skin of some lower vertebrates (hagfish, lamprey and chimaera).* Comp. Biochem. Physiol., B., **53**, 295–298 (1976).
14. WEISEL G.F., *The integument of the paddlefish, Polyodon spathula.* J. Morphol., **145**, 143–150 (1975).
15. WHITEAR M., MITTAL A.K., LANE E.B., *Endothelial layers in fish skin.* J. Fish. Biol., **17**, 43–65 (1980).
16. WHITEAR M., *The skin of fish, including cyclostomes.* In: Biology of the Integument, 2. Vertebrates. J. Bereiter-Hahn, A.G. Matolsy, and K.S. Richards, eds, Springer Verlag, Berlin, 8–64 (1984).

Received December 14, 2000.

Faculty of Biology
Spl. Independenţei 91–95,
Bucharest

STRUCTURE OF HUMAN FETAL MEMBRANES AT TERM AND IMMUNOHISTOCHEMICAL EVIDENCE OF CHONDROITIN SULPHATE

MARINELA BUNEA, MARIA CALOIANU, LUCIA MOLDOVAN,
ANCA OANCEA, LIDIA CONSTANTINESCU

The aim of this study was to characterize by light microscopy the structure of human fetal membranes at term including the umbilical cord, under normal conditions and chondroitin sulphate location by immunohistochemistry, using specific monoclonal antibodies. Optic microscopy revealed a cellular dynamics both at the amniotic epithelium and chorion level, and a connective tissue-rich umbilical cord. Immunohistochemical investigations by light microscopy at the level of free membranes and umbilical cord demonstrated a high immunoreactivity of chondroitin sulphate, especially in amniotic epithelium microvilli, fibroblast and compact layer, but also in Wharton connective tissue and around umbilical vessels. This distribution demonstrates chondroitin sulphate role in maintaining the tissue integrity and in preserving the biomechanical properties of embryonic annexes meant to foetus protection.

1. INTRODUCTION

Human foetus is surrounded by extraembryonic (fetal) membranes that protect it against external environment and contribute to material exchange between mother and foetus. These are embryonic annexes formed and maintained only during pregnancy [1], the survival of embryo and subsequently of the foetus being impossible without them.

Bourne [2] described the general anatomy of the fetal membranes as a multilayered system. The amnion consists of an avascular epithelium that lines a special connective tissue composed by three layers: the compact, fibroblast and spongy sheet. The chorion exhibits two distinct layers: the cellular and reticular one onto the trophoblastic mass.

Placenta represents the most important organ for fetal development. It is highly vascularized, exhibits unusual cell types, a unique connective structure and secretion products. Matrix component provides the strength and elasticity to the tissue. This extracellular matrix consists mainly of collagens (I, III, IV, V, VI), glycosaminoglycans (chondroitin sulphate and hyaluronic acid) and some glycoproteins (laminin and fibronectin).

Glycosaminoglycans are the glucidic components of proteoglycan macromolecules that are covalently bound to a protein core [3]. The chondroitin sulphate (CS) appears to be expressed in mesenchymal connective tissue and is

REV. ROUM. BIOL. – BIOL. ANIM., TOME 45, N° 2, P. 183–190, BUCAREST, 2000

synthesized by fibroblasts [4]. CS has important roles in matrices, especially binding to collagen to regulate the thickness of collagen fibrils, both being responsible for the strength of the fetal membranes [5].

There are few works concerning the changes of these macromolecules in embryogenesis [6] and pregnancy [7]. It is known the fact that at term placenta has 69% CS [8], the remainder being constituted of the other glycosaminoglycans (hyaluronic acid, dermatan and heparan sulphate), but the amount of CS is increased in early stages of pregnancy. Some authors support the presence in a very large quantity (75%) of CS at extraembryonic level [9].

The aim of this study was to characterize the structure of human extraembryonic membranes at term and CS location at this level by immunohistochemistry under light microscopy.

2. MATERIALS AND METHODS

Sample drawing: fragments of human placenta, free membranes and umbilical cord were taken within 10 minutes after birth, from 10 women-patients. The samples were obtained from normal births, both vaginal and by Caesarian section.

For **light microscopy,** the tissue fragments were fixed in Bouin, dehydrated in alcohols, clarified in toluene and embedded in paraffin wax. The sections (5 micrometers) were cut and mounted on glass slides treated with albumin for classic morphological studies and with gelatinized water for immunohistochemistry. For light microscopy, lamella were stained with hematoxylin-eosin.

For **immunohistochemical studies** of CS location, the sections were deparaffinated and rehydrated, then immersed in 0.3% hydrogen peroxide for 30 minutes to remove any endogenous peroxidases, thereby reducing background artefacts. Tissue was then washed in 0.1 M phosphate buffer saline (PBS). All incubations were performed in a humid chamber. Then we proceeded for the nonspecific antigens blocking using 2% bovine serum albumin (BSA) in PBS followed by an overnight incubation in primary antibody (antiCS monoclonal antibody; Sigma, C-8035) diluted 1:150 in 2% BSA in PBS. After washing, the samples were maintained for 1 hour in the presence of secondary antibody (peroxidase-conjugated goat anti-rabbit IgG; Sigma) diluted 1:150 in PBS. Substitution of the primary antibody with PBS was used as a control. After that, peroxidase reaction was developed using 3, 3–diaminobenzidine tetrahydrochloride for a few minutes. Sections were then dehydrated in alcohols and mounted.

3. RESULTS

The present study was to carry out at the level of free fetal membranes ("amnion & chorion reflectum"), of membranes from placenta and umbilical cord structures taken after birth from patients with normal pregnancies.

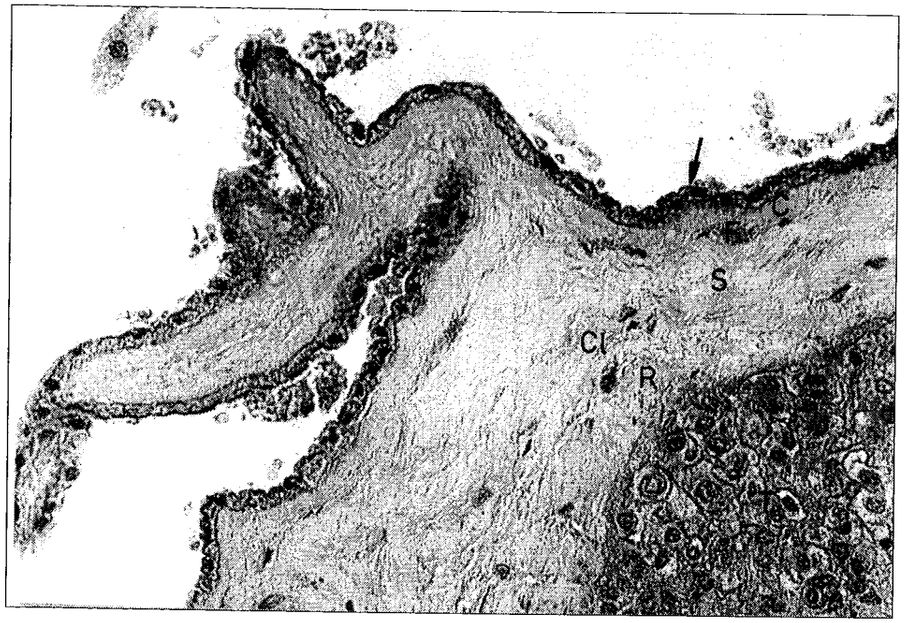

Fig. 1 – Light microscopy view of amniotic epithelium of free membranes at term. The epithelium (arrow) delimits an amniotic connective tissue (compact, fibroblast, spongy layer) and the chorionic one (cellular and reticular layer) which protects trophoblast cell mass (*T*) (× 25; hematoxylin-eosin).
C – compact layer; *F* – fibroblast layer; *S* – spongy layer; *Cl* – cellular layer; *R* – reticular layer.

Fig. 2 – Light microscopy view of the pseudomembrane (arrowheads) delimiting the chorionic connective tissue (*CCT*) from trophoblastic mass (*T*). One may notice irregular, large trophoblast cells (large arrow) with voluminous nuclei (× 40; hematoxylin-eosin).

Fig. 3 – Transverse section at the level of chorionic villi. In villous connective tissue there are fetal capillaries (arrow) and macrophages (arrowhead), externally surrounded by trophoblast (*) (× 10; hematoxylin-eosin).

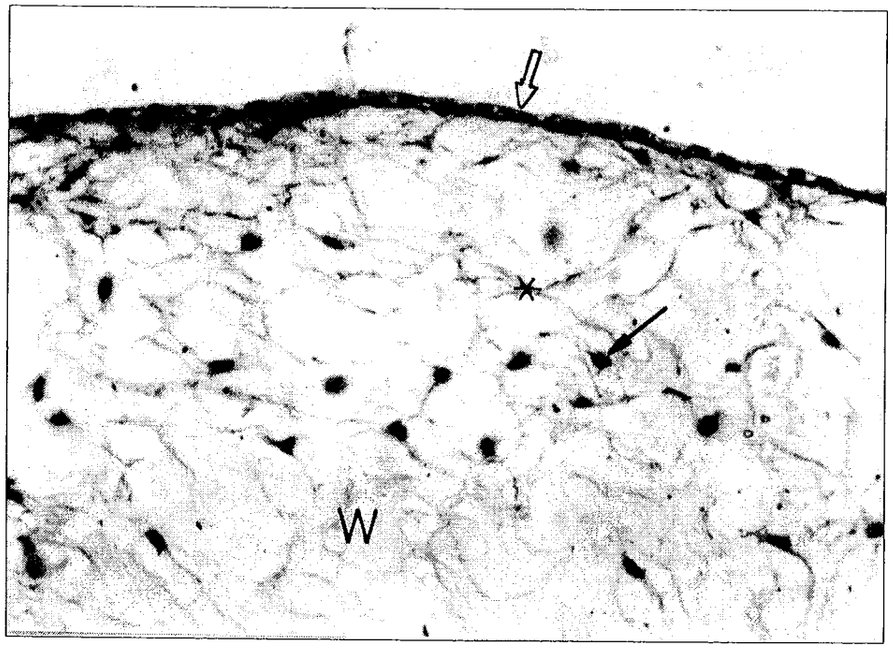

Fig. 4 – Amniotic epithelium (empty arrow) structure at the surface of human umbilical cord at term. Wharton jelly (*W*) with fibroblast type cells (arrow) and connective fibres (*) are noticed (× 40; hematoxylin-eosin).

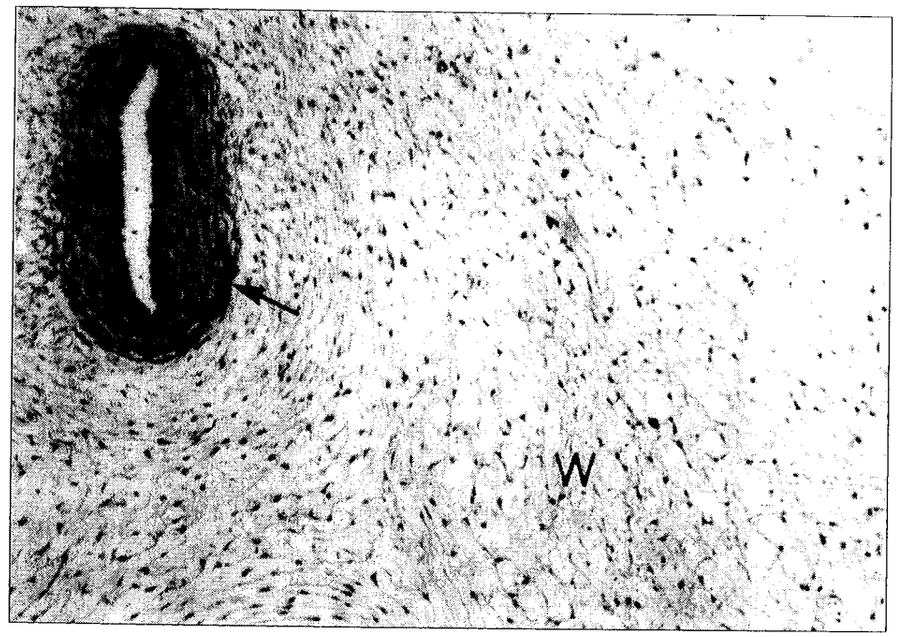

Fig. 5 – Umbilical artery (arrow) surrounded by Wharton connective tissue (*W*) (× 10; hematoxylin-eosin).

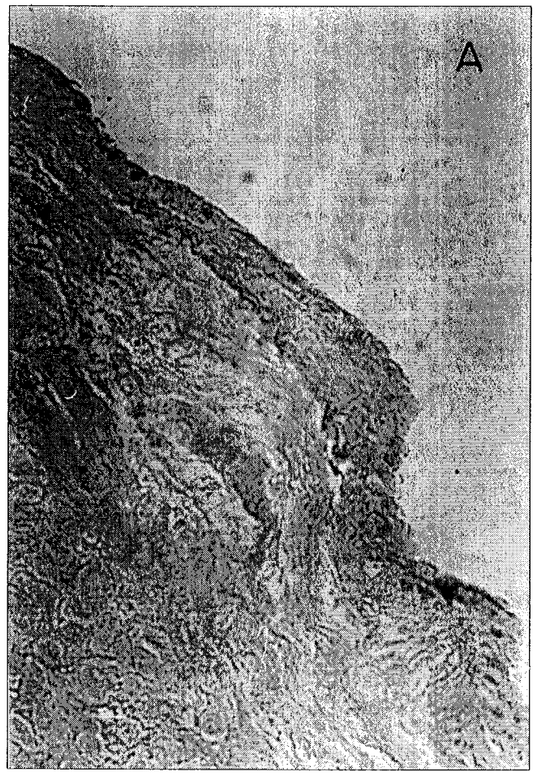

Fig. 6 *A–B* – CS immunohistochemistry in light microscopy at the level of fetal membranes at term.
CS presence was noticed especially in amniotic epithelium (*Ep*)
and the underlying connective tissue (*CT*) (× 25);
A – control (without antiCS primary antibody – no immunohistochemical reaction).

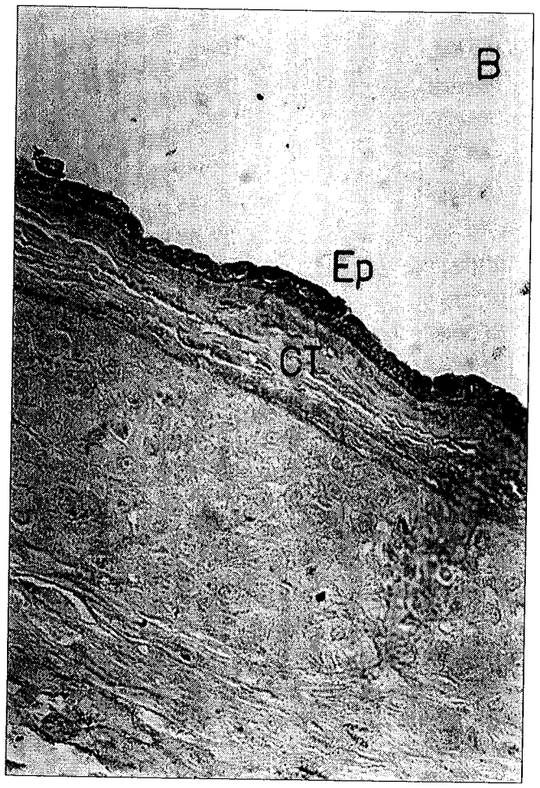

Fig. 6 *A–B*
B – sample (incubated with antiCS primary antibody – after immunohistochemical reaction).

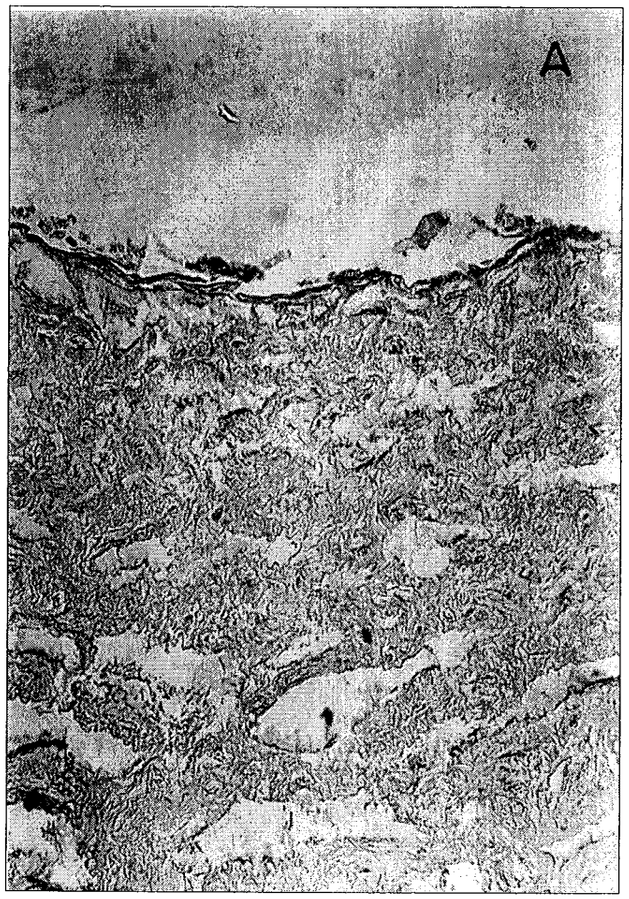

Fig. 7 *A–B*– CS revealed by light microscopy immunohistochemistry at the level of Wharton connective tissue (*W*) in umbilical cord at term. Immunoreactivity is very strong at the level of mesenchymal cells (arrow). The epithelium (*Ep*) shows no reaction (× 16); *A* – control (without antiCS primary antibody – no immunohistochemical reaction).

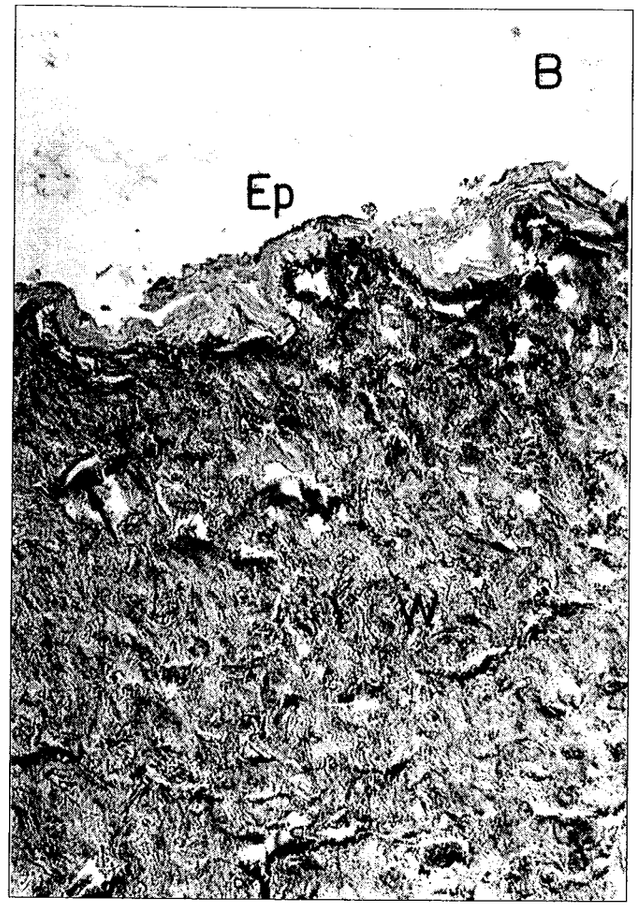

Fig. 7 *A–B*
B – sample (incubated with antiCS primary antibody – after immunohistochemical reaction).

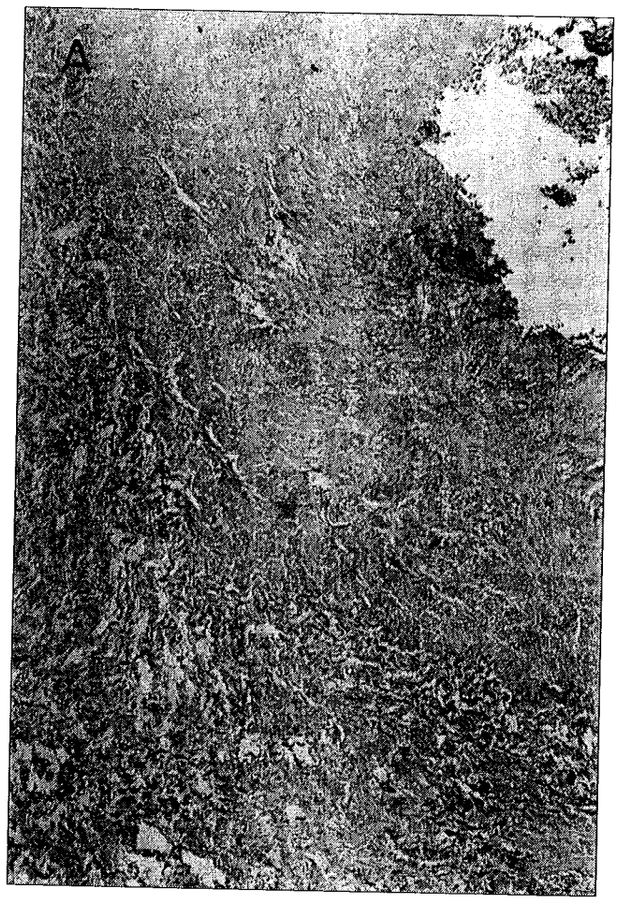

Fig. 8 *A–B* – CS immunohistochemistry by light microscopy at the level of vascular region in umbilical cord. High immunoreactivity is observed in perivascular area (∗) while the vascular wall (*V*) exhibits a weak reaction (× 6.3);
A – control (without antiCS primary antibody – no immunohistochemical reaction).

Fig. 8 *A–B*
B – sample (incubated with antiCS primary antibody – after immunohistochemical reaction).

Amnion is a structure consisting of an avascular, thin epithelium, with cuboidal cells at this late stage of pregnancy (Fig. 1). Beneath the epithelium there is an amniotic connective tissue consisting of several layers: compact, fibroblast and spongy sheet. The compact layer exhibits only a dense fibrilar component with no cellular profiles. Under this, one lies a fibroblast sheet, as a variable region of dispersed mesenchymal cells. The spongy (intermediate) layer is a fibrilar sheet and delineates the underlying chorionic extracellular matrix.

Chorion is a more complex extraembryonic component of a slight different structure at the free membranes level (chorion laeve) compared to placenta (chorion frondosum). Our light microscopy studies showed that in free membranes, the chorion exhibited a very rich cell component, structurally different, represented by large trophoblast cells of irregular shapes (Fig. 1, Fig. 2) with voluminous nuclei. These cells form the chorionic mass, above which, looking at the amnion, two layers of connective tissue belonging to chorion are distinct: cellular and reticular layers separated by chorionic mass through a pseudomembrane structurally different from the amniotic basement membrane (Fig. 2).

In the placenta, the chorion (chorion frondosum) shows a number of fine ramifications, the chorionic villi (Fig. 3) well developed by the end of pregnancy.

Tertiary chorion villus is a mature, complex structure with a trophoblast on the external side and connective tissue on the internal side.

The trophoblast is differentiated into an internal layer, cytotrophoblast (Langhans layer) and an external layer, syncytiotrophoblast. The latter is a multinucleated cell layer formed during the repeated divisions of cytotrophoblast cells (Fig. 3). Syncytial trophoblast exhibits microvilli as a brush border, which increase the area of villous absorption. In the villous core very large and ramified fetal capillaries were noticed at this late age of pregnancy, as well as a macrophage population (Hofbauer cells) with a phagocytary role. Hofbauer cells are large, round and have a voluminous nucleus and a rich cytoplasm. They are embedded in a mass of connective tissue.

Umbilical cord exhibits an unistratified, amniotic epithelium (Fig. 4) on its surface, in which the cells are flattened and different in appearance compared to the amniotic epithelium at the level of free membranes. The epithelium lies on a mucopolysaccharide gelatinous connective tissue called "Wharton jelly" containing typical cells (fibroblasts) with cytoplasm extensions, collagen fibers and basic substance.

In its inner part there are two umbilical arteries (Fig. 5) with thick muscular walls and an umbilical vein surrounded by a rich "Wharton jelly".

The immunohistochemical study of CS at the level of embryonic annexes demonstrates the CS location in free membranes, particularly at the apical pole of amniotic epithelial cells where microvilli occur (Fig. 6*A, B*). In amniotic and chorionic connective tissues one may notice a relatively uniform distribution of CS, the latter

being more evident in the compact and fibroblast layer and is associated with some fibers. Also, we can notice the presence of CS at the pseudomembrane level.

In umbilical cord, CS distribution is rich in Wharton jelly at the level of fibroblasts and amniotic basement membrane (Fig. 7*A, B*). The amniotic epithelium, which covers the umbilical cord, presents no reaction which means that it is not involved in secretion of CS, although the basement membranes show positive reactivity. It was noticed the presence of small amounts of CS in umbilical blood vessel wall, but perivascularly the reactivity is very strong, an accentuated brown color being developed (Fig. 8*A, B*). In figure 8B it is also shown the occurrence of CS in the vascular wall, but less comparative with perivascular area.

4. DISCUSSION

The fetal membranes covering the amniotic cavity are composed of the amnion and chorion that are adjacent structures exhibiting many cell types and an extracellular matrix.

The amnion consists of an epithelium and the amniotic connective tissue, both with no vascular and nervous components. The epithelial cells at term are different from those at early ages of pregnancy, when they are of flattened shapes, as our original studies have shown [unpublished results]. The absence at the amniotic level of a nervous component was also noticed in the other initial studies [1, 10]. Because of the absence of the vascular and nervous compartment, it was suggested that the viability of the amnion be maintained through chorionic vascularization [11].

The epithelium lies on a connective tissue consisting of several layers: compact, fibroblast and spongy sheet, results which are similar to previous studies [2]. The connective tissue provides the amnion with resistance to pressure and mechanical shocks. First of these, the compact layer represents the main collageneous support of the amnion [10], having a thickness of 5–20 micrometers [12]. The previous studies [13] demonstrated that the spongy layer consists of mesodermal cells, which exhibit a phagocytic role. Amnion delimits a cavity with amniotic fluid in which there is the foetus. The fluid protects it while ensuring its mobility. When the foetus is ejected by amniotic fluid pressure, amnion contributes to the uterine cervix dilatation. The amniotic epithelium continues at the level of umbilical cord, covering it.

Although connective tissues, both of amnion and chorion are adjacent, our original studies [unpublished results] proved their different affiliation to the two membranes, due to the fact that in early pregnancy, their attaching is either incomplete or even is absent as earlier researches described [14, 15].

Chorionic villi are of three types: primary villi, represented by trophoblast extensions, secondary villi containing in addition chorionic mesoderm

(extraembryonic) and tertiary villi containing all these components plus fetal capillaries. They represent the functional unit of the placenta since here exchanges between mother and foetus occur [11] and the hormones necessary to maintain the pregnancy are produced as well [16, 17].

With villous growth and capillary extension, the cytotrophoblast becomes discontinuous, due to the fusion of some cytoplasm of Langhans cells with the syncytium, at some regions [18]. Chorionic villi are separated by the intervillous space existing between them, in which maternal blood vessels are opening. In this way, maternal blood directly contacts the chorionic villi, and gas and material exchanges between mother and foetus take place.

Our previous studies [unpublished results] on immature human placenta (8–10 weeks) revealed the abundant presence of macrophages compared to this stage. This fact demonstrates the very important role of these cells at early stages, when certain critical moments can influence the evolution of embryo and even of foetus, or may threaten their survival. Some researchers [15] suggested that the Hofbauer cells may well represent an important sentinel population that is able to accumulate some unwanted products during disturbed gestation and also, they are a challenge for pathologists.

The umbilical cord is an embryonic annex particularly important for foetus life, protecting umbilical vessels [19], two arteries and one vein, and providing the link between placenta and foetus; it is a tubular, twisted and compressible structure [15] and it does not contain lymphatic vessels and nervous cells [11]. The arteries carry the blood from the foetus to the placenta and the blood is returned to the foetus through the vein [1].

Although the umbilical vessels have, generally speaking, a similar structure with the other vessels of the same size in the body they lack typical elastic membranes and they have the ability to allow leukocytes to pass their walls in infectious conditions [11].

CS is an extracellular matrix glycosaminoglycan that regulates cell adhesion, growth, migration, differentiation, gene expression [20] and repair [21]. Also, it participates in the cell – matrix interactions by effectively modulating the cellular phenotype via high affinity binding sites [22]. CS is highly negatively charged and is able to attract ions and water molecules, thus giving proteoglycans special physical properties of maintaining the connective tissues hydrated and making them resilient to compressive forces [7]. The analysis of glycosaminoglycans from fetal membranes [9] indicated that more than 85% of the uronic acid content of this tissue is CS and Inoue and Iwasaki [23] isolated the CS – dermatan sulphate copolymers from umbilical cord as a major glycosaminoglycan component of this tissue.

There are very few studies concerning CS regarding the fetal membranes, particularly biochemical aspects being outlined. It was proceeded some immunofluorescence [9] and immunohistochemical studies at the umbilical cord level [24], knowing that the immunochemistry assay with monoclonal antibodies

began after 1990 only. Daugaard *et al.* [24] evaluated the immunohistochemical staining of CS versus the conventional histochemical methods (Alcian Blue and a modified PAS stain) and results indicated that the use of antibodies against CS is superior to the other methods.

Our studies indicated a positive reaction at the microvilli level in the amniotic epithelial cells comparative with controls, results supported by the previous immunofluorescence studies [9].

At the umbilical cord level there is a strong reactivity of CS in the "Wharton jelly", especially perivascularly, similar to the prior data [24]. This fact demonstrates the CS rich content surrounding the blood vessels, protecting and supporting them. A weak positive reaction was developed in vascular wall while the amniotic epithelium showed no reactivity.

Our previous studies [unpublished results] demonstrated CS presence in immature placenta (8–10 weeks) in higher amount compared to the same structure at term, CS ratio diminishing as placenta matures.

Knowing the role played by this glycosaminoglycan in some biological processes such as tissue integrity as well as maintaining and functioning of specialized matrices (basement membrane) [9], we may say that CS is very important in embryonic annexes, which are dynamic structures.

CS presence at the level of amnion fibroblastic layer and around fibroblasts of umbilical cord connective tissue demonstrates that they represent the source of glycosaminoglycans in embryonic annexes.

Its distribution around the blood vessels suggests CS role as a protective agent of vascular walls. Due to its hydrating properties, a consequence of its ability to retain the water, CS helps to maintain fetal membrane elasticity and to increase their mechanical resistance in order to ensure the foetus protection. In addition, as the foetus grows, the extraembryonic membranes have to enlarge themselves and to allow the fetal movements within the amniotic cavity [25]. In spite of this fact, they have to keep their properties throughout the pregnancy.

5. CONCLUSIONS

We conclude that the embryonic annexes are dynamic structures because the amniotic and mesenchymal cells are still in function and produce matrix components at term.

We noticed differences regarding morphological aspects of the amniotic cells at the free membranes level and onto the umbilical cord.

The immunohistochemical study shows a large distribution of CS at term, being located in specialized structures like blood vessels, amniotic microvilli and basement membranes.

REFERENCES

1. K. BENIRSCHKE, *Placenta*, Encycl. Hum. Biol., 6, 829–834 (1997).
2. G.L. BOURNE, *The microscopic anatomy of the human amnion and chorion*, Am. J. Obstet. Gynecol., **79**, 1070–1073 (1960).
3. LENA KJELLEN, U. LINDAHL, *Proteoglycans: structures and interactions*, Ann. Rev. Biochem., **60**, 443–475 (1991).
4. E. RUOSLAHTI, *Structure and biology of proteoglycans*, Ann. Rev. Cell Biol., **4**, 229–255 (1988).
5. A.D. HOYES, *Ultrastructure of the mesenchymal layers of the human amnion in early pregnancy*, Am. J. Obstet. Gynecol., **106**, 557–562 (1970).
6. H.A. THOMPSON, B.S. SPOONER, *Proteoglycan and glycosaminoglycan synthesis in embryonic mouse salivary glands: effects of beta-D-xyloside, an inhibitor of branching morphogenesis*, J. Cell Biol., **96**, 1443–1447 (1983).
7. M. YANAGISHITA, *Proteoglycans and hyaluronan in female reproductive organs*. In: Jolles P., ed., Proteoglycans, Birkhauser Verlag Basel/Switzerland, 1994, pp. 179–190.
8. W.D. WAGNER, H.A. ROWE, JANICE R. CONNOR, *Biochemical characteristics of dissociatively isolated aortic proteoglycans and their binding capacity to hyaluronic acid*, J. Biol. Chem., **258**, 11136–11142 (1983).
9. M.J. BRENNAN, A. OLDBERG, M.D. PIERSCHBACHER, E. RUOSLAHTI., *Chondroitin/dermatan sulfate proteoglycan in human fetal membranes. Demonstration of an antigenically similar proteoglycan in fibroblasts*, J. Biol. Chem., **259**, 13742–13750 (1984).
10. S. PARRY, J. F. STRAUSS III, *Premature rupture of the fetal membranes*, New Engl. J. Med., **338**, 663–670 (1998).
11. K. BENIRSCHKE, *Placenta: implantation and development*, Encycl.Reprod., **3**, 848–855 (1999).
12. J.D. APLIN, S. CAMPBELL, T. ALLEN, *The extracellular matrix of human amniotic epithelium: ultrastructure, composition and deposition*, J. Cell Sci., **79**, 119–136 (1985).
13. H. WESER, P. KAUFMANN, *Lightmicroscopical and histochemical studies on the chorionic plate of the mature human placenta*, Arch. Gynakol., **225**, 15–30 (1978).
14. J.D. BOYD, W.J. HAMILTON, *The Human Placenta*, Heffer, Cambridge/UK, 1972.
15. K. BENIRSCHKE, *Remarkable placenta*, Clin. Anat., **11**, 194–205 (1998).
16. H.J. KLIMAN, *The placenta revealed*, Am. J. Pathol., **143**, 332–336 (1993).
17. H.J. KLIMAN, *Trophoblast to human placenta*, Encycl. Reprod., **4**, 915–923 (1999).
18. A.C. ENDERS, *Formation of syncytium from cytotrophoblast in the human placenta*, Obstet. Gynecol., **25**, 378–386 (1965).
19. H.J. KLIMAN, *Umbilical cord*, Encycl. Reprod., **4**, 915–923 (1999).
20. M. SLATER, C.R. MURPHY, *Chondroitin sulfate and heparan sulfate proteoglycan are sequentially expressed in the uterine extracellular matrix during early pregnancy in the rat*, Matrix Biol., **18**, 125–131 (1999).
21. J.R. COUCHMAN, D.R. ABRAHAMSON, K.J. MCCARTHY, *Basement membrane proteoglycans and development*, Kidney Int., **43**, 79–84 (1993).
22. T. SCHAEFER, M. ROUX, H.W. STUHLSATZ, R. HERKEN, B. COULOMB, T. KRIEG, H. SMOLA, *Glycosaminoglycans modulate cell-matrix interactions of human fibroblasts and endothelial cells in vitro*, J. Cell Sci., **109**, 479–483 (1996).

23. S. INOUE, M. IWASAKI, *Dermatan sulfate-chondroitin sulfate copolymers from umbilical cord. Isolation and characterization*, J. Biochem (Tokyo), **80**, 513–521 (1976).
24. S. DAUGAARD, L. STRANGE, T. SCHIODT, *Immunohistochemistry of chondroitin sulfate and keratan sulfate. Two monoclonal antibodies evaluation*, Histochem., **95**, 585–589 (1991).
25. GYLLIAN D. BRYANT-GREENWOOD, *The extracellular matrix of the human fetal membranes: structure and function*, Placenta, **19**, 301–312 (1997).

Received October 4, 2000.

National Institute for Biological Science
296 Spl. Independenței
Bucharest

COLLAGEN AND GLYCOSAMINOGLYCAN GEL EFFECT ON EPITHELIAL WOUND HEALING IN RABBIT EYES

LUCIA MOLDOVAN*, OTILIA ZĂRNESCU**,
MARINELA BUNEA*, LIDIA CONSTANTINESCU*

Cornea regeneration following an injury occurs gradually in three distinct stages: cell migration, cell proliferation and cell adhesion. Duration and contribution of each phase vary depending both on wound nature and its size and depth. In this context, the purpose of our study was to estimate a collagen and glycosaminoglycan gel (COL-GAG) effect on regeneration of cornea injured by keratotomy at epithelium level. Superficial incisions of about 0.1 mm depth were made in the cornea of albino rabbit eye in its central region. In each animal, an eye was periodically treated for 4 days with COL-GAG gel and the other was not treated (control). Evaluation of biopolymeric gel effect was made also by comparing the changes at cellular level, which occurred during reepithelization process. For this purpose, wounded cornea fragments were analyzed in light microscopy, electron microscopy, and fluorescent microscopy. At latent phase of regeneration (the first 4–6 hours following the injury), a massive mobilization of polymorphonuclear leukocytes is noticed at wounded level, followed by epithelial cell migration. Six hours following the wounding, the reepithelization process is evident and is much more advanced in the treated eyes. The complete regeneration of corneal epithelium was evident after 3 days only in the cases of treated eyes. During the same period of time, between the cells of regenerated epithelium, the presence of desmosomes and interdigitate junctions was evidenced. These results demonstrate that COL-GAG gel speeds reepithelization of corneal wound, the healing being carried out 24 hours earlier than in untreated eyes.

1. INTRODUCTION

Restoration of tissue functions following an incision is an objective of major importance in cornea surgery. In this context, the treatment of persistent and recurrent wounds of corneal epithelium is a very significant clinical problem.

Corneal epithelium functions as a barrier to infections, maintains stromal hydration and is essential for a normal visualization. Previous studies concerning the wounded cornea regeneration largely established the events that occurred during its healing process. Thus, the main stages of cornea regenerating process are cell migration, cell proliferation and cell adhesion [1]. Each phase duration and contribution vary depending both on the wound nature and its size and depth. The rapid reepithelization of the wounded cornea is essential for visual rehabilitation and the prevention of ocular infection [2].

REV. ROUM. BIOL. – BIOL.ANIM., TOME 45, N° 2, P. 191–196, BUCAREST, 2000

In cases when corneal epithelium is subjected to traumatisms, the regenerating process is directed firstly to reestablish the epithelial layer continuity and later, to develop the adhesions accumulated in the underlying tissue. Usually, in order to help reepithelization and to minimize the discomfort for patients with persistent deficiencies of corneal epithelium, contact lenses and appropriate drugs are used [3], [4], [5], [6] and [7].

Hydrophilic contact lenses do not provide a full transportation of oxygen to cornea, especially when the eyelids are closed, which may lead to epithelial and stromal oedema, corneal nonvascularization and infectious corneal ulcers [5].

The purpose of this work was to evaluate the effect of a biomaterial as gel containing collagen and glycosaminoglycans on the regeneration of the corneal epithelium wounded by keratotomy. Based on this study we tried to determine, in an animal model, whether this gel diminishes the period of corneal epithelial wound healing.

2. MATERIALS AND METHODS

Gel preparation. The preparation used for testing is a viscous solution of collagen and glycosaminoglycans-keratan sulphate and chondroitin sulphate at a ratio of 4:0.6:0.4. To this solution, a mixture of two antibiotics neomycin (0.5%) and bacitracin (0.35%) was added. Collagen and glycosaminoglycans were extracted from bovine cornea by previously described methods [8], [9].

Animals and treatment. The study was performed on 12 eyes of 10–12 months-old albino rabbits, on which incisions were made by keratotomy at epithelium level of about 0.1 mm cornea depth and 3 mm long, in its central region. In each of the six rabbits, an eye was periodically treated with COL-GAG gel (sample) and the other was not treated (control). The treatment was performed by application of the preparation (0.1 ml) at different periods of time: 1h, 2h, 6h, 12h and daily, respectively, for 4 days.

Tissue processing. For light microscopy, wounded cornea fragments were fixed in Bouin' fixative, embedded in paraffin, sectioned at 7 μm and stained with hematoxylin-eosin.

For transmission electron microscopy (TEM), the tissue fragments were fixed in 0.1 M cacodylate buffer (*p*H 7.4), containing 2.5% glutaraldehyde and 2% paraformaldehyde. Then, they were cut into small pieces and postfixed with 1% OsO_4 in 0.1 M cacodylate buffer for 2h. The pieces were dehydrated in ethanol and included in Epon 812. Ultrathin sections were obtained with an MT 7000 ultramicrotome stained with uranyl acetate and lead citrate and examined in transmission electron microscopy (Philips EM 208 S).

For fluorescence microscopy, corneas were fixed in saline phosphate buffer with 10% formol for 24h. After fixation the tissue fragments were washed in the same buffer and stained *in toto* with DAPI (4,6-diamino-2-phenyl indole). Then, a fluorescent microscope Zeiss Jena provided with mercury lamp and corresponding filters for DAPI visualized the sections.

3. RESULTS

The process of wounded cornea remodeling was evaluated on albino rabbit eyes wounded by keratotomy at epithelium level. The evaluation of collagen and glycosaminoglycan biomaterial effect was made by comparing the changes occurred during the healing process of treated eyes and untreated ones.

In the first stage, the wound healing was estimated in terms of decrease of the wounded zone length during the four day-treatment. Cornea healing occurred in two distinct phases: a latent phase in which the wound size decreased not significantly and a linear phase, in which the wound diminished rapidly. The latent phase lasted about 6h, both for corneas treated with polymeric gel and those untreated. In the healing phase, the treated eyes exhibit a much more rapid rate of healing (Table 1). The average time for wound healing was of 72h for the treated corneas and of 96h for the untreated ones.

Table 1

Average length of incision for COL-GAG gel treated and untreated corneas

Time after wounding (h)	Treated cornea (mm)	Untreated cornea (mm)
0	2.95	3.14
6	2.90	2.93
12	2.87	2.65
24	2.10	1.85
36	1.20	0.90
72	0.22	0.08
96	0.10	0.01

By light microscopy, it is found a mobilization of polymorphonuclear leukocytes at epithelial wound level in the latent stage, which is more pronounced in treated eyes (Fig. 1*A*), compared to controls (Fig. 1*B*).

Two hours after wounding, epithelial cells begin to migrate in the form of bundles or individual cells onto the cornea surface. This migration was evidenced by fluorescent microscopy (Fig. 2). Six hours following the wounding, the process of epithelium recovery is evident and it is more advanced in treated eyes. At ultrastructural level, it was noticed that in epithelial cells surrounding the wound numerous microfibrils appear disposed in bundles (Fig. 3).

After three days following the keratotomy, epithelium was completely regenerated in the treated eyes only. At the level of untreated corneas, epithelium

regenerated after 4 days. But, it was found that the adhesion between epithelium and stroma is not as tight as in the case of treated corneas (Fig. 4*A*, *B*). At the same period of time, between the cells of regenerated epithelium, desmosomes and interdigitate junctions were often present (Fig. 5).

4. DISCUSSION

Our light, electron and fluorescent microscopy observations demonstrate that collagen and glycosaminoglycan gel speeds reepithelization of keratotomy wounds in the rabbit cornea. The repairing of superficial corneal keratotomy using collageneous compresses was previously reported [10], [11], [12], when it was demonstrated the positive action of exogenous collagen on the process of wound healing. Our results obtained on rabbit eyes reveal a considerable difference as concerns the changes occurring in the process of healing the treated eyes compared to controls.

One of the important events in the regenerating process is the epithelial cells' migration into the wound edge including a latent phase and a linear phase of regeneration [13], [14].

In the latent phase (first hours following the wounding) it were found a mobilization of polymorphonuclear leukocytes and a desquamation of superficial cells determining the progressive thinning of the epithelium at the wound edge. Polymorphonuclear leukocytes' appearance one hour following the cornea wounding is similar to that previously reported by Lee et al. [15]. An accumulation of polymorphonuclear cells, arriving principally via the tear fluid, occurs along the wound edge and later can be seen over the surface of the wound, exhibiting a higher mobilization in the eyes treated with collagen and glycosaminoglycan gel.

In the linear phase of regeneration, it is noticed epithelial cell migration over the wounded tissue, both in the form of individual cells and in small groups. This aspect was outlined in our study by marking the wounded tissue with DAPI nuclear dyestuff. At this stage, polymorphonuclear leukocytes disappear and epithelial cell migration is accompanied by their proliferation in order to restore the normal thickness of epithelium. Previous researches correlated cell migration to increased synthesis of glycoproteins and an intensification of glycogen metabolism, serving as the energy source [16]. Also, it was demonstrated, on the mouse cornea, that migration of epithelial cell occurs in a centripetal manner, from the limbus towards the cornea center [17].

The complete regeneration of epithelium was noticed in corneas treated with COL-GAG gel earlier than in controls. The positive effect of collagen matrices is determined by optimization of the environment into which the migration of epithelial cells occurs, thus ensuring the trauma minimizing and preventing epithelial cell desiccation in the migration stage.

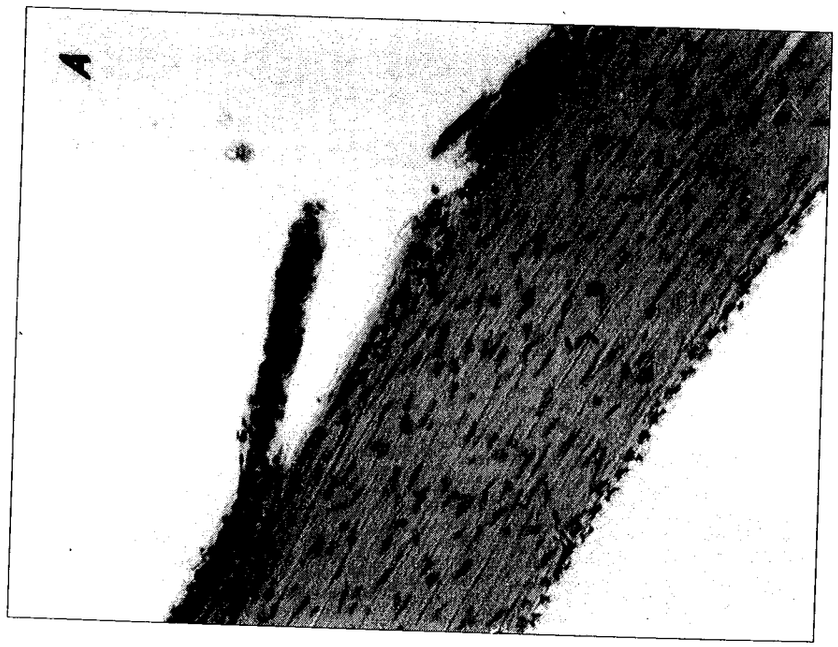

Fig. 1 – Light micrograph of rabbit cornea wounded by keratotomy, one hour following the injury. One can notice that in treated eyes (*A*) there is a higher mobilization of polymorphonuclear leukocytes compared to untreated eyes (*B*).

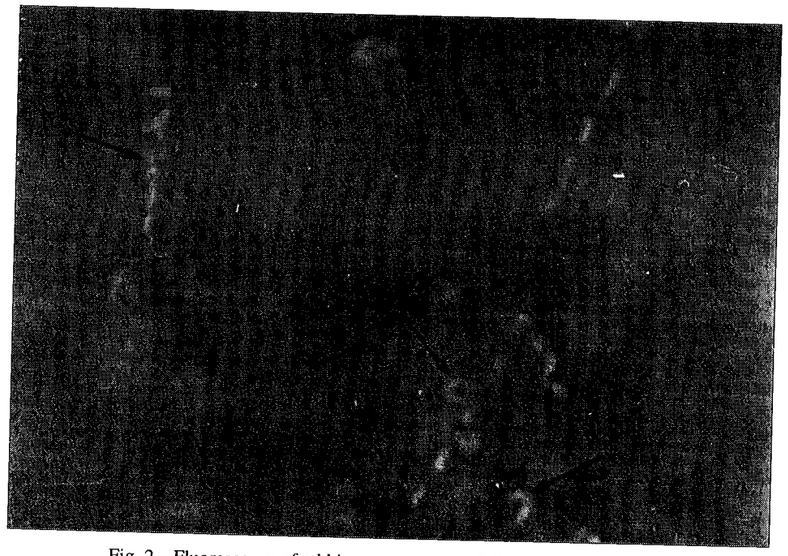

Fig. 2 – Fluorescence of rabbit cornea, 2 hours following the wounding. It is revealed the epithelial cell migration onto cornea surface in the form of bundles, individual cells or small groups.

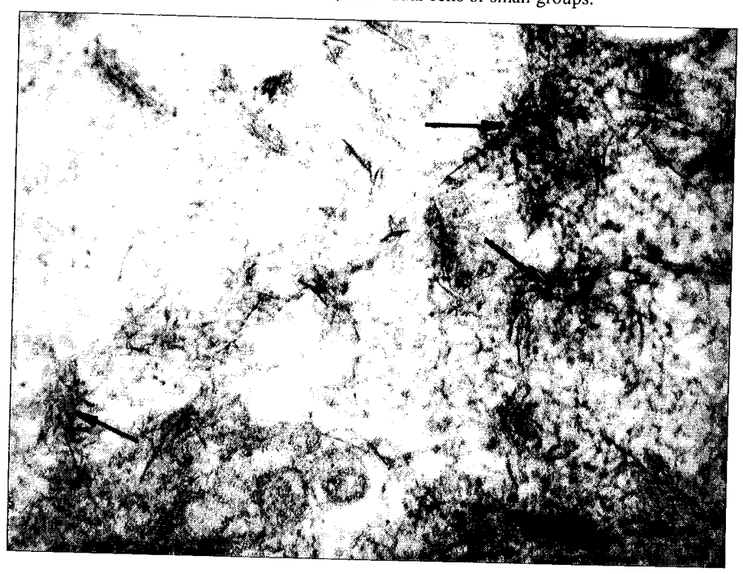

Fig. 3 – Electron micrograph of microfibrils arranged in bundles in epithelial cells surrounding the wound (×75000).

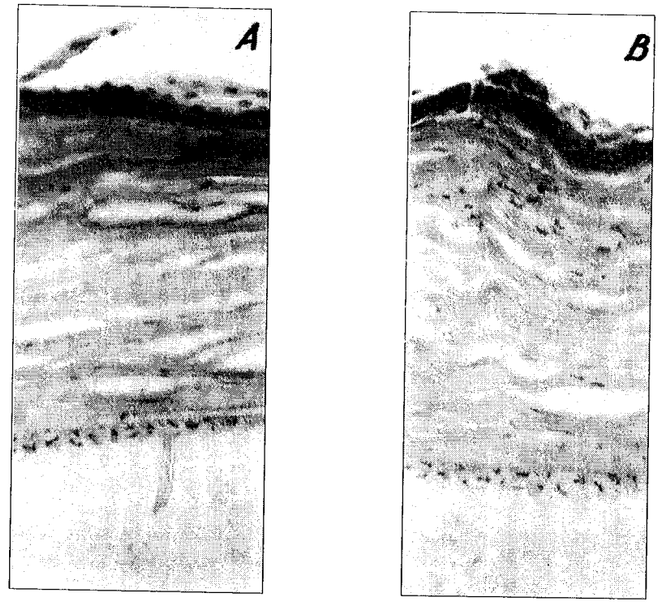

Fig. 4 – Rabbit corneas wounded by keratotomy 4 days after wounding. One may notice that the adhesion between epithelium and stroma is tighter in the case of treated corneas (*A*) compared to the untreated ones (*B*).

Fig. 5 – Interdigitate junctions between the cells of regenerated epithelium (×55000).

During migration, epithelial cells develop cell – substrate focal contacts, which are, specialized cytoskeletal complexes in which stress fibers are involved [18]. In hemidesmosomes' absence, intracellular action can mediate these attachments through surface adhesion molecules, such as integrins that have a role of receptors for extracellular matrix collagen. In our study, exogenous collagen and glycosaminoglycans may constitute an adequate matrix for epithelial cells [19].

The results of this study demonstrate that collagen and glycosaminoglycan gel improve the process of wound reepithelization in the rabbit cornea, the healing being performed 24h earlier than in untreated eyes.

REFERENCES

1. H.S. DUA, J.A.P. GOMES, A. SINGH, *Corneal epithelial wound healing*, Brit. J. Ophthalmol., **78**, 401–408 (1994).
2. I.M. RAWE, S.J. TUFT, K.M. MEEK, *Proteòglycan and collagen morphology in superficially scarred rabbit cornea*, Histochem. J., **24**, 311–318 (1992).
3. S.D. KLYCE, *Transport of Na, Cl and water by the rabbit corneal epithelium at resting potential*, Am. J. Physiol., **228,** 1446 (1975)
4. R.A. THOFT, E.F. MOBILIA, *Complications with therapeutic extended wear soft contact lenses*, Int. Ophthalmol. Clin., **21,** 197 (1981).
5. C.H. DOHLMAN, S.A. BORUCHOFF, E.F. MOBILIA, *Complications in use of soft contact lenses in corneal disease*, Arch. Ophthalmol., **90**, 367 (1965).
6. S.N. FYODOROV, Z.I. MOROZ, Z.I. KRAMSKAYA, S.N. BAGROV, T.S. AMSTISLAVSKAYA, A.V. ZOLOTAREVSKY, *Complex conservative treatment of endothelial and epithelial corneal dystrophy using therapeutic collagen coating*, Vestn. Oftalmol., **101,** *6,* 33–38 (1985).
7. H.D. PERRY, L.W. HODES, J.A. SEEDOR, E.D. DONNENFELD, T.F. MCNAMARA, L.M. GOLUB, *Effect of doxycycline (Hyclate) on corneal epithelial wound healing in the rabbit alkali – burn model*, Cornea, **12**, 379–82 (1993).
8. LUCIA MOLDOVAN, OANA CRACIUNESCU, MARINELA BUNEA, MARIA CALOIANU, *Extraction and purification of collagens from corneal stroma*, Rom. J. Biol. Sci., 1–2, **II**, 5–16 (1998).
9. LUCIA MOLDOVAN, OANA GHEORGHIU, FLORENTINA CUTAŞ, MARIA CALOIANU, *Fractionation of glycosaminoglycans from bovine corneal stroma*, Analele Univ. Bucureşti, *XLIII*, 28–33 (1994).
10. J.M. FRANTZ, B.M. DUPUY, H.E. KAUFMAN, R.W. BEUERMAN, *The effect of collagen shields on epithelial wound healing in rabbits*, Am. J. Ophthalmol., **108,** *5*, 524 (1989).
11. J.V. AQUAVELLA, J.J. RUFFINI, J.A. LOCASCIA, *Use of collagen shields as surgical adjunct*, J. Cataract. Refract. Surg., **14**, 492 (1988).
12. D.E. POLAND, H.E. KAUFMAN, *Clinical uses of collagen shields*, J. Cataract. Refract. Surg., **14,** 489 (1988).
13. D.M. MAURICE, *The biology of wound healing in the corneal stroma*, Cornea, **6**, *3*, 162–168 (1987).
14. H.S. DUA, J.V. FORRESTER, E.J. COHEN, P.R. LAIBSON, *Clinical observations on corneal epithelial cell migration in humans*, Invest. Ophthalmol. Vis. Sci.(suppl), **34**, 1017 (1993).
15. R.E. LEE, P.F. DAVISON, C. CINTRON, *The healing of linear nonperforating wounds in rabbit corneas of different ages*, Invest. Ophthalmol. Vis. Sci, **23,** *5*, 660–665 (1982).

16. I.K. GIPSON, M.J. WESTCOTT, N.G. BROOKSBY, *Effects of cytochalasins B and D and colchicine on migration of the corneal epithelium*, Invest. Ophthalmol. Vis. Sci., **22**, 633 (1982).
17. R.K. BUCK, *Measurement of centripetal migration of normal corneal epithelial cells in the mouse*, Invest. Ophthalmol. Vis. Sci., **18,** 767–784 (1979).
18. R.M.R. GARANA, W.M. PETROLL, W.-T. CHEN, I.M. HERMAN, I.P. BARRY, P. ANDREWS, H.D. CAVANAGH, J.V. JESTER, *Radial keratotomy. II. Role of the myofibroblast in corneal wound contraction*, Invest. Ophthalmol. Vis. Sci., **33**, *12*, 3271–3282 (1992).
19. B. LAUWERYNS, J.J. VAN DEN OORD, R. VOLPES, B. FOETS, L. MISSOTTEN, *Distribution of very late activation integrins in the human cornea*, Invest. Ophthalmol. Vis. Sci., **32**, 2079–85 (1991).

Received November 16, 2000.

*National Institute for Biological Sciences
296 Spl. Independenţei, Bucharest

**University of Bucharest
Faculty of Biology
90–95 Spl. Independenţei, Bucharest

AVIS AUX COLLABORATEURS

La «Revue roumaine de biologie – Série de biologie animale» publie des articles originaux d'un haut niveau scientifique de tous les domaines de la biologie animale: taxonomie, morphologie, physiologie, génétique, écologie, etc. Les sommaires des revues sont complétés par d'autres rubriques, comme: 1. La vie scientifique, qui traite des manifestations scientifiques du domaine de la biologie (symposiums, conférences, etc.); 2. Comptes rendus des plus récentes parutions dans la littérature.

Les auteurs sont priés de présenter leurs articles en double exemplaire imprimés, de préférence sur une imprimante laser et espacés à double interligne. Le contenu des articles sera introduit sur des disquettes dans un langage connu, préférablement Word 6.0. La composition et la mise en vedette seront faites selon l'usage de la revue: caractères de 11/13 points pour le texte, de 12/14 points pour le titre de l'article et de 9/11 pour les annexes (tableaux, bibliographie, explication des figures, notes, etc.) et le résumé en anglais de 10 lignes au maximum, qui sera placé au début de l'article. Il est obligatoire de spécifier sur les disquettes le nom des fichiers ainsi que le programme utilisé.

Le matériel graphique sera envoyé sur disquette, scanné, avec les mêmes spécifications. En l'absence d'un scanner, le matériel graphique sera exécuté en encre de Chine sur papier calque.

Les tableaux et les illustrations seront numérotés en chiffres arabes dans l'ordre de l'apparition. Les titres des revues seront abrégés conformément aux usages internationaux.

Les textes ne doivent pas dépasser 10 pages (y compris les tableaux, la bibliographie et l'éxplication des figures).

La responsabilité pour le contenu des articles revient exclusivement aux auteurs.